Differentially expressed proteins in prostate cancer and functional characterization of proteins with altered expression

I n a u g u r a l d i s s e r t a t i o n

zur

Erlangung des akademischen Grades

doctor rerum naturalium (Dr. rer. nat.)

an der Mathematisch-Naturwissenschaftlichen Fakultät

der

Ernst-Moritz-Arndt-Universität Greifswald

vorgelegt von

Ramesh Ummanni

geboren am 15.05.1978

Hyderabad, India

Dekan: .....

1. Gutachter: .....

2. Gutachter: .....

Tag der Promotion: .....

This thesis is dedicated to my parents and family members

Results of this work are part of the following publications and manuscripts:

Zimmermann U, **Ummanni R**, Junker H, Venz S, Teller S, Giebel J, Walther R. Establishing a protein signature from prostate tissue biopsies. Urologe A. 2007 Sep;46(9):1089-91.

Ummanni R, Junker H, Zimmermann U, Venz S, Teller S, Giebel J, Scharf C, Woenckhaus C, Dombrowski F, Walther R. Prohibitin identified by proteomic analysis of prostate biopsies distinguishes hyperplasia and cancer. Cancer Letters, 2008, 266: 171-185

Ummanni R, Teller S, Junker H, Zimmermann U, Giebel J, Walther R. Altered expression of TPD52 regulates apoptosis and migration of prostate cancer cells**.** *Manuscript in revison (FEBS Journal)*

Ummanni R, Lehnigk U, Zimmermann U, Woenckhaus C, Walther R, Giebel J. Immunohistochemical expression of caspases 1 and 9, uncleaved caspases 3 and 6, cleaved caspases 3 and 6 as well as bcl-2 in benign prostate epithelium (BPE) and prostate cancer (PCa). *Manuscript submitted*

Table of contents

Abbreviations

2-DE	2-dimentional gel electrophoresis
aa	Amino acid
APS	Ammonium persulphate
at al.	and others
AMACR	Alpha-methylacyl-CoA-racemase
AR	Androgen receptor
bp	Base pairs
BPE	Benign prostate epithelium
BPH	Benign prostate hyperplasia
BSA	Bovine serum albumin
CDS	Coding sequence
CHCA	α-Cyano-4-hydroxycinnamic acid
CHAPS	3-[(3-Cholamidopropyl)dimethylammonio]-propanesulfonate
COFRADIC	Combined FRActional DIagonal Chromatography
dd H_2O	Deionized distilled water
DEPC	Diethyl pyrocarbonate
DIOC	Dihexyloxacarbocyanine iodide
DNA	Deoxyribonucleic acid
dNTP	Deoxyribonucleic acid triphosphate
DDT	Dithiothreitol
DHT	Dihydroxy testosterone
DRE	Digital rectal examination
E coli	*Escherichia coli*
EDTA	Ethylendiamintetraacetic acid
EGTA	Ethylenebis(oxyethylenenitrilo) tetraacetic acid
ESI	Electrospray ionization
FFPE	Formalin-fixed paraffin-embedded
FPC	Familial prostate cancer
FCS	Fetal calf serum
For	forward

GFP	Green Fluorescent Protein
GST	Glutathione -S-Transferase
h	Hour
HDC	Hereditary prostate cancer
HEPES	Hydroxyethyl piperazinyl ethanesulfonic acid
HUGO	Human Genome Organization
HRP	Horseradish peroxidase
IgG	Immunoglobulin G
IGF-1	Insulin-like growth factor-1
IP	Immunoprecipitation
IPTG	Isopropyl β-thiolgalactoside
IPG	Immobilzed pH gradient
IEF	Isoelectric focusing
kDa	kilodalton
LB	Luria Bertani medium
LCM	Laser capture microdissection
MALDI	Matrix Assisted Laser Desorption Ionization
MCS	Multiple cloning site
min	Minute
mRNA	messenger ribonucleic acid
MS	Mass spectrometry
MW	Molecular weight
NMR	Nuclear magnetic resonance
OD	Optical density
PAGE	polyacrylamide gel electrophoresis
PF-2D	Two-dimensional liquid-phase proteome profiling
PCR	Polymerase chain reaction
PCa	Prostate cancer
PI	Propidium iodide
PIN	Prostatic intra epithelial neoplasia
PHB	Prohibitin
PMSF	Phenyl methyl sulphonylfluoride

PPAP	Prostatic acid phosphatase
Prx1	Peroxiredoxin-1
PSA	Prostate specific antigen
rev	Reverse
rpm	Rotations per minute
RPLP0	Ribosomal protein large P0
RT	Room temperature
SPC	Sporadic prostate cancer
SDS	Sodium dodecyl sulphate
SELDI	Surface-enhanced laser desorption/ionization
ShRNA	Small hairpin RNA
TEMED	N,N,N',N'-Tetramethylethylenediamine
TPD52	Tumor protein D52
TOF	Time of flight
TRUS	Trans-Rectal Ultrasound
sec	Second
SEM	Standard error of the mean
U	Unit

1 Introduction

1.1 Anatomy and physiology of Prostate

In Greek the word “prostates” means “to stand before”. Anatomist Heropilus named it as such because the prostate stood before the testes, as he observed it. The prostate is a part of the male reproductive system. It is located in the pelvis below the urinary bladder and in front of the rectum surrounding urethra [1]. The prostate is divided into three zones: the peripheral zone, transition zone and central zone. The function of these different zones is not clear; however, in the young adult prostate gland, the peripheral zone is composed of 65-70% of the glandular tissue, the transition zone 10-15% and the central zone 20-25% [2,3]. The whole organ is encapsulated in a fibrous prostatic capsule. The prostate gland is comprised of 30–50 glands arranged in acini, which empty into the prostatic urethra, the tube that connects the prostate gland with the bladder. Each acinus lined with luminal secretory epithelial cells, basal cells and neuroendocrine cells. The luminal epithelial cells secrete fluid to nourish semen during intercourse [4].

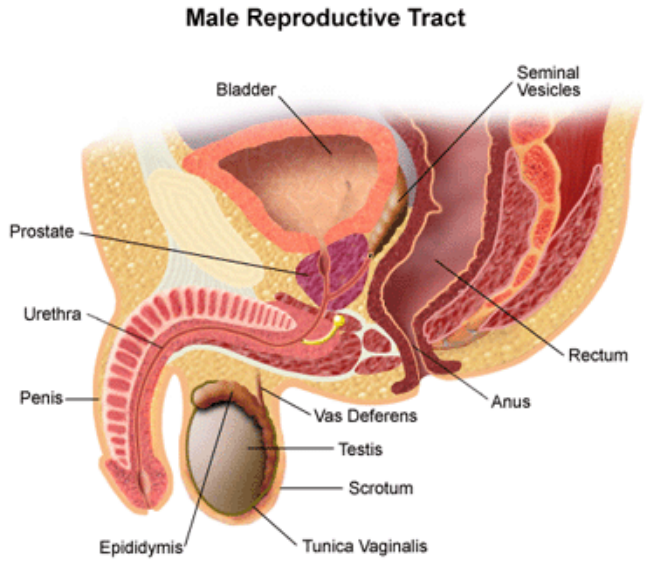

Figure 1: Anatomy of the male reproductive system, courtesy from Rush University Medical Center, Illinois, USA.

1.2 Epidemiology and Etiology Prostate cancer

1.2.1 Incidence and Mortality

Prostate cancer was first reported in 1817 by George Langstaff [5]. Prostate cancer is the most common cancer among the men in western countries. In the year 2005 in the

United States, there were an estimated 230,000 new cases of prostate cancer (PCa) and 30,000 deaths due to this cancer [6]. An estimated 48,650 German men were diagnosed with this disease and 11,839 died from PCa (www.rki.de). World health organization (WHO) announced that, 679,023 new cases and 221,002 deaths from PCa were recorded world wide in 2002. The specific causes for PCa remains unknown [7]. The known risk factors for PCa related to age, race, diet, lifestyle, genetic predisposition (family history for PCa). The incidence rate of PCa differs with ethnicity and origin. The high incidence rate is found in USA and North Europe compared to Asian countries [8,9].

1.2.2 Age

The primary risk factor for PCa is age. It is more common in men over 60 and less common in men below 45 years. Most of the tumors will be diagnosed at the age of 70 [10]. Autopsy studies have shown that approximately 30 % of men over the age of 50 and 80% of men in their 70s have microscopic evidence of prostate cancer [11,12]. This indicates that the most men will get PCa if they live long and die due to PCa most likely.

1.2.3 Genetic background

A man's genetic background contributes to his risk of developing prostate cancer. PCa are divided in to three different epidemilogical forms; Familial (FPC), Hereditary (HDC) and Sporadic (SPC). The PCa patients with no family history for cancer are referred as SPC and this form constitutes about 80% of all PCa cases. SPC occurs due to the somatic mutations. FPC is defined as a clustering of PCa cases among the members of the family. HPC is a subtype of FPC which occurs through the genetic inheritance linked to PCa susceptible genetic abberations. These two forms account for about 20% of all PCa cases recorded [13]. Men who have a brother or father with prostate cancer have twice the usual risk of developing prostate cancer [14]. A study on twins from north Europe suggest more risk risk for PCa in monozygotic twins compared to heterozygotic twins and reported that only 40% of PCa risk by inherited factors and 50% by other factors [15]. However no single gene is responsible for prostate cancer, many genes have been implicated. Several loci such as 1q24-25, 1q36, 1q42.2-43, 8p22, 8q21, 17q-21 etc. are identified as susceptible and associated with PCa. Two genes *BRAC1* and *BRAC2* that are risk factors for ovarian and breast cancer have significant implications for PCa [16,17]. Also genetic polymorphisms of

IGF1 [18,19] vitamin D receptor [20] and *GST-T1* [21] have been found to be associated with PCa risk. Epigenetic changes such as promoter hypermethylation for transcriptional silencing for GST-P1 expression strongly associated with PCa progression [22-24].

1.2.4 Diet

Dietary amounts of certain food, vitamins and minerals can contribute to prostate cancer risk. High intake of fat (which produce transfatty acids) and meat will have high risk for PCa [25]. Many studies have reported that dietery intake of tomatos rich in lycopene a carotenoid with antioxidant property decrease the risk for PCa [26,27], but it was challenged recently [28]. Other dietery factors that may decrease PCa risk have been reported are omega-3-fatty acids, vitamin D and E [29], minerals zinc and selenium [30].

1.2.5 Alcoholism and smoking

The role of alcohol and smoking is not clear. High alcohol intake may increase the risk. Many studies have shown no correlation for PCa risk with alcoholism and smoking.

1.2.6 Race and Ethnicity

The rate of men dying from prostate cancer has varied, depending on their race and ethnicity. In some areas of the USA, the risk of the disease is 80% higher in blacks than in Caucasians; Black men were more likely to die of prostate cancer than any other group. Chinese, Japanese [31] Soviet Union [32] and other Asian men have the lowest incidence of prostate cancer while men in North America and Northern Europe have the highest incidence [33]. But immigrants from these regions have more risk for PCa [34,35]. Despite the ethnic and geographical variations in the incidence of overt disease, the incidence of latent disease has been found to be similar in all populations, suggesting that environmental factors may influence the aggressiveness of prostate cancer.

1.2.7 Environmental factors

Migration studies show that the incidence of prostate cancer in immigrants moving from low-risk to high-risk countries can increase with successive generations. An environmental factor that has been proposed as possibly responsible for the changes in incidence is exposure to industrial chemicals such as cadmium [36], lead [37] and zinc [38].

A higher risk has also been suggested in farming possibly due to occupational exposure to chemicals used as fertiliser or in pest control [39,40].

1.2.8 Sexual behaviour

There is some suggestion that the risk of prostate cancer may be increased in men who become sexually active at a young age, who have multiple sexual partners, or who contact a sexually transmitted disease. However, the evidence for this hypothesis is inconclusive and the finding could represent a hormonal effect.

1.3 Hormonal control of prostate

In the adult, prostate gland size and function is maintained through a homeostatic balance between the process of cell renewal (proliferation) and cell death (apoptosis). This balance is regulated by hormones secreted by the endocrine system, mainly androgens, of which testosterone is the major circulating form. Most testosterone (97%) circulates in the bloodstream bound to one of two proteins, either sex hormone binding globulin (SHBG) or albumin. A small percentage of testosterone (2–3%) remains unbound and it is thought to affect the glandular cells of the prostate. The enzyme 5 alpha-reductase catalyzes the conversion of testosterone to dihydroxy testosterone (DHT). DHT binds to androgen receptors (AR) within the glandular cells, then targets within the cell nucleus, specific DNA sequences known as androgen response elements, that activate cell functions, including growth and proliferation. PCa and normal prostate cells require androgens for their growth. Therefore, androgen depletion may kill PCa cells.

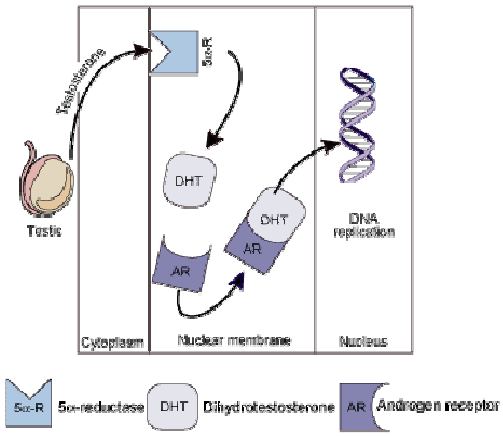

Figure 2: The role of androgens testosterone and DHT action in physiological function of the prostate gland. Courtesy from prostate cancer online

1.4 Prostate cancer

1.4.1 Prostate cancer progression

Carcinogenesis is a multi-step accumulation of genetic lesions that may eventually result in uncontrolled cellular proliferation, and/or a decrease in cell death or apoptosis. The molecular pathology of prostate cancer is not clear, but environmental, dietery, lifestyle, infection or inflammation of prostate and androgens, mainly testosterone, are thought to play a part in initiating and promoting PCa. The defects in molecular pathways that are responsible for its initiation, development and progression are still remains unclear. Various growth factors, such as epidermal growth factor and insulin growth factor and mutations in the AR may also play a role the development and/or progression of prostate cancer. At least 95% of prostate cancers are adenocarcinomas, they arise in the glandular tissue or acini derived from the epithelial cells of the prostate [41]. Most prostate cancers (60–70%) arise in the PZ of the prostate, with 5–15% arising in the CZ and the remainder developing in the TZ [42,43].

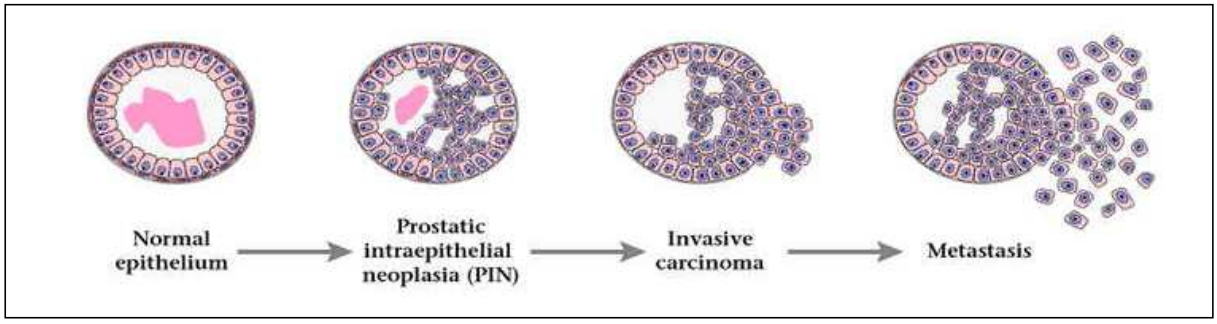

Figure 3: Steps involved in prostate cancer progression. Courtesy Memorial Sloan-Kettering Cancer Center

1.4.2 Prostatic intraepithelial neoplasia

Prostatic intraepithelial neoplasia (PIN) is now accepted as the most likely pre-invasive stage of PCa. Its role as the preinvasive stage of cancer was recently confirmed [44,45]. PIN coexists with cancer in more than 85% of cases in PZ [46], the clinical importance of recognizing PIN is based on its strong association with PCa. PIN is associated with intermediate genotypic and phenotypic abnormalities between and normal and PCa. PIN is classified into two grades, low grade (PIN I) and high grade (PIN II, PIN III) [47,48]. Increasing PIN associated with the loss of basal cell layer which lost completely in cancer

[49]. Although there is no proof that PIN is a cancer precursor, it has been suggested that most patients with PIN will develop cancer within ten years.

1.4.3 Classification of PCa

1.4.3.1 Grading

Gleason grading is most accepted system to describe aggressiveness of PCa histopathologically. Gleason score is assigned based on microscopic appearance of cancer tissue. In grade 1, tissue resembles normal whereas, in grade 5, almost all glands are lost and tissue appears like sheet of cells. The final score is a combination of two different scores from dominant and common grades. The Gleason score is important because higher Gleason scores are associated with worse prognosis [50,51].

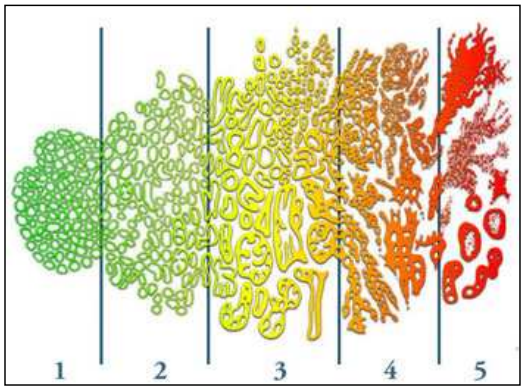

Figure 4: Gleason grading system to classify prostate cancer depending on its aggressiveness. Courtesy Providence Cancer Institute

1.4.3.2 Tumor staging

For better treatment of cancer it is necessary to know the disease stage. The most common system is the four-stage TNM system which describes primary tumor (T), tumor in lymph nodes (N) and metastasis (M). In the TNM system, clinical T1 and T2 cancers are found within the prostate, while T3 and T4 cancers have spread elsewhere in the body [52].

1.4.4 Diagnosis

Prostate cancers are usually slow-growing. In many cases the disease does not reach a stage where it becomes clinically significant. Screening for prostate cancer involves the digital rectal examination (DRE) and the prostate specific antigen (PSA) blood test. Either of these tests alone cannot detect cancer. Both tests together are valuable methods in

detecting this life threatening cancer. Consequently, a pathological PSA value and/or DRE necessitate further diagnostic procedures, such as the trans-rectal ultrasound (TRUS) examination with multiple biopsies from the prostate. Latest research investigations suggests that sampling of increased biopsies improves the PCa detection [53-55]. Patients with high PSA levels (> 4 ng/ml) and negative biopsies require annual testing of PSA and further biopsies to exclude PCa.

1.4.5 Biomarkers for early diagnosis of PCa

Since the introduction of PSA, the detected incidence has increased dramatically [56]. However, PSA is neither tissue nor gender specific and small amounts are also detected in the endometrial, breast, adrenal and renal tumors. Moreover, PSA can be secreted from benign as well as malignant cells of the prostate [57,58]. Therefore, the serum PSA value correlates closely with both, BPH and PCa. Most men will have PSA level between 4-10 ng/ml [59] which demands better tools for early diagnosis of cancer in these patients to save life.

Several markers for PCa have been reported but only a few potential markers have been identified such as AMACR [60,61]. The only test which can fully confirm the diagnosis of prostate cancer is a biopsy, the removal of small pieces of prostate tissue for microscopic examination. Although some parameters including measurement of free and total PSA value [62-64], human glandular kallikrein-2 [65,66] and insulin growth factor-1 in blood serum, immunohistochemistry of Ki-67 proliferation index [67,68] and CD44 have been employed, a reliable marker to decide whether further biopsies are indicated has not yet been established. Consequently, it is necessary to develop novel diagnostic methods to improve early detection of PCa. Recently a new blood test for early prostate cancer antigen-2 (EPCA-2) was reported for PCa diagnosis and staging [69,70].

1.4.6 Treatment

The prognosis and treatment options depend on tumor stage, patient’s health, age and/or weather cancer diagnosed early. For tumors that are localized within the prostate, radiation therapy, watchful waiting and a surgery called radical prostatectomy are common treatment options [71]. The tumors that spread the capsule prostate can't be cured with either radiation or surgery. They can be treated with hormone ablation (high level of androgens

helps the PCa to grow) therapy that delays the cancer growth. Deficient markers to diagnose cancer before it escapes from gland and the limited treatment options highlights the need of developing advanced methods for early diagnosis and treatment. Gene and/or protein expression profiling of prostate cancer tissues may provide a chance to identify potential markers and new drug targets for early diagnosis and effective treatment to save cancer patients life.

1.5 Proteomics

1.5.1 Highlights of proteomics technology

The term **"proteome"** coined in 1994 to describe the expressed proteins by genome of a cell at a particular time under specific conditions. The aim of **"proteomics"** is to identify, characterize, and quantify all proteins involved in a particular pathway, organelle, cell, tissue, organ, or organism to obtain comprehensive data about that system and to correlate expression level changes and/or protein modifications associated with conditions of the system such as disease state etc.

The completion of the Human Genome Sequencing Project by International Human Genome Sequencing Consortium and Celera Genomics represents a major achievement in modern science in 2001 [72,73]. According to HUGO, human genome size is about 3,200 Mbp. Only two percent of the human DNA makes genes, the remaining DNA are important but as yet unknown functions. One of the interesting findings about the human genome is the number of genes found in between 20,000 to 35,000 (the precise number is still is in the controversy). In human DNA, gene prediction is very difficult due to open reading frame (ORF), alternative splicing, repetitive sequences and low density exons. So, verification of a gene product by proteomic analysis is necessary step in gene annotation. It is clear that array based gene expression profiling studies measuring mRNA levels are insufficient to analyze it protein complement of cells. Recent studies indicate that there is no correlation between mRNA expression levels and the level of its encoded proteins [74,75]. In addition to that one gene one protein concept, one gene codes for six to eight protein [76]. There may be several thousands of proteins are included in human total proteins due to splice variants [77], processing of mRNA [78] and posttranslational modification [79]. These biological complexities can be unravelled by proteomics approach which helps to understand molecular mechanisms to integrate signals in cellular systems [80].

Even if we identify all protein coding regions in the human genome, we will still be missing necessary information, because genomic information does not allow efficient prediction of all the post translational modifications observed in proteins. The number of different protein molecules expressed by the human genome is more than number generally considered by genome scientists. Genomics focuses on the information of one target molecule, DNA, in the nucleus of cells. Proteomics focuses on the identification, localization, and functional analysis of the protein make-up of the cell. Proteins are the functional units of the cells and their expression changes dramatically with the organism and conditions of the host cells. Protein signature of the cells is very important because most diseases are manifested at the level of protein activity. To really understand biological processes in disease progression, we need to understand how proteins function in and around cells under a given disease state. Such information will help to identify new targets that can be used in diagnosis, treatment and prognosis of disease.

Proteomics comprises all comprehensive, high-throughput technology platforms enabling us to display and identify the largest possible number of proteins in a proteome, and to determine how they are related to each other though changes in expression levels or modifications according to the state of the system under study.

1.5.2 Classification of proteomics technology

Structural proteomics is the dtermination of protein structures. This is achieved by protein expression combined with X-ray crystallography and NMR spectroscopy. It also involves analyses of primary structure (amino acid sequencing) and tertiary structures to identify common structural motifs and how they relate to diverse protein functions. Structural analysis can contribute to identifying the functions of newly discovered genes or to showing where drugs bind to a target protein or how proteins interact with each other.

Functional proteomics is the determination of function of newly identified proteins and protein-protein interactions. It includes applications of protein purification and mass spectrometry and physical methods like direct affinity capture method [81,82] and yeast two-hybrid assays [83], coimmunoprecipitations [84] and coprecipitation [85] can be used to study protein interactions.

Expression proteomics is the large scale analysis of protein expression. The main aim of expression proteomics is to identify all or a set of interested proteins in protein

samples to identify differentially expressed and proteins that are present or absent under particular variations. For example, a particular protein is specifically altered in expression under certain disease condition it can be used as a marker for the diagnosis or a new drug target. In protein expression studies, to separate proteins different methods such as gel based two-dimensional gel electrophoresis (2D SDS-PAGE) or gel free methods like liquid chromatography or PF 2D (Two-dimensional liquid-phase proteome profiling). In PF 2D, proteins are by IEF in first dimention and hydrophobic chromatography in second dimension. Following separation, protein expression profile analyzed by suitable software and interested proteins will be identified by mass spectrometry combined with the available protein database.

1.5.3 Two-dimensional gel electrophoresis

Two-dimensional gel electrophoresis (2-DE) is one of the best experimental tools for the reliable separation of thousands of proteins in a single gel consists of a pair of electrophoretic separations. As described previously, the first dimension isoelectric focusing (IEF) separates proteins based on their charge whereas the second dimension SDS-PAGE separates proteins according to their molecular weights. The result is an array of protein spots, each spot representing a single or few proteins depending on the sample. In addition to this 2-DE can separate proteins based on their modifications.

The original 2-DE with carrier ampholyte generated pH gradients in polyacrylamide tube gels was first described by P.H. O'Farrel and J. Klose in 1975 [86,87]. It has not been widely used due to limitations of original technique and results analysis. Bjellqvist et al. in 1982 developed an alternative method to prepare immobilized pH gradients [88]. The new 2-DE methods use immobilized pH gradient gels for IEF and other developments have provided an opportunity to achieve better resolution, reproducibility and result analysis [89,90]. Immobilzed pH gradient (IPG) based 2-DE separations have more advantages than ampholyte based 2-DE such as high protein loading [91] and samples can be applied during rehydration of the precast IPG strips [92]. With the recent advances in 2-DE, each gel can resolve approximately 2000 protein spots representing proteome map of the sample. Visualization of proteins requires highly sensitive, reproducible and mass spectrometry compatible methods to detect and identify very low amount of protein. Routine staining techniques include Coomassie blue, colloidal Coomassie blue and silver nitrate staining

procedures. However, silver staining is not compatible for mass spectrometry due to formaldehyde used in staining procedure [93]. There are some alternative silver staining protocols were reported with a lot of changes to original staining method [94,95]. With recent developments in protein staining methods have developed fluorescent dyes such as SYPRO® Ruby, Flamingo™ and Deep Blue become more important and are commercially available. The fluorescent dyes are be able to detect 0.1 ng of protein per spot and is suitable for mass spectrometry and have replaced the conventional staining methods.

2-DE has some disadvantages over the advantages in post genomics approach. It is very difficult to resolve and detect low abundant proteins, hydrophobic proteins, proteins with very high or low MW and highly acidic or basic pI on 2D gels. Some of these problems have been overcome by recent developments in 2-DE technology.

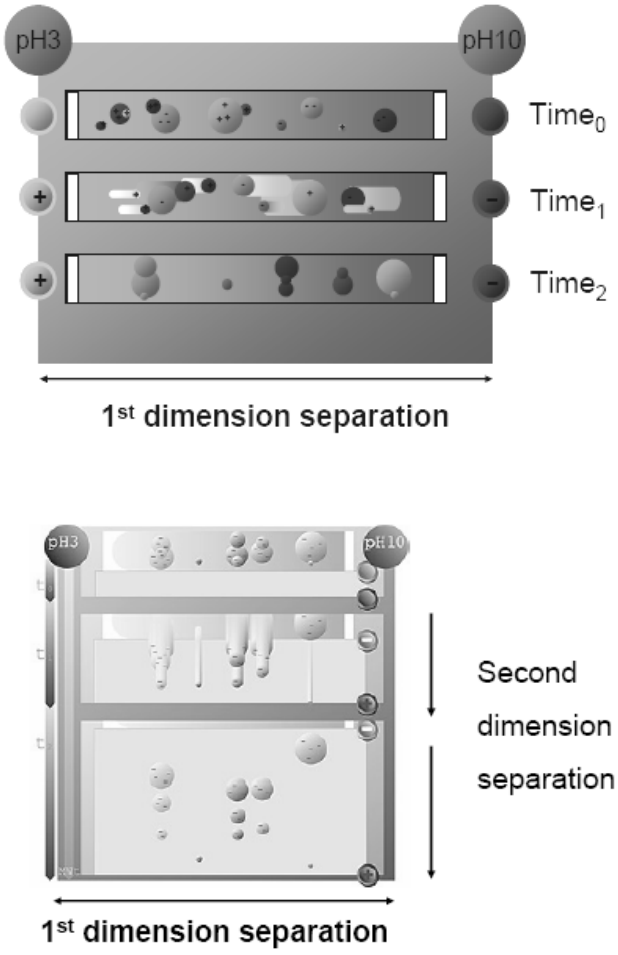

Figure 5: Illustrations of 2-DE, (A) Isoelectric focusing for separation of proteins in first dimension and (B) Separation of proteins based on their molecular weight in second dimension.

1.5.4 Mass spectrometry

The two basic developments Matrix-Assisted Laser Desorption/Ionization (MALDI) [96] and electrospray ionization (ESI) [97] in analytical chemistry laid a fundamental stone for latest improvements in proteomics. Mass spectrometry (MS) based methods for the identification of gel-separated proteins is important platform technologies for proteomics. With basic instrumentation in mass spectrometry technology, recent developments have provided new machines for proteomic applications.

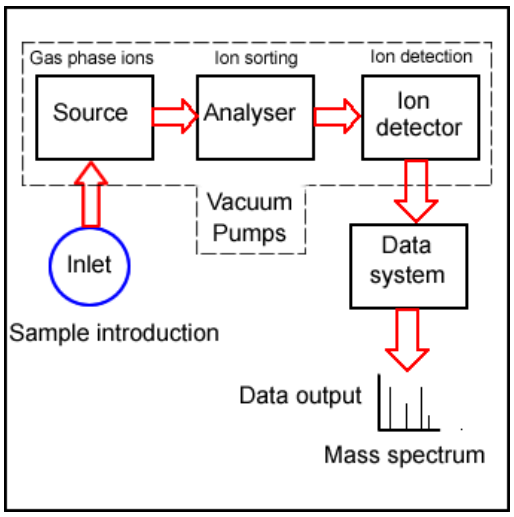

Figure 6: Basic components included in the mass spectrometer.

For identification of proteins in MS, first step is proteolysis of unknown protein with proteases (e.g. Trypsin) to generate short peptides. In MALDI, the protein digest is co-crystallized with matrix which is weak organic acid. Then the pulsed laser energy applied onto matrix-analyte mixture to desorb analytes from solid matrix producing singly charged ions. In ESI, a high voltage potential is applied to a liquid sample as it passes through a small capillary. In contrast to MALDI, electrospray peptides are desorbed into the gas phase following evaporation generating multiple charged ions. The accelerated ions in the electric field of mass spectrometer fly towards detector according to their mass to charge ratio (m/z). The detector will collect the ions and generate proportional electrical signal which is recorded as a function of m/z by recorder finally converted as mass spectra. The mass spectrum generated by MALDI/ESI provides masses of the analyzed peptides. The peptide list of protein can be finger print of the digested protein. The list of peptide masses is then

matched with the theoretical peptides generated by the same proteolytic enzyme in data base SEQUEST or Mascot [98]. This is known as peptide mass finger printing (PMF) [99,100].

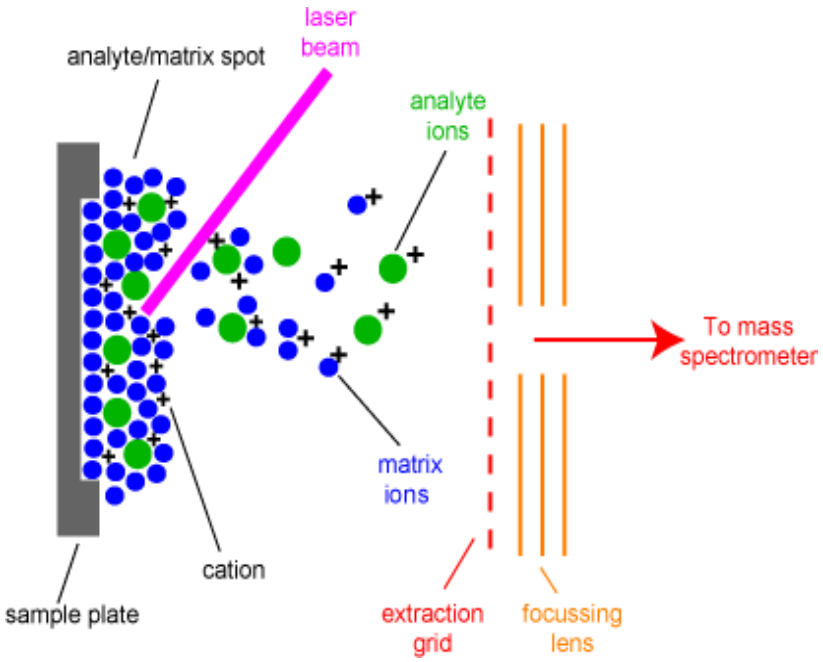

Figure 7: Matrix Assisted Laser Desorption Ionization (MALDI). Pulsed laser on matrix-analyte mixture results in vaporization of the matrix and acceleration of the ions. The ions entered in flight tube separated according to their m/z ratio and recorded by recorder. Courtesy University of Bristol

Generally the mass analyzed in MS is not sufficient for unambiguous protein identification. A MS/MS spectrometer based on either ESI or MALDI can be used to analyze proteolytically derived peptides for subsequent protein identification. In MS/MS, the selected peptide ions are fragmented by soft ionization and spectra were recorded. Generated MS/MS spectras represents an amino acid sequence tag of the peptides to support or confirm identification by PMF data.

Alternative to 2-DE coupled mass spectrometry, other proteomic methods are available. The gel-free proteomic techniques such as LC-MS/MS, PF-2D, MudPIT [101], LC-ICAT [102] can be used for protein identification in complex mixtures. Recent technology, COFRADIC that isolates predefined peptides decreases the complexity of the analytes for MS/MS analysis there by increases the number of identified proteins of a sample [103].

1.6 Prostate cancer proteomics

There are limited tools for PCa screening and diagnosis among them currently PSA test is in use. It has been shown that PSA test alone is not reliable but together with DRE and TRUS it can facilitate PCa diagnosis. Differential proteomics technology provides an opportunity for analysis of global protein expression of prostate tissue from different clinical states such as cancer, hyperplasia and prostatitis to find markers for early diagnosis and prognosis of PCa. Also, potential candidate proteins can be used to develop new therapeutic strategies for PCa [104,105]. In 1985 Guevara et al. first reported first 2-DE protein profile of prostate fluids[106]. Proteomic reports on prostate fluids indicate that a series of prostatic acid phosphatase variants have been elevated in BPH prostatic fluids where as decreased or absent in PCa samples [106]. A protein specifically present in PCa patients was undetectable in normal tissue and BPH [107]. Proteomic analysis of urine samples collected from normal men, patients diagnosed with either BPH or cancer and prostatectomized men reported few potential markers to distinguish different clinical situations [107-109]. Recently a multiplex panel of urine transcripts was reported to optimize multiplex urine biomarker tests for more accurate detection of PCa [110]. Urinary calgranulin B/MRP-14 [109], alpha methylacyl coenzyme A racemase (AMACR), and transcripts for GSTP-1 [111] and PCA3 (DD3) [112] were identified as potential novel markers for PCa. A PubMed-based search on studies of urinary markers for prostate cancer published since 1985 onwards emphasized further work is needed to identify and validate 'signature markers' indicative of prostatic malignancy [113]. In the past years, the investigation of prostate cancer tissue specimens was more and more focused on biomarker discovery and understanding of the cancer pathophysiology. Most studies were performed on surgically obtained materials [114,115] and preparation of homogenous samples for protein analysis is necessary. Recent developments such as automated high throughput laser capture microdissection (LCM) allow sampling of homogenous cell populations for biomarker discovery [116-118]. The protein expression profiling studies have been carried out on both formalin-fixed paraffin-embedded (FFPE), ethanol fixed paraffin embedded tissues and radical prostatectomy specimens and detected altered protein patterns [119,120]. Also 2-DE studies were performed with snap frozen or fresh prostate tissue blocks [115,121,122]. However, proteomic studies on PCa identified a lot of differentially expressed proteins and some were reported as potential markers but clinical application of these markers is mostly missing [123-127].

Alternative to the analysis of tissue specimens, body fluids such as blood can be analyzed which may provide means to overcome tissue sampling. Blood is expected to be rich source of novel PCa specifc biomarkers and improve accurate diagnosis and prognosis of the disease and its progression. Early prostate cancer antigen (EPAC), a nuclear matrix protein, has been identified as a novel PCa marker in blood [69,70]. Instead of single marker allowing diagnosis, a panel of markers can be identified by serum SELDI profiles [128]. Another alternative to tissue, urine and blood, seminal plasma might be the original source of markers for prostatic malignancy [129,130]. However, seminal plasma has not yet received much attention for biomarker discovery. Although Pilch et al. reported a large-scale proteomic analysis of seminal plasma [130], to the best of my knowledge, there is no report available dealing with the detection of novel seminal markers for PCa.

Prostate needle biopsies are gold standard for diagnosing prostate cancer that enables a more direct and complete molecular characterization of prostate cancer. To date, not much attention is focused on prostate biopsies for the investigation of biomarkers. Proteomic analysis of prostate biopsies would enable biomarker investigations of pathologically characterized clinical samples. In this thesis, we have drawn our attention towards proteomic analysis of prostate biopsies. Recently, in parallel to our report [131], proteomic data on prostate biopsies has been reported [132].

There are many reports assessing different proteins for their potential in PCa diagnosis and their role in PCa malignancy. Although there are several promising marker candidates available, the majority of these need further validation. However, it is clear that study design for proteomic analysis of clinical samples is very important to enable to find appropriate proteins associated with disease progression. Mischak et al. reported a set of guide lines for clinical proteomic studies [133]. Advances in proteomics technology provide an excellent opportunity to characterize the modified or unmodified proteins, involved in tumorigenesis and cancer progression. Further, the functional characterization of the potential target proteins may provide useful information to understand the molecular insight of cancer progression which may help to develop new therapeutic strategies.

1.7 Caspases in prostate cancer

It is well known that tissue homeostasis in the normal prostate gland (as in most other organs) is maintained by the quantitative relationship between the rate of cell proliferation and the rate of apoptotic cell death [134,135]. Thus, apoptosis plays an important role in the development of the prostate and in the normal process of prostatic glandular self-renewal. Consequently, dysregulation of apoptosis could represent an important mechanism of prostate carcinogenesis.

The most prominent executioners of apoptosis are represented by the family of caspases comprising initiator (caspases-1, -2, -4, -5, -8, -9 and -10) and effector caspases (caspases-3, -6, and -7) [136,137]. Caspases are cysteine proteases and synthesized as inactive proenzymes [138]. On activation (cleavage), effector caspases can cleave a broad range of intracellular targets and thus leads to apoptosis. Activation of caspases and initiation of different apoptotic pathways depends on the cell type [139]. In a few cell type's, the active caspase-8 activates executioners such as caspases-3, -6 and -7 in a mitochondrial independent manner. In contrast, in other cell types apoptosis involves mitochondrial death signals mediated by Bcl-2 family proteins. Here, active caspase-8 cleaves Bid into a tBid (truncated form of Bid) that translocates to the mitochondria, promoting the release of cytochrome *c* into the cytosol [140]. This, in turn leads to the formation of the apoptosome and subsequently to the activation of caspase-3. Caspase-1 (known as interleukin-1β-converting enzyme) is also required for apoptosis [141] and Caspase-9 activity is dependent on cytosolic factors [142]. Cytochrome *c* release from mitochondria initiates activation of caspase-9 which subsequently activates caspase-3 as an important executioner of apoptosis [143,144]. Caspase-6 as an important effector caspase can activate caspase-3 that results in apoptosis. The Bcl-2 gene product is a potent inhibitor of apoptosis, since it stabilizes the mitochondrial membrane and blocks the release of cytochrome *c*. In turn, cytochrome *c* can bind to caspase-9 which triggers the activation of caspase-3 [145,146]. Taken together, a variety of proteins e.g. caspases and members of the Bcl-2 family are involved in tissue homeostasis but there is only sparse information on the role of caspases in PCa.

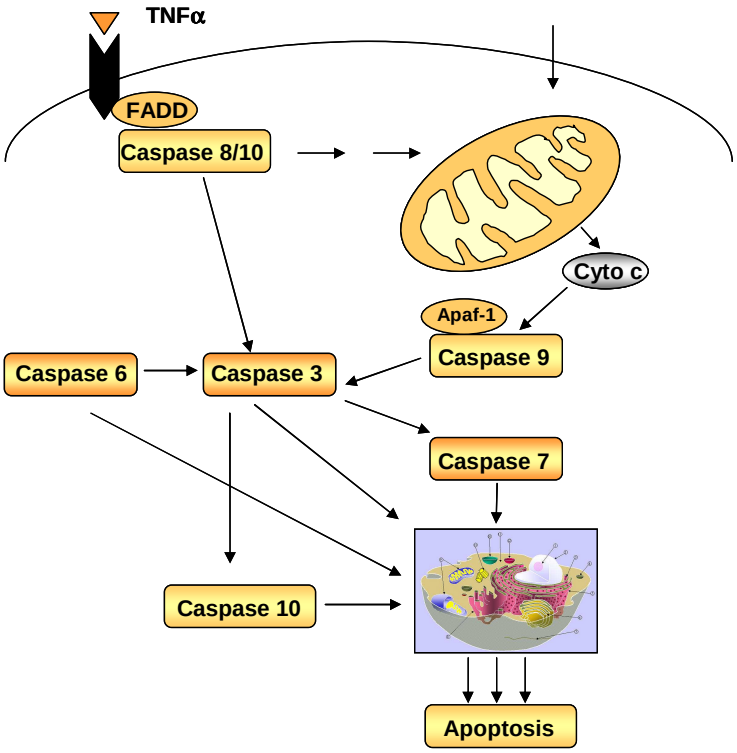

Figure 8: Extrinsic and intrinsic pathways involved in activation of caspase cascade for apoptosis.

Aims of the study

- **Optimization of the two-dimensional gel electrophoresis for proteome analysis of prostate biopsies.**

- **Generation of proteome maps of PCa and BPH tissue from biopsy specimens.**

- **Identification of differentially expressed proteins in prostate biopsies (PCa versus BPH)**

- **Functional characterization of altered proteins using, cell culture models to evaluate potential candidates for diagnosis, prognosis and therapeutical targets**

2 Materials and methods

2.1 Materials

2.1.1 Instruments

Equipment	Company
2-DE equipment	Bio-Rad/GE Healthcare
3D Rocking Platform STR 9	Stuart scientific
Rolling incubator	Karl Hecht
Agarose gel electrophoresis apparatus	Armin Baack
Autocool/Autogene II	Grant
Bead mill	Sartorious
BioPhotometer	Eppendorf
Centrifuge 5415 R	Eppendorf
Centrifuge GR422	Jouan
Centrifuge KR22i	Jouan
Centrifuge MR 1822	Jouan
CO_2-Incubator US Autoflow	Nuaire
Combs	Bio-Rad, Owl
Cover glasses	Marienfeld/Roth
Disposable cuvette	Plastibrand
Electroblotter	Owl
Electrophoresis Power Supply E833	Consort
FACS Calibur™ System	BD Biosciences
Filter Whatman paper	Schleicher & Schuell
Half micro cuvettes	Greiner, Nunc.
Haptotactic migration plates	Costar
Heating block	Grant
IPG Phor	GE Healthcare
Image Station 440CF	Kodak
Incubation chamber B15	Heraeus
Inverse microscopy (Televal 3)	Carl-Zeiss-Jena
Laminar air flow bench	Biohit
LightCycler 480	Roche
Luminometer Centro-LB 960	Berthold Technologies
4800 MALDI TOF/TOF™ Analyzer	Applied Biosytems
Mastercycler® ep *realplex*	Eppendorf

Microscope IX-70 (with fluorescence equipment)	Olympus
Microscope BX-50	Olympus
Microtome for sectioning of paraffin blocks	Leica microsystems
Microwave	Micromaxx
Master cycler	Eppendorf
MS1 mini Shaker	IKRR
Multi Temp III	Pharmacia Biotech
Nitrocellulose membrane Protran®	Whatman
Nuc Trap® columns	Stratagene
Tube Falcon (15 ml, 50 ml)	Greiner, Nunc.
pH meter	Orion
Power PACK P25	Biometra
Precision balance AC210S Analytic	Sartorius
PP tube (13 ml)	Sarstedt
Reaction containers (1.5 ml, 2.0 ml)	Greiner, Nunc.
Scanner (FS-700 laser densitometer)	Bio-Rad
SDS-PAGE apparatus (Mini and Midi gel)	Biometra
Shaker innova™ 4330	New Brunswick Scientific
Microscopic slides	R.Langenbrinck
Spectrophotometer	Pharmacia Biotech
Spot cutter (Proteome Works TM)	Bio-Rad
Spot Handling Workstation Ettan	GE Healthcare
Sterile aids of the cell culture	Greiner, Nunc.
Sterile filters milli pore	Schleicher & Schuell
Table top centrifuge	Eppendorf
Thermo mixer compact	Eppendorf
Tissue homogenizer	OMNI International
Unipack 250 (Power Supply)	Uniequip
UV-light TFL-20M	Biometra
Vortex mixer	Janke & Kunkel

2.1.2 Chemicals

Chemicals	**Manufracturers**
6-aminohexanoic acid	Sigma
Acetic acid	Roth

Acetone	Laborchemie Apolda
Agarose	Invitrogen
Agarose peq Gold Universal	Peqlab
Adenosine triphosphate (ATP)	Boehringer Mannheim
Ammonium persulphate	GibcoBRL
Bromophenol blue	Phamacia
Bovine serum albumin (BSA), 100x stock solution	New England Biolabs
Bovine serum albumin (BSA), Fraction V	Roth
Calcium chloride ($CaCl_2$)	Sigma
CHAPS	Roth
Chloroform/Isoamylalcohol	Roth
Coomassie brilliant blue G-250	FERAK
Coomassie brilliant blue R-250	FERAK
Cover fluid	GE Healthcare
D-Glucose	Merck
Diaminobenzidine	Sigma
DEPC	Roth
Dimethyl formamide	Roth
DMSO	Roth/Sigma
dNTPs	Roth/Fermantas
DHT	Sigma
Dihexyloxacarbocyanine iodide [$DiOC_6$]	Molecular probes
DTT	Roth/Merck
EDTA	GibcoBRL
EGTA	GibcoBRL
Ethanol	Roth
Ethidium bromide	Stratagene
FACS buffer	Invitrogen
Formaldehyde	Merck
Glutamine	GibcoBRL
Glutathione (reduced)	Sigma
Glycerol	Sigma
Glycine	Roth
Guanidinium chloride	GibcoBRL
HEPES	Sigma
H_2O_2	Roth

Isopropanol	Merck
IPTG	Sigma
2-Mercaptoethanol	Merck
Methanol	Roth
MOPS	Roth
MTT	Sigma
Neo mount	Merck
Saponin	Sigma
Sodium bicarbonate (Na_2HCO_3)	Laborchemie Apolda
Sodium chloride (NaCl)	Roth
Sodium dihydrogenphosphate	Laborchemie Apolda
Sodium dodecyl sulphate (SDS)	Roth
Sodium hydroxide (NaOH)	Chemapol, Lachema
Sodium pyruvate	PAA
Sodium pyrophosphate	Sigma
Paraformaldehyde	Merck
PMSF	Sigma
Ponceau S	Serva
Phosphoric acid	Roth
Potassium acetate	Laborchemie Apolda
Potassium chloride (KCl)	Merck
Potassium hydrogen phosphate	Sigma
TEMED	Jena pharm
Tris	Roth
Triton X-100	FERAK
Tween 20	Sigma
Water (MS grade)	JT Baker

2.1.3 Kits and solutions ready to use

Biocarta detection sytem for immunohistochemistry	Biocarta
Roti®-Blue	Roth
Complete™ Mini Protease inhibitor	Roche
DAKO® Fluorescent Mounting medium	Dako
DNA-ladders	New England Biolabs
Dual Luciferase™ Reporter Assay system	Promega

Glutathione Sepharose™ 4 B	GE Healthcare
IPG buffer	GE Healthcare
IPG strips	GE Healthcare
Lipofectamine™ 2000	Invitrogen
LumiGlo Reagent A (20x) and Peroxide B (20x)	Cell Signaling
M-MLV RTase	Promega
PageRuler, prestained protein marker	Fermentas
PeqGOLD plasmid miniprep	Peqlab
PeqGOLD gel extraction kit	Peqlab
Protein G Sepharose™ 4 Fast Flow	Pharmacia
QIAprep Spin Plasmid Maxiprep Kit	QIAGEN
QIAquick PCR-purification Kit	QIAGEN
QIAquick Gel-extraction Kit	QIAGEN
real MasterMix for SYBR® Green	Eppendorf
SYPRO® Ruby	Bio-Rad
X-ray film	Agfa
X-rayfilm-developer, -fixer	Agfa
Roti®-Block	Roth
Rotiphorese® Gel 30	Roth
Reverse Transcription reagents	Promega
TRIZOL Reagent	Invitrogen
Trypsin MS grade	Promega

2.1.4 Enzymes and inhibitors

T4-polynuclotide kinase (PNKinase)	New England Biolabs
Pwo-DNA polymerase	Peqlab
Restriction enzymes	New England Biolabs
RNasin	Promega
Shrimp alkaline phosphatase (SAP)	Fermentas
T4- DNA-Ligase	Fermentas
Taq-DNA-Polymerase	Invitrogen/Peqlab
Trypsin EDTA	PAA Laboratories
Soyabean trypisn inhibitor	PAA Laboratories

2.1.5 Antibodies

Primary antibodies:	
Anti-cyt-c antibody, polyclonal rabbit	Santa Cruz Biotechnology
Anti-Flag M2 antibody, monoclonal mouse	Sigma
Anti-GFP antibody, monoclonal mouse	Roche
Anti-GAPDH antibody, monoclonal mouse	Abcam
Anti-AKT antibody, polyclonal rabbit	Cell Signaling
Anti-phospho AKT Ser473antibody, polyclonal, mouse	Cell Signaling
Anti-Prx-1 antibody, polyclonal, rabbit	LabFrontier
Anti-Prohibitin antibody, polyclonal, mouse	Abcam
Anti-Caspase 3	Cell Signalling
Anti-Caspase 1	Acris
Anti-Caspase 9	Santa Cruz Biotechnology
Anti-Caspase 6	Cell Signalling
Anti-Caspase 3 cleavced	Cell Signalling
Anti-Caspase 6 cleaved	Cell Signalling
Anti-Bcl-2	Biosource
Secondary antibodies:	
Anti mouse IgG HRP-linked antibody	Cell Signaling
Anti rabbit IgG HRP-linked antibody	Cell Signaling
Anti rabbit Cy^{TM}2 green antibody	Dianova
Anti mouse Cy^{TM}3 red antibody	Dianova

2.1.6 Cell lines and materials used in cell culture

Cell lines/Reagents	**Suppliers**
LNCaP prostate cancer cell line	DSMZ
MCF-7 breast cancer cell line	DSMZ
100x penicillin/streptomycin	PAA Laboratories
10x Trypsin soyabean inhibitor	PAA Laboratories
10x Trypsine/EDTA	PAA Laboratories
FCS	Hyclone
Glucose solution 40% sterile	Braun

HEPES 1M sterile	PAN Biotech
OptiMEM	GibcoBRL
RPMI-1640	GibcoBRL
Sodium pyruvate 100 mM sterile	PAA Laboratories
Sodium bicarbonate	Sigma

2.1.7 Microbial cultures and culture medium used

***E.coli* strains**	**Genotype**	**Suppliers**
E.coli BL21 codon plus	F– *ompT hsdS*(r_B– m_B–) *dcm*+ Tet^r *gal l* (DE3) *endA* Hte *[argU proL* Cam^r]	Stratagene
E.coli XL1-Blue	recA1 endA1 gyrA96 thi-1 hsdR17 supE44 relA1 lac [F proAB $lacI^qZ\Delta M15$ Tn10 (Tet^r)]	Stratagene

Agar Noble	GibcoBRL
Bacto-yeast extract	DIFCO Laboratories
Bacto-tryptone	Roth
Ampicillin (50 mg/ml)	Roth
Kanamycin (30 mg/ml)	Roth
Tetracyclin (50 mg/ml)	Invitrogen
LB medium	10 g tryptone 5 g yeast extract 5 g NaCl dissolved in 1 liter of dd H_2O and pH adjusted to 7.5 with NaOH Sterilized in autoclave
LB-agar medium	15 g Agar Noble dissolved in 1 liter of dd H_2O and sterilized in autoclave

2.1.8 Primers

2.1.8.1 Primer sequences for RT and real-time PCR

TPD52 sense: 5’ –GAGGAAGGAGAAGATGTTGC- 3’,

TPD52 antisense: 5’ -GCCGAATTCAAGACTTCTCC -3’

Prohibitin sense: 5’ –GTGGAGTGCAGGACATTGTG -3’,

Prohibitin antisense: 5’ –TGAGTTGGCAATCAGCTCAG -3’,

RPLP0 sense: 5’ –TTGTGTTCACCAAGGAGGAC -3’,

RPLP0 antisense: 5’ –GACTCTTCCTTGGCTTCAAC -3’

2.1.8.2 Oligonucleotides for cloning

pEGFP-N3-TPD52

Forward 5’ –GCTA**CTCGAG**CCATGGACCGCGGCGAGCAAGGT -3’

Reverse 5’ –CACTT**GGTACC**CAGGCTCTCCTGTGTCTTTTC -3’

psiCHECK™2-TPD52

Forward 5’ –GCTA**CTCGAG**CCATGGACCGCGGCGAGCAAGGT -3’

Reverse 5’ –CACTT**GCGGCCGC**TCACAGGCTCTCCTGTGTCTT -3’

pFLAG-CMV-1-TPD52

Forward 5’ –GCTA**GCGGCCGC**ATGGACCGCGGCGAGCAAGGT -3’

Reverse 5’ –CACTT**GGATCC**CAGGCTCTCCTGTGTCTTTT-3’

pGEX-6P1-TPD52

Forward 5’ - GCTA**GGATCC**ATGGACCGCGGCGAGCAAGGT - 3’

Reverse 5’-CACTT**GCGGCCGC**TCACAGGCTCTCCTGTGTCTTTTC-3’

pETM-11-TPD52

Forward 5’ - GCTA**CCATGGC**CATGGACCGCGGCGAGCAAGGT - 3’

Reverse 5’- CACTT**GGATCC**TCACAGGCTCTCCTGTGTCTTTTC-3’

- Restriction sites highlighted in bold

2.1.8.3 shRNA sequences cloned in to pSUPER-neo-gfp RNAi system

Forward (204)	5'–GATCCCCGCGGAAACTTGGAATCAATTTCAAGAGAAT TGATTCCAAGTTTCCGCTTTTTA –3'
Reverse (204)	5'–AGCTTAAAAAGCGGAAACTTGGAATCAATTCTCTTGA AATTGATTCCAAGTTTCCGCGGG –3'
Forward (350)	5'-GATCCCCGTTGGCTCAGTCATCACCAATTCAAGAGATT GGTGATGACTGAGCCAACTTTTTA –3'
Reverse (350)	5'-AGCTTAAAAAGTTGGCTCAGTCATCACCAATCTCTTGA ATTGGTGATGACTGAGCCAACGGG –3'
Forward (103)	5'–GATCCCCGAGCAGGAAGAGCTAAGAATTCAAGAGATT CTTAGCTCTTCCTGCTCTTTTTA –3'
Reverse (103)	5'–AGCTTAAAAAGAGCAGGAAGAGCTAAGAATCTCTTGA ATTCTTAGCTCTTCCTGCTCGGG –3'

2.1.8.4 Sequencing primers

T3 Primer	5'-CTTTAGTGAGGGTTAAT-3'
pEGFP-N3-For	5'-ACGGTGGGAGGTCTATATAA-3'
pEGFP-N3-Rev	5'-ACCACCCCGGTGAACAGCTC-3'

2.2 Plasmids

2.2.1 pEGFP-N3 (Clontech) and its derivative

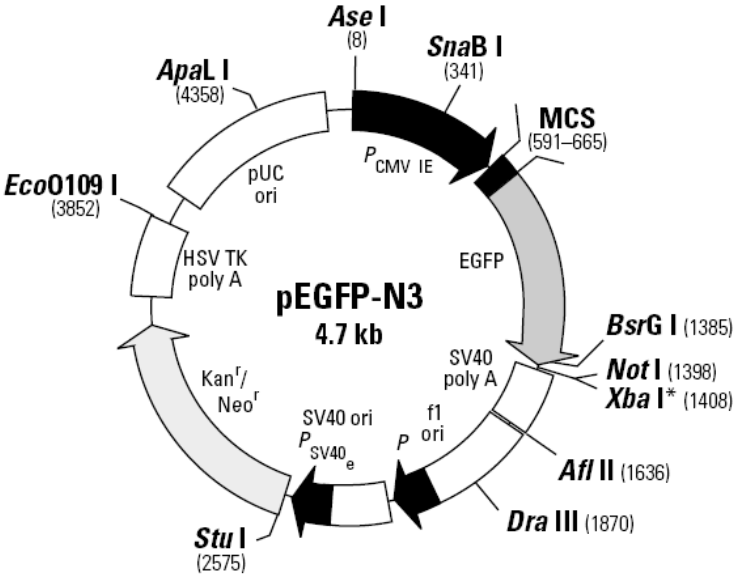

Multiple cloning site:

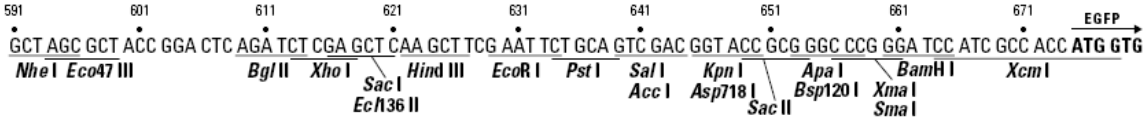

pEGFP-N3: It encodes a mutant GFP which has been optimized for brighter fluorescence and higher expression in mammalian cells. The MCS in pEGFP-N3 is in between the promoter of CMV and the EGFP coding sequences. Genes cloned into the MCS will be expressed as fusions to the N-terminus of EGFP. Fusions to the N-terminus of EGFP retain the fluorescent properties of the native protein allowing the localization of the fusion protein *in vivo*. Presence of antibiotic resistance to Neomycin/G418 provides an opportunity to make, stable transformants for EGFP fusion protein expression.

pEGFP-N3-TPD52: The gene encoding for TPD52 (isoform 3) amplified from cDNA derived from LNCaP total RNA amplified in PCR and cloned between *XhoI and Kpn1* cleavage sites in MCS.

2.2.2 pSuper.neo.gfp (Oligo Engine) and its derivative

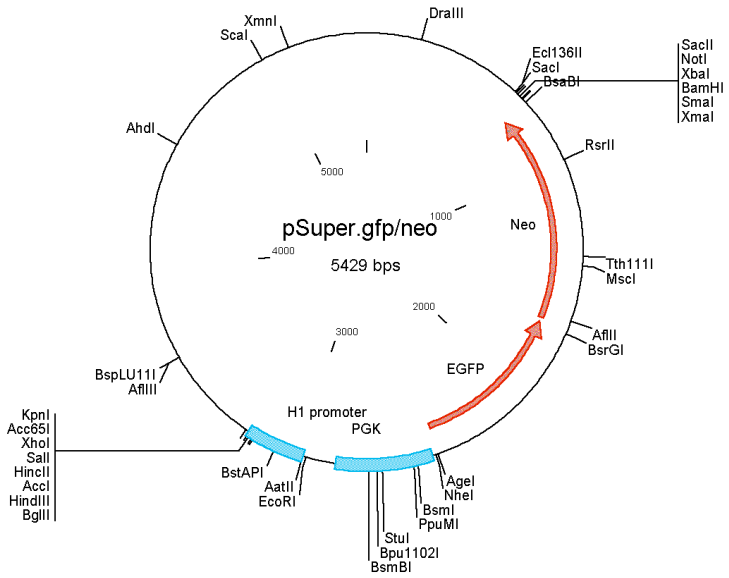

pSuper.neo.gfp: This expression vector uses the polymerase-III H1-RNA gene promoter, as it produces small RNA transcripts without a poly(A) tail. The transcripts have transcriptional start site and a termination signal consisting of five thymidine residues. The recombinant vector can produce transcripts which can fold back to form short hairpin loop like structures. The short hairpin loop precursor transcript is quickly cleaved to produce functional siRNA in cells to degrade target mRNA. Presence of antibiotic resistance to aminoglycoside Neomycin provides an opportunity to make stable clones for down regulation of protein of interest and to overcome problems of tranfection efficiency.

pSuper.neo.gfp-shTPD52: The forward and reverse oligonucleotides of shRNA(204), shRNA(350) and shRNA(103) hybridized to form double strands and cloned into vector between *BglII* and *HindIII* restriction site in MCS.

2.2.3 psiCHECK-2 (Promega) and derivative

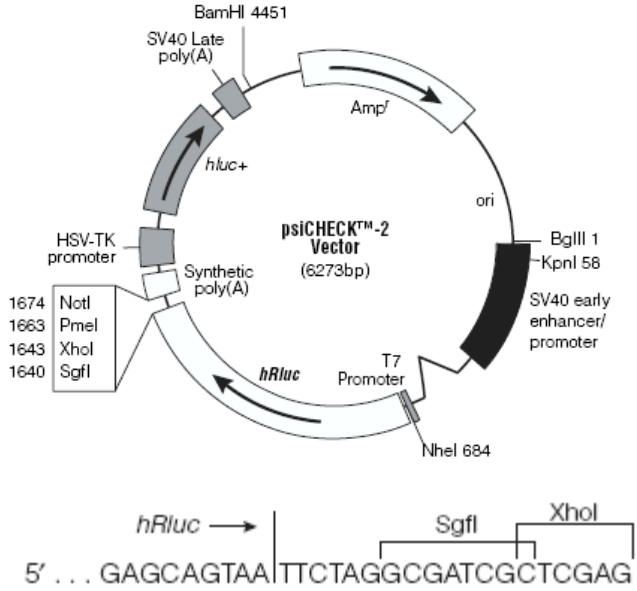

Multiple cloning site:

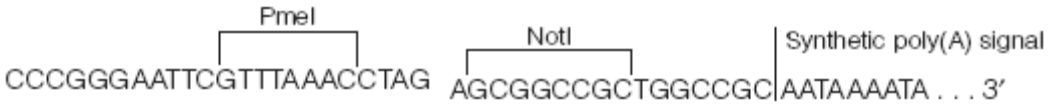

psiCHECK-2: The siCHECK vectors uses SV40 promoter for expression of *Renilla* luciferase as primary reporter gene. Also it consists of synthetic firefly luciferase for intraplasmid normalization of transfection. The target gene is cloned at 3´ *Renilla* luciferase gene and the recombinant vector is co-transfected and vectors expressing potential shRNA or siRNA in to cells. If a specific shRNA/siRNA binds to the target mRNA and initiates the RNAi process, the mRNA of *Renilla* luciferase fused with gene of interest will be cleaved and subsequently degraded, decreasing the *Renilla* luciferase signal.

psiCHECK-2.TPD52: The cDNA coding for TPD52 amplified using specific oligonucleotide primers in PCR and inserted between *Not1* and *Xho1* restriction sites in MCS.

2.2.4 pGEX-6P-1 and derivative

Multiple cloning site:

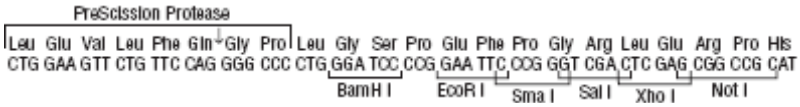

pGEX-6P-1: In pGEX vectors the protein expression is under the control of the *tac* promoter, which is induced by the lactose analog isopropyl β-D thiogalactoside (IPTG). All pGEX vectors are also engineered with an internal *lac*Iq gene. The *lac*Iq gene product is a repressor protein that binds to the operator region of the *tac* promoter, preventing expression until induction by IPTG, thus maintaining a tight control over the expression of the insert. pGEX-6P PreScission Protease vectors offer the most efficient method for cleavage and purification of GST fusion proteins. The GST fusion system has been used successfully in many applications including molecular immunology, the production of vaccines, protein-protein interactions and DNA-protein interactions.

pGEX-6P-1-TPD52: The derivative of original vector for GST-TPD52 fusion protein expression was generated by insertion of TPD52 cDNA between *BamHI* and *Not1* restriction sites in MCS.

2.2.5 pCMV-Tag 1 and derivative

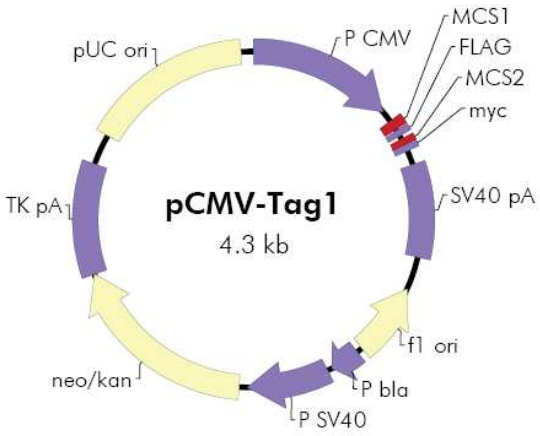

Multiple cloning site:

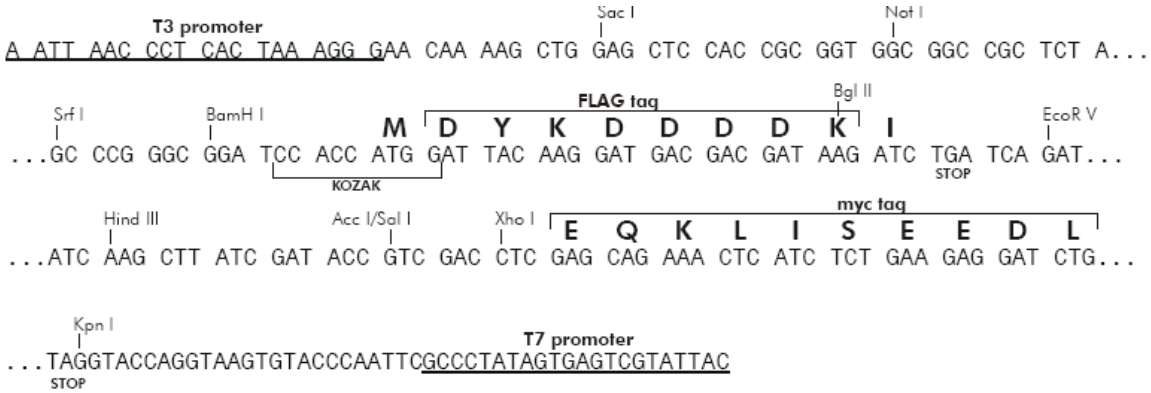

pCMV-Tag 1: It is an epitope tagging vector designed for gene expression in mammalian cells. A target gene inserted into the pCMVTag1 vector can be tagged with the FLAG® epitope (N-terminal, C-terminal, or internal tagging), the c-myc epitope (C-terminal) or both the FLAG (N-terminal) and c-myc (C-terminal) epitopes. Tagged constructs generated in the pCMV-Tag 1 vector can be transfected into mammalian cells. Hence the tagged gene product can be easily characterized using commercially available tag-specific antibodies. Epitope tagging can be used to localize gene products in living cells, identify associated proteins, track the movement of fusion proteins within the cell, or characterize new proteins by immunoprecipitation.

pCMV-Tag 1-TPD52: This derivative was generated by inserting TPD52 cDNA between *Not1* and *BamHI* restriction sites to generate N-terminal tag to TPD52 and further used to study immunofluorescence and immunoprecipitation.

2.2.6 pETM-11 and its derivative

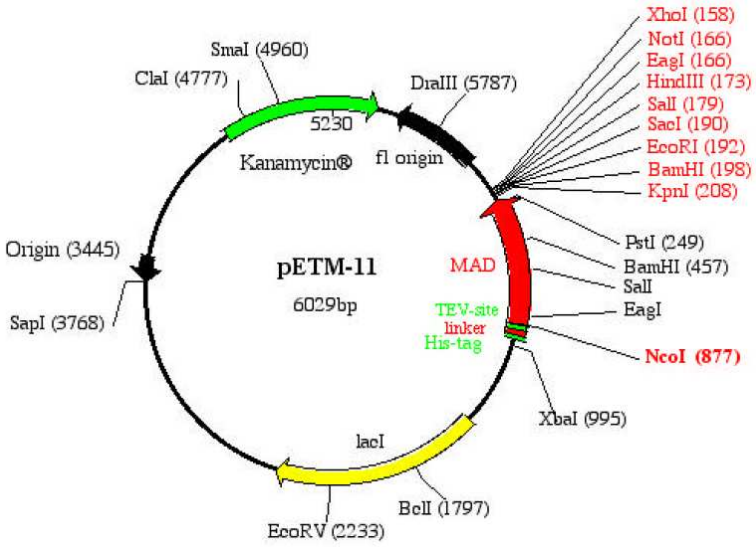

Multiple cloning site:

```
                                        TEV site          NcoI
ATGAGCGATTACGACATCCCCACTACTGAGAATCTTTATTTTCAG GGCGCCATGGCGGCG
TACTCGCTAATGCTGTAGGGGTGATGACTCTTAGAAATAAAAGTC CCGCGGTACCGCCGC
MetSerAspTyrAspIleProThrThrGluAsnLeuTyrPheGln|GlyAlaMETAlaAla

GCGGTTCGGATGAAC..612bp..GACAGTCACAAGGCGTGTCTTGGTCTCTAACTAGTG
CGCCAAGCCTACTTG...MAD...CTGTCAGTGTTCCGCACAGAACCAGAGATTGATCAC
AlaValArgMetAsn..204aa..AspSerHisLysAlaCysLeuGlyLeu***

                                        NotI
      BamHI        SacI                 EagI
KpnI         EcoRI         SalI HindIII         XhoI   His-tag
GTACCGGATCCGAATTCGAGCTCCGTCGACAAGCTTGCGGCCGCACTCGAGCACCACCAC
CATGGCCTAGGCTTAAGCTCGAGGCAGCTGTTCGAACGCCGGCGTGAGCTCGTGGTGGTG
                                                  HisHisHis
```

pETM-11: In pET vectors the protein expression is under the control of the *lac* promoter, which is induced by the lactose analog isopropyl β-D thiogalactoside (IPTG). The pETM-11 sytem produce an N-terminal histidine $(His)_6$ tagged protein and most efficient method for purification of recombinant proteins using metal chelate affinity chromatography. The TEV protease specific amino acid site between tag and protein facilitates to cleave $(His)_6$ tag from protein of during or after purification.

pETM-11-TPD52 derivative: The derivative of original vector for $(His)_6$-TPD52 fusion protein expression was generated by insertion of TPD52 cDNA between *NcoI* and *NotI* restriction sites in MCS.

2.3 Methods

2.3.1 Clinical Samples

Tissue samples and patient data were obtained after informed consent. The study was approved by the local ethics committee of the University of Greifswald and performed in accordance with the declaration of Helsinki.

A total of 13 biopsies have been collected from each patient with elevated PSA value by the Clinic of Urology, University of Greifswald, Germany. From these, twelve have been used for pathological evaluation and one randomly chosen biopsy from each patient was snap frozen. The histopathological investigation including H&E staining was assessed by two experienced pathologists from the Department of Pathology, University of Greifswald, Germany. Based on 12 biopsies the pathology report showed that at least 3 biopsies were scored as cancer positive. After pathological evaluation 23 patients (12 PCa, 11 BPH) were selected. The serum PSA levels of these patients were determined and all patients had a range between 4.7 to 14.7 ng/ml (Mean PSA value = 8.21 ng/ml). The mean age of the selected patients was between 50-79 years (Mean age = 64.78 years) and Gleason score between 2 to 7 (Mean score = 4.16). To verify proteomic data by immunohistochemistry the Department of Pathology, University of Greifswald, Germany provided 21 paraffin-embedded radical prostatectomized specimens.

2.3.2 Cell culture

The Prostate carcinoma cell line LNCaP was purchased from DSMZ and maintained in RPMI1640 (Invitrogen, Germany) supplemented with 10% FCS, 100 units/ml penicillin and streptomycin, 4.5 g/L glucose, 1 mM sodium pyruvate, 1.5 g/L sodium bicarbonate and 10 mM HEPES. Cells were grown in an incubator at 37°C with constant supply of 5% CO_2 and split after reaching 85 to 90% confluence. To split cells from culture bottles, the medium was discarded and cells were washed with PBS (1×) and incubated with an appropriate volume of 2× Trypsin/EDTA for 2 min at 37°C. The trypsin activity was neutralized by adding 10 ml of medium containing FCS. Followed by centrifugation (1500 rpm, 4°C for 4 min) cells were split according to the number. For freezing the cells, after trypsinization followed by centrifugation cells were resuspended in FCS containing 10% DMSO. The cell suspension was dispenced into cryo-vials placed in a cryo-freezing container filled with isopropanol and stored at -70°C for 24 hour and then stored in liquid

nitrogen. To revive cells from cryo-vials, the vial from liquid nitrogen was allowed to thaw at 37°C and diluted with culture medium. The cells were pelleted by centrifugation (1500 rpm, 4°C for 4 min), and supernatant was discarded. The cells were then resuspended in appropriate medium and seeded into a culture bottles. Cells were regularly tested for mycoplasma contamination using the MycoAlert™ Mycoplasma Detection Kit (Cambrex).

2.3.3 Preparation of protein extracts/RNA from cell lines

Isolation of total proteins or RNA for further analysis carried out in special lysis buffers depending on sample requirements in next experiments. For Luciferase assays cells were harvested in passive lysis buffer. To perform 2-DE or western blots proteins directly lysed in 2D lysis buffer or RIPA buffer for immunoprecipitations. The protein and RNA were prepared separately from same sample as mentioned in the section 2.3.2. In GST pulldown assays cells were lysed in lysis buffer containing protease inhibitor cocktail. All the buffers were prepared as mentioned bellow.

1x Lysis buffer (GST pulldown assay)	25 mM Tris-HCl pH 7.4 50 mM NaF 0.1 M NaCl 5 mM EGTA 1 mM EDTA 1% Triton X-100 10 mM Sodium pyrophosphate
Passive lysis buffer (Luciferase assay)	Promega Corporation
RIPA buffer (Immunoprecipitation)	50 mM Tris-HCl pH 7.5 150 mM NaCl 1% NP 40 and 0.1%SDS 0.5% Sodium-deoxycholate
2D Lysis buffer	8 M urea 2 M thiourea 4% CHAPS 40 mM Tris-base 65 mM DTT

2.3.4 Protein /RNA preparation from biopsies

Approximately, 6-10 mg of prostate biopsiy was homogenized in 0.5 ml of TRIzol® Reagent in a bead mill. 0.1 ml of chloroform was added to the homogenate which was mixed vigorously for 15 sec and incubated for 3 min at room temperature. The phases were separated by centrifugation at 12000×g for 15 min at 4°C. RNA remaining in the aqueous phase was precipitated with isopropanol and used for mRNA analysis in quantitative real time PCR. DNA remaining in the interphase layer and phenolic phase was recovered by ethanol precipitation and centrifugation at 2500×g for 5 min. Proteins in the supernatant were then precipitated by isopropanol (0.75 ml per 0.5 ml of TRIzol® Reagent used for initial homogenization) followed by centrifugation at 12000×g for 10 min at 4°C. After precipitation the protein pellet was washed extensively in 0.3 M guanidinium chloride in 95% ethanol followed by 100% ethanol [147,148]. Protein pellets were vacuum dried and resuspended directly in 2D lysis buffer. The protein concentration of the extracts was determined by a modified Bradford assay [149]. After dilution of 2 µl of tissue protein extract to 100 µl with 2-D lysis buffer and dd H_2O, 1.9 ml of reagent was added to each sample and incubated for 10 min in dark. Protein concentration was measured in spectrophotometer at 595nm using different concentration of BSA as a reference. Total RNA was stored in 70% ethanol at -20°C for real time PCR.

2.3.5 Two-dimensional gel electrophoresis (2-DE)

The first dimension Iso electric focussing was carried out by using 24 cm immobilized pH gradient dry strips (IPG) with a linear pH 4-7 gradient. For analytical gels 150 µg protein was filled up to 450 µl with rehydration buffer (8 M urea, 2 M thiourea, 2% CHAPS, 50 mM DTT) supplemented with 0.5% (v/v) IPG buffer pH 4-7. IPG strips were passively rehydrated overnight at 20°C. For preparative gels 650 µg of protein pooled from equal amounts of samples was used. Proteins were separated by the IPGphor unit using a programmed voltage gradient at 20°C with a current limit of 50 µA per strip for total of 50 kVh. After IEF, the IPG strips were equilibrated in buffer 1 (0.375 M Tris-HCl pH 8.8, 6 M urea, 20% glycerol, 2% SDS and 130 mM DTT) and buffer 2 (15 min each) containing 135 mM iodoacetamide instead of DTT.

Second dimension was performed in PROTEAN® Plus Dodeca™ Cell system. The equilibrated strips were applied to the top of 12.5% SDS-PAGE gels and sealed with 1%

agarose prepared in SDS-Tris-glycine buffer with traces of bromophenol blue as a tracking dye to monitor electrophoresis. Electrophoresis was performed with constant voltage (80V) at 20°C until the dye front reached the bottom of the gel. After electrophoresis analytical gels were fixed in 40% methanol, 10% acetic acid for 3 hrs with constant shaking, and washed in double distilled water 3 times (30 min) each. Gels were then covered with SYPRO® Ruby protein gel stain overnight in the dark with gentle agitation. After staining gels were washed with 10% methanol, 7% acetic acid to reduce the background fluorescence followed by double distilled water before imaging. Preparative gels were stained with Roti®-Blue, a colloidal coomassie brilliant blue G250 stain. Briefly, gels were fixed in 40% methanol, 15% acetic acid for at least 4 hrs and then immersed in colloidal staining solution overnight. To remove background staining gels were washed in 20 % methanol.

2.3.6 Imaging and analysis

SYPRO® Ruby stained gel images were scanned at 100-µm resolution using FS-700 molecular dynamics laser densitometer using PDQUEST software (Version 7.3.3 Basic Bio-Rad). Image analysis was carried out with PDQUEST 2-D analysis software package (Version 7.4, Bio-Rad). Gel images were compared as groups of BPH and PCa for consistent qualitative and quantitative differences. To ensure that variations in spot size and intensity between gels in the match set are due to differential expression, all gels were normalized using the total spots density normalization tool and changes in expression level were restricted to greater than 1.5fold.

2.3.7 Mass spectrometry

Preparation of peptide mixtures for MALDI-TOF-TOF - Protein identification was performed as described recently [150]. Briefly, proteins were excised from Colloidal Coomassie Brilliant Blue stained 2-DE gels using a spot cutter. Digestion with trypsin and subsequent spotting of peptide solutions onto the MALDI-targets were performed automatically in the Ettan Spot Handling Workstation. Gel pieces were washed 50 mM ammoniumbicarbonate/ 50% (v/v) methanol and with 75% (v/v) ACN. After drying trypsin solution containing 20 ng/µl trypsin in 20 mM ammoniumbicarbonate was added and incubated at 37°C for 120 min. For peptide extraction, gel pieces were covered with

50% (v/v) ACN / 0.1% (w/v) TFA and incubated for 30 min at 37°C. The peptide containing supernatant was transferred into a new micro plate and the extraction was repeated. The supernatants were pooled and dried completely at 40°C for 220 min. Peptides were dissolved in 0.5% (w/v) TFA / 50% (v/v) ACN and spotted on the MALDI-target. Then, matrix solution (50% (v/v) ACN / 0.5% (w/v) TFA) saturated with CHCA was added and mixed with the sample solution by aspirating the mixture five times. Prior to the measurement in the MALDI-TOF instrument, the samples were allowed to dry on the target 10 to 15 min.

MALDI-TOF-MS - The MALDI-TOF measurement of spotted peptide solutions was carried out on a 4800 MALDI TOF/TOF™ Analyzer. The spectra were recorded in reflector mode in a mass range from 800 to 3700 Da with an internal one-point-calibration on the autolytic fragment of trypsin (mono-isotopic $(M+H)^+$ m/z at 2211.104, signal/noise ≥10). Additionally MALDI-TOF-TOF analysis was performed for the 5 strongest peaks of the TOF-spectrum after subtraction of peaks corresponding to background or trypsin fragments. The internal calibration was automatically performed as one-point-calibration if the mono-isotopic arginine $(M+H)^+$ m/z at 175.119 or lysine $(M+H)^+$ m/z at 147.107 reached a signal to noise ratio (S/N) of at least 5. After calibration a combined database search of MS and MS/MS measurements was performed using the GPS Explorer software v3.5 (Applied Biosystems, Foster City, USA). Peak lists were compared with the SwissProt rel.49 restricted to human taxonomy or IPI human v3.12 database using the Mascot search engine 1.9 (Matrix Science Ltd, London, UK). Peptide mixtures that yielded at least twice a mowse score of at least 53 for SwissProt or at least 59 for IPI database results were regarded as positive identifications.

2.3.8 Sodium Dodecyl Sulfate-Poly Acrylamide Gel Electrophoresis (SDS-PAGE)

For protein and western blot analysis SDS-PAGE was performed. The SDS-PAGE gel consists of a stacking gel and a resolving gel. The resolution of proteins depends on the protein size and percentage of acrylamide. For casting the gel, the resolving gel was prepared as mentioned below and poured between two glass plates. To get even surface 2/3 (V/V) isopropanol and water was overlaid on top of the gel and allowed to stand at room temperature for polymerization. After polymerization the isopropanol was drained, the stacking gel solution was poured and a polypropylene comb was inserted to make wells for

sample loading. Further the gel was allowed to stand to polymerize stacking gel. To prepare samples, 10-30 µg of protein were mixed with 5 µl of 6x protein sample loading buffer (350 mM Tris-HCl pH 6.8, 10.3% SDS, 36% glycerol, 5% β-mercaptoethanol and a pinch of bromophenol blue) and filled up to 30 µl with ddH_2O. Prior to loading samples were boiled at 95°C for 4 min and kept on ice immediately. Then samples were loaded in the sample wells of the stacking gel. The electrophoresis was carried out in Tris-Glycine buffer (192 mM Glycine, 24.8 mM Tris and 0.1% SDS) for 15 min at 120 V till the proteins enter into resolving gel and further continued at 150 V till the tracking dye reached 5 mm above the bottom of the gel. Standard molecular weight makers were used along with samples to determine the MW of protein samples. The recipe for casting gels as mentioned in next page.

Components for 12% SDS-PAGE	Stacking solution / mini gel	Resolving solution / mini gel
Resolving gel buffer 1.5 M Tris-HCl, pH 8.8	---	2.5 ml
Stacking gel buffer 1.5 M Tris-HCl, pH 6.8	0.25 ml	---
Rotiphorese® Gel 30	0.8 ml	4.2 ml
dd H_2O	1.4 ml	3.1 ml
10 % (W/V) SDS	25 µl	100 µl
10 % (W/V) APS	25 µl	100 µl
TEMED	2.5 µl	5 µl

2.3.9 Western blotting

To perform western blot, protein extracts were separated on 12% SDS-PAGE and electrophoretically transfered onto the nitrocellulose membrane by semi-dry method. In semi-dry transfer Whatman filter papers (3 mm thick) and nitrocellulose membrane were pre cut according to size of the gel. Prior to transfer, the gel and three papers soaked in cathode buffer. The membrane and three papers were soaked in anode buffer. All pre soaked materials were placed in semi-dry transfer apparatus as shown figure 9 and blotting carried out with constant power supply (1 mA/cm^2 membrane) for 1 h.

Figure 9: The illustration showing set up for western blot to transfer proteins from acrylamide gels onto nitrocellulose membrane.

After protein transfer, membrane was stained with Ponceau S solution (0.2% Ponceau S in 3% Trichloroacetic acid) for 2 min to see efficiency of electrophoretic transfer. The membrane was destained in ddH_2O to visualize the protein bands and further destained with TBST (20 mM Tris, 138 mM NaCl, pH 7.6 and 0.1% Tween 20) for blotting. Blocking was carried out in 1× Rotiblock solution followed by incubating the membrane with primary antibody (diluted in 5% (W/V) BSA dissolved in TBST) overnight at 4°C. Excess antibodies were removed by washing with TBST. Incubation with secondary antibody conjugated to HRP (anti mouse or anti rabbit IgG) was done for 1 h at room temperature. After three washes the reaction was developed by the addititon of LumiGLO substrate. The emitted light was captured on X-ray film.

Anode buffer 1	Anode buffer 2	Cathode buffer
0.3 M Tris in 20% methanol	25mM Tris in 20% methanol	40 mM 6-aminohexanoic acid

To reprobe the Western blot membranes with another antibody, they were incubated with stripping buffer (50 mM Tris-HCl pH 6.8, 2% SDS and 50 mM DTT) at 50°C for 30 min. The membranes were then washed with TBST buffer (3×5 min) and blocking was carried out with blocking solution followed by incubating with primary antibody.

2.3.10 Histopathological evaluation

Formalin fixed prostatectomy specimens were dehydrated and embedded in paraffin according to standard protocols. The 5 µm paraffin sections were sliced and mounted on glass slides. The sections were incubated at 40°C overnight, deparaffinized using xylene (2×10 min), hydrated with a series of decreasing ethanol concentrations (96%, 80%, 70%, and 50% each 5 min) and finally with distilled water (2×5 min). The slides were immersed in hematoxylin for 5 min and flushed with running tap water for 10 min. After rinsing with dH_2O slides were placed in eosin for 10 min and then dehydrated with increasing alcohol series (80% (1×5 min), 96% (2×5 min) and absolute alcohol (1×5 min)) and neo clear. HE stained sections were mounted in neo mount. Histological diagnosis, Gleason grading of biopsies and radical prostatectomy sections was performed on hematoxylin and eosin (HE) stained paraffin sections prepared from the same patients included for proteomic analysis and immunohistochemistry [151,152]. Further histological grading of tumors confirmed by two experienced pathologists from the Department of pathology, University of Greifswald.

2.3.11 Immunohistochemistry

Formalin fixed prostatectomy specimens obtained from patients were dehydrated and embedded in paraffin according to standard protocols. The 5 µm paraffin sections were sliced and mounted on glass slides. The sections were prepared for deparaffinized and hydrated as described in section 2.3.8. Endogenous peroxidase activity was blocked by peroxydazed 1 for 5 min. Then samples were heated in the microwave oven for antigen retrieval (10 mM citrate buffer, pH 6.0, 20 min, 700W). Slides were allowed to cool in citrate buffer slowly. After washing (de-ionised water 1×5 min, PBS-buffer pH 7.4, 2×5 min) slides were incubated with blocking solution (10 min). Slides were washed with PBS (2×5 min) and incubated overnight with primary antibody at 4°C. After washing (PBS, 2×5 min) slides were incubated with secondary antibody (4plus Universal Immunoperoxidase detection system, Biocarta) followed by washing in PBS (2×5 min). Finally, the slides were incubated with Streptavidin-HRP solution (10 min), washed (PBS, 2×5 min) and bound antibody was visualized with 0.1% diaminobenzidine in PBS containing 0.01% H_2O_2 (5 min). Slides were counter stained with hematoxylin (1 min), washed in tap water (10 min), dehydrated and mounted in neo mount. Control reactions to

demonstrate specificity of antibody binding were done by omitting the primary antibody. Photographs were taken on a BX50 microscope equipped with a DP 10 digital camera.

2.3.12 Amplification of target genes by PCR

To clone cDNA of the genes of interest into different vectors requires a large number of copies. This can be achieved by amplification of specific region of DNA using PCR. In PCR, a thermostable DNA polymerase initiate and extend the synthesis of target DNA using two oligonucleotide primers complement to opposite strands that flanking the region of interest in cDNA template. The reaction conditions were optimized and performed to amplify specific targeted genes. The PCR products were checked on ethidium bromide-agarose gel electrophoresis. The reaction mixture and conditions for amplifications are mentioned in the following table. Conditions for PCR reactions were as follows: 1 cycle of 95°C for 2 min and 34 cycles of 95°C for 30 s, 60°C for 45 s and 72°C for 2 min (extension time 1 min/1 kb). For final extension step at 72°C for 5 min and hold at 4°C for 2 h. The PCR reaction mixture was prepared as mentioned in the following table.

Per each PCR reaction	Amount/Volume
cDNA /DNA template	2.5 µl /50-200 ng
10× buffer complete	5 µl
dNTPs (10 mM)	2 µl
For. and Rev.primer (10 µM)	2 µl each
Pwo-Taq polymerase	0.5 µl
ddH_2O	...
Total volume	50 µl

2.3.13 Restriction digestion of DNA

A restriction endonuclease is an enzyme that cuts double-stranded DNA. Restriction enzymes recognize a specific sequence typically four to twelve nucleotides and produce a double stranded cut in the DNA. The digestion reaction was set according to the amount and dilution of DNA for further applications. The digestion reaction mixture was prepared with required amount of DNA, suitable restriction enzyme buffer (10×), BSA (10×), restrction enzymes 2.5 to 10 units and ddH_2O. The reaction mixture was incubated at 37°C for 2 h. Digested DNA was analysed using agarose gel electrophoresis. For dephosphorylation of

vector, 2-4 U of the Shrimp alkaline phosphatase was added to the digestion mixture and further incubated for 1 h at 37°C. Finally linearized plasmids or restricted DNA were purified by agarose gel electrophoresis followed by gel extraction. The digestion reaction was set as mentioned in the following table.

Restriction digestion reaction	Amount/Volume
Circular vector/ PCR product	1 µg/ 10 µl
10× BSA	5 µl
Restriction enzymes mixture	2 µl
ddH_2O	...
Total	50 µl

2.3.14 Annealing and phosphorylation of oligonucleotides

Two complementary DNA oligos were hybridized to form a small double-stranded DNA sequence before cloning in to pSUPER-neo-gfp vector. The separate oligos (0.05 µM) were dissolved in 50 µl of sterile ddH_2O. The annealing reaction was performed by mixing 2 µl of each oligo together with 48 µl of annealing buffer (100 mM NaCl and 50 mM HEPES pH 7.4). For annealing, the mixture was incubated at 95°C for 4 min and then at 70°C for 10 min. The annealed oligos were allowed to cool down slowly to room temperature. For phosphorylation of oligos, annealed oligos were incubated with phosphorylation buffer at 37°C for 30 min. Further PNK kinase was heat inactivated by incubating at 70°C for 10 min.

Phosphorylation of oligos	Volume
Annealed oligos	5 µl
T4 ligase buffer (usually contain 1mM ATP)	2 µl
PNK kinase	1 µl
ddH_2O	12 µl
Total	20 µl

2.3.15 DNA ligation

Ligation reaction was carried out to insert dsDNA fragments of interest or shRNA oligos in to desired vectors. After isolation of restricted fragments or annealed oligos and

linearized vector ligation reaction mixture was prepared as mentioned below. Ligation reaction was performed at 22°C for 1 h and incubated at 65°C for further 15 min to inactivate ligase. The ligation reaction was set according to the following table.

Ligation reaction	Volume/amount
Restricted Vector	2-4 µl/ 1 µg
Restricted dsDNA	5-10 µl/ 100 ng
10× buffer for T4 ligase	2 µl
T4 ligase	2 µl
ddH_2O	...
Total	20 µl

2.3.16 Preparation of competent cells

A single colony of *E. coli* XL1blue strain was inoculated in 2 ml LB medium and grown for overnight. The overnight culture was diluted 100 fold in the LB medium and cultivated at 37°C with constant shaking (200 rpm) until cell density reached OD_{600} of 0.4 - 0.6 (approx. 3 h). The culture was kept on ice for 30 min and then centrifuged at 4000 rpm for 15 min at 4°C to harvest cells. The cell pellet was resuspended in 30 ml of RF1 buffer and incubated on ice for 2 h. The cells were pelleted again by centrifugation, resuspended in 8 ml of RF2 buffer and further incubated on ice for 15 min. Aliquots of 100/200 µl volume of the competent cells were transfered into a pre-chilled sterile microfuge tube further flash frozen in the liquid N_2. The competent cells were stored at -80°C for next use.

RF1 buffer	RF2 buffer	LB medium
75 mM KCl 50 mM KCH_3COOH 50 mM $MnCl_2$ 10 mM $CaCl_2$ 15% (v/v) Glycerol	10 mM MOPS 10 mM KCl 75 mM $CaCl_2$ 15% (v/v) Glycerol	As mentioned in materials section 2.1.7

2.3.17 Bacterial transformation

Heat shock transformation method is used to transform the bacteria with the recombinant plasmid DNA or ligation mixture. To transform bacteria, approximately 100 ng

plasmid DNA or the whole ligation mix was added to 100 µl freshly thawed competent cells and incubated for 20 min on ice. The complete mixture was subjected to heat shock at 42°C for 60 sec followed by incubation on ice for 2 min. Then 1 ml of LB medium with out antibiotics was added to the mixture and incubated at 37°C with constant shaking at 250 rpm. After 1 hr 250 µl of the culture applied (spread plate method) on LB agar plates containing appropriate antibiotics. The plates were incubated at 37°C overnight.

2.3.18 Screening for positive clones

Rapid screening for clones with plasmid containing foreign DNA fragment of interest was performed by colony PCR. The clones were inoculated into 0.5 ml of LB medium containing appropriate antibiotic and grown for 2 h. For a PCR reaction, 2 µl of the culture was used. PCR reaction performed under the similar conditions used for the amplification of the targeted gene from cDNA. The PCR mixtures were separated on 1% agarose gel electrophoresis and observed for the presence of interested amplified insert of known size. The positive clones containing amplified insert were used for the prepartion of minipreps for DNA sequncing. For screening of the clones expressing pSUPER-neo-gfp-sh RNA, restriction digestion was performed to see insert release of known size. The sequence of the cloned PCR fragment or shRNA was confirmed by DNA sequencing (Seqlab, Göttingen, Germany).

2.3.19 Preparation of glycerol stocks

20% glycerol stocks were prepared to store clones of interest for the future use. After confirmation of clones by DNA seqencing, recombinant plasmids were transformed into bacteria as dscribed in section 2.3.15. A single colony was inoculated in 2 ml of LB medium containing appropriate antibiotics and grown for 12-14 h. To prepare the stock, 800 µl of the culture was mixed with 200 µl of sterile 98% glycerol in a 1.5 ml tube, flash frozen in liquid N_2 and stored immediately at -80°C.

2.3.20 Transfection of cells

To transfect cell lines with recombinant or normal vectors Lipofectamine 2000™ a cationic liposome has been used. To perform transfections, appropriate number of cells was seeded into culture dishes and grown for 18 h to reach nearly 80% of confluency. The

transfection mixture was prepared as described by transfection reagent supplier. The necessary amount of DNA diluted in OptiMEM and Lipofectamine 2000™ also diluted in the equal volume of OptiMEM in seperately and incubated for 5 min at RT. The DNA to lipid ratio used was 1:1.5 (µg:µl). The diluted DNA and Lipofectamine were mixed in one tube and allowed to form DNA-liposomes complexes for 20 min at RT. For transfection DNA-liposome complexes were added drop wise on the surface of the medium in culture dishes. Then the cells were incubated at 37°C in CO_2 incubator.

2.3.21 Measurements of mRNA by semiquantitative or quantitative real time PCR

Semiquantitative RT-PCR or quantitative real time PCR for the measurement of transcripts for targeted proteins was performed. Briefly, RNA was isolated from the same biopsies that were used for the proteome analysis using TRIzol® Reagent according to the manufacturer's protocol. The cDNA was prepared by reverse transcription of 1 µg total RNA. The total RNA was mixed with oligo $(dT)_{15}$ primer and incubated at 70°C for 5 min then immediately transfer onto the ice. The contents were mixed with RT master mix containing M-MLV Reverse Transcriptase, buffer, RNase inhibitor and dNTPs. The complete RT reaction mixture was incubated at 42°C for 1 h and then the cDNA was denatured at 94°C for 5 min finally diluted to 100 µl with ddH_2O.

To measure transcripts of interest, primers were designed using OligoPerfect™ Designer (Invitrogen, Germany) and synthesized by Invitrogen, Germany. Semiquantitative RT-PCR was performed using the Mastercycler. The PCR for the target and house keeping gene was performed in parallel and the reaction mixture prepared as mentioned in following table. Conditions for RT PCR reaction were as follows: 1 cycle of 94°C for 3 min and 35 cycles of 94°C for 20 s, 60°C for 30 s and 72°C for 30 s. Final extension strp for 5 min at 72°C. At the end of the PCR 15 µl of each sample subjected to agarose gel electrophoresis for relative quantification of target gene expression.

Quantitative real time PCR was performed on the Mastercycler® ep *realplex* using SYBR Green kit. PCRs for the targeted and house keeping genes were performed in duplicates and mean relative expression levels were reported. Conditions for real time PCR reaction were as follows: 1 cycle of 94°C for 3 min and 40 cycles of 94°C for 20 s, 60°C for 30 s and 68°C for 30 s. At the end of the PCR samples were subjected to a melting analysis to confirm specificity of the amplicon. Relative quantification of target was estimated by software

based on $\Delta\Delta C_T$ method. Statistical tests of significance have been computed by a non-parametric two-tailed Mann Whitney test performed at the 95% confidence interval. The reaction mixtures were prepared to perform PCR as mentioned in the following table.

Reverse transcription reaction mixture		RT-PCR reaction mixture	
Total RNA	1 µg	cDNA	2.5 µg
Oligo-dT-primer (0.5 µg/µl)	1 µl	10× PCR buffer with $MgCl_2$	5 µl
add DEPC water to 13.5 µl		dNTP mix (10 mM)	1 µl
5× M-MLV RT buffer	4 µl	For primer (10 mM)	2 µl
dNTP mix (10 mM)	1 µl	Rev primer (10 mM)	2 µl
M-MLV Reverse Transcriptase	1 µl	Taqpolymerase	0.5 µl
RNasin	0.5 µl	Sterile ddH_2O	36 µl
Total reaction volume	20 µl	Total reaction volume	50 µl

Real-time PCR reaction mixture	
SYBR Green 20× in 2.5× buffer	9 µl
For. primer (1mM)	4µl
Rev. primer (1mM)	4 µl
Diluted cDNA	3 µl
Total volume	20 µl

2.3.22 Agarose gel electrophoresis

Agarose gel electophoresis has been used to separate and analyse dsDNA. After electrophoresis the DNA bands can be visualized by ethidium bromide staining. The resolution of DNA is dependent on DNA size and percentage of the gel. The gel was prepared by solubilizing the agarose in 1× TAE buffer (40 mM Tris-acetate, pH 8.3, 1 mM EDTA, pH 8.0) and boiling in a microwave oven. Agarose melted in TAE allowed to cool down to 60°C and the ethidium bromide (10 mg/ml dd H_2O) was added to a final concentration 0.5 µg/ml.Then the mixture poured into a gel platform fixed on flat surface with out any air bubbles. An appropriate comb was inserted to load samples onto gel. The DNA samples were prepared in 10× DNA loading buffer (0.2 mM EDTA, pH 8.0, 25 %

(w/v) sacharose, 0.25 % (w/v) bromophenol blue) to 1× and loaded onto the gel. The electrophoresis was performed in TAE buffer with constant current (80 mA) supply until the tracking dye reached 10 mm above the end of gel. The separated DNA was visualized under UV light and moleclar weight of the unknown bands compared with known marker included in samples.

Agarose gel (%)	Effective range of resolution of linear DNA fragments (kb)
0.5	30 to 1
0.7	12 to 0.8
1.0	10 to 0.5
1.2	7 to 0.4
1.5	3 to 0.2

2.3.23 Gel extraction of DNA

For cloning of restriction digested DNA fragments into desired vector, the restriction reaction mixture needs to be purified before ligation. To purify, the restricted DNA fragments were separated on ethidium bromide agarose gel and the interested bands were excised from gel by visualizing under UV-light. The DNA was extracted by using PeqGOLD gel extraction kit (Peq lab) according to the protocol mentioned by the manufacturer.

2.3.24 Isolation of plasmid DNA from bacteria

Minipreps were prepared by using PeqGOLD plasmid miniprep kit I. To prepare minipreps, a single colony of bacteria transformed with the plasmid was inoculated into 3 ml of LB medium with appropriate antibiotics and grown for 12-16 h. The cells were harvested by centrifugation at 10000×g for 5 min. From the pelleted cells plasmid was isolated according to the standard protocol mentioned by manufacturer. After elution, the concentration plasmid DNA was measured in spectrophototmeter by taking OD at 260nm.

For large scale isolation of plasmid DNA, QIAprep Spin Plasmid Maxiprep Kit was used. For maxiprep prepertion, first a single colony was inoculated in 3 ml of LB medium

with appropriate antibiotics and grown for 8 h, and then cultivated in 100 ml of same medium for overnight (12-16 h). Cultured bacteria were harvested by centrifugation at 4500 rpm for 15 min and plasmid DNA was isolated according to the standard protocol mentioned by manufacturer. Finally the DNA pellet was washed with 70% ethanol and dissolved in 300 µl of ddH_2O. Isolated plasmids were stored either at 4°C or –20°C.

2.3.25 Formaulas for calcultion of moleculr weight and concentration

MW of dsDNA = [number of basepairs] × [660 Da]

MW of ssDNA = [number of basepairs] × [330 Da]

MW of ssRNA = [number of basepairs] × [340 Da]

Concentration of DNA or RNA mg/ml = $A_{260} \times x\varepsilon \times f$

A_{260} = absorbance at 260 nm

$x\varepsilon$ = extinction coefficient

f = dilution factor

1 A_{260} unit of dsDNA = 50 µg/ml H_2O

1 A_{260} unit of ssDNA = 33 µg/ml H_2O

1 A_{260} unit of ssRNA = 40 µg/ml H_2O

2.3.26 Downregulation of TPD52

To downregulate TPD52 in LNCaP cells, we designed different shRNA pairs directed against three splice variants of TPD52 using oligoengine programme and synthesized by Invitrogen. shRNA oligos were annealed and phosphorylated as described in section 2.3.12 and cloned into pSUPER.neo-gfp vector between *BglII* and *HindIII* restriction sites. The inserted oligonucleotide sequences were confirmed by test digestion and also sequencing of recombinant vector with T3 sequencing primer. The shRNA expressing vectors were screened for their antisence activity using psiCHECK™2. This vector enables the monitoring of changes in expression of a target gene fused to the reporter gene *Renilla* luciferase. In psiCHECK™2-TPD52 the gene encoding for TPD52 was cloned into the multiple cloning region located down stream of the *Renilla* translational stop codon. Measurement of *Renilla luciferase* activity indicates RNAi effect. The two vectors

psiCHECK™2-TPD52 and pSUPER-neo-gfp-shRNA were co-transfected in 1:10 ratio into LNCaP cells. The luciferase activity was measured after 48 h using the Dual- Glo™ Luciferase Assay Sytem, In Luciferase assay firefly luciferase expression facilitates the determination of relative expression of reporter gene.

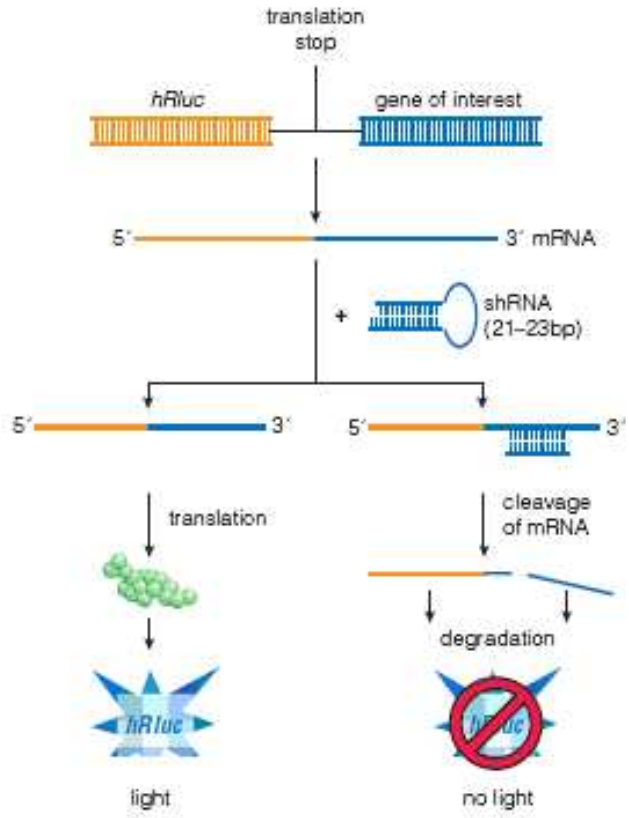

Figure 10: Mechanism of action of the siCHECK™ Vectors.

2.3.27 MTT assay for cell proliferation

The effect of TPD52 overexpression on proliferation of the prostate carcinoma cell line LNCaP was measured by the MTT (3-(4, 5-dimethylthiazol-2-yl)-2, 5-diphenyltetrazolium bromide) proliferation assay. In brief, 4×10^4 cells were grown in 24 well plates at 37°C/5% CO_2 for 20h. Cells were then transfected with EGFP- or EGFP-TPD52 vector by the Lipofectamine™ 2000 method. After 24 h of post transfection, MTT solution was added to the wells and cells were incubated for additional 4h at 37°C/5% CO_2. After solubilization buffer was added, formazan production was measured at 570nm and the

measured OD is directly proportional to the rate of cell proliferation. Cell proliferation assays were performed with and without Dihydroxy testosterone (DHT). The results of cell proliferation were plotted in graphs from the mean values of three independent experiments, each carried out with triplicate samples. For calculation of significance, a t-test was performed using Graph Pad Prism version 3.0.

2.3.28 Cell migration assay

To study the influence of TPD52 on cell migration hapototactic cell migration test was performed after overexpression of EGFP-TPD52 in LNCaP or MCF-7 cells. Haptotactic cell migration assays were performed in Transwell chambers according to Zhang et al. Porous membranes were coated on the bottom surface with vitronectin (10 µg/ml) or collagen type I (10 µg/ml) for 1h at 37°C. LNCaP or MCF-7 cells were transfected with EGFP or EGFP-TPD52 expressing vectors using Lipofectamine™ 2000 and grown at 37°C/5% CO_2 for 24h. Transfected cells were then trypsinized and washed in the presence of soyabean trypsin inhibitor with the migration buffer (RPMI-1640, 2 mM $CaCl_2$, 1 mM $MgCl_2$, 0.2 mM $MnCl_2$ and 0.5% BSA). Cells were resuspended in migration buffer and 1×10^5 cells were added onto the top of the membrane. The cells were allowed to move through it and bind vitronectin or collagen type I at 37°C for 6 h in migration buffer filled in the lower chamber. After removal of remaining cells in the upper chamber, membranes were fixed in PBS with 4% formaldehyde and cells were counted using an inverse fluorescence microscope. To investigate activation of Akt/PKB pathway, EGFP-TPD 52 or EGFP alone positive cells were seeded on pre coated plates with either vitronectin or BSA and allowed to attach for different time intervals. Then the attached cells were harvested in 2-D lysis buffer and subjected to western blot with Akt and phospho Akt specific antibodies. The steps involved in migration assay as represented in figure 11.

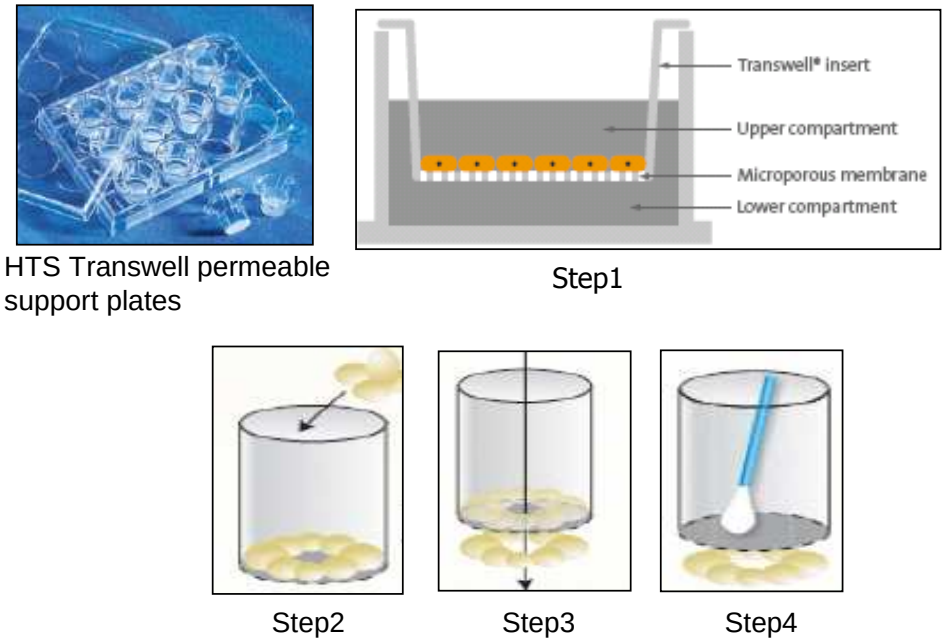

Figure 11: Schematic representation of the steps involved in haptotactic cell migration assay to study the influence of proteins on the cell attachment and migration towards various integrin specific ligands.

2.3.29 Propidium iodide uptake (PI) for cell death

Cell death was analysed with propidium iodide (PI) uptake. Propidium iodide incorporates into DNA of ethanol fixed cells, allowing the measurement of the DNA content. In DNA analysis, cells are stained with fluorescent dyes such as propidium iodide (PI), which intercalate into double-stranded nucleic acids. The fluorescence signal intensity of the PI is directly proportional to the amount of DNA in each cell. PI is not able to penetrate an intact membrane of the viable cells facilitates measurement of dead cell population. To measure cell death cells were harvested with trypsin, washed with PBS and fixed in 2 ml of 70% ethanol for 30 min at -20°C. After centrifugation cells were resuspended in PBS containing 1% glucose (w/v), 50 µg/ml RNase and 50 µg/ml of PI and incubated for 20 min in dark at room temperature. After washing with PBS buffer, PI uptake was analysed by FACS on FL-2 fluorescence detector. 20,000 events were recorded for each condition. Flow cytometry data were analysed using WinMDI software.

2.3.30 Caspase 3 and Caspase 9 activity determination

Caspase-3 and Caspase-9 activities were measured 48 h after downregulation of TPD52 using fluorogenic substrates Ac-DEVD-AMC and DEVD-AFC respectively. Harvested cells were lysed with caspase lysis buffer (10mM Tris-HCl, 10mM Sodium

phosphate buffer pH 7.5, 130 mM NaCl, 1% TritonX-100 and 10 mM $Na_2P_20_7$) and incubated with the respective substrate (25 µg/ml) in 20 mM HEPES (pH7.5), 10% Glycerol, 2 mM DTT at 37°C for 2 h. The release of AFC was analyzed by fluorimeter using excitation/emission wavelength of 390/510 nm. Relative caspase activities were calculated as the ratio of values between mock transfected and transfected cells. Paclitaxel was used as a positive control.

2.3.31 Measurement of mitochondrial membrane transmembrane potential ($\Delta\psi_m$)

To investigate the apoptotic signal, cytofluorometric analysis of mitochondrial transmembrane potential ($\Delta\psi_m$) was performed. Changes in the $\Delta\psi_m$ were detected by measuring the accumulation of the cationic lipophilic fluorochrome dihexyloxacarbocyanine iodide [$DiOC_6$] in the mitochondrial matrix, which is directly proportional to $\Delta\psi_m$ [153]. $\Delta\psi_m$ was determined 48h after downregulation of TPD52. To harvest TPD52 depleted cells for analysis, medium was collected into the labeled tubes and centrifuged at 4°C, 1500 rpm for 1 min, and then the supernatant was discarded. The attached cells were harvested with trypsin and diluted in medium to inhibit the trypsin activity. Then the cells were added to the pellet and centrifuged for 1 min at 1500 rpm. The supernatant was discarded and the cells were resuspended in 1 ml of medium with 50 nM DiOC, and incubated for 30 minutes at 37°C in dark. After incubation, the cells were centrifuged and resuspended in 300 µl of PBS and kept in the dark on ice. In measurement, 20,000 cells were analysed by FACS. Results were analysed by using Cell Quest software.

2.3.32 GST fusion protein expression and GST pull down assay

The GST and GST fusion proteins were expressed in *E. coli* BL21 codon plus strain and purified using affinity chromatography with Glutathione Sepahrose® 4B.

Preparation of GST fusion proteins: A recombinant vector expressing GST-TPD52 fusion protein was generated by cloning the coding region of the human TPD52 (variant 3) cDNA from LNCaP cells into the vector pGEX-6P1 (GE Healthcare Life Sciences). Insertion of the *BamHI/NotI* digested PCR product into the *BamHI/NotI* restriction sites of the vector resulted in a C-terminal fusion of TPD52 to GST. The sequence of the cloned PCR fragment was confirmed by DNA sequencing (Seqlab, Gottingen, Germany). For expression of GST-TPD52 fusion protein or GST alone, the recombinant or empty vector was transformed into

E. coli strain BL21 CodonPlus™. An overnight culture of BL21 transformed with the pGEX-6P1-TPD52 construct or empty vector was diluted in larger volume of LB medium with appropriate antibiotics and allowed to grown at 37°C with constant shaking to reach log phase (OD_{600} = 0.6 to 1.0). To induce protein expression, 100 mM IPTG was added to the final concentration of 0.2 mM and the culture was allowed to grown for additional 4 h under same conditions. Then the cells were harvested by centrifugation at 4500×g and 4°C for 15 min. For purification of the protein, cell pellets were resuspended in pre-chilled PBS containing 1% Triton-X 100 and lysed by sonication. The cell debris was removed by centrifugation at 4500×g and 4°C for 30 min. After centrifugation the lysate was incubated with PBS-equilibrated Glutathione Sepharose® 4B beads for 30 minutes at room temperature on rotating shaker. The beads were washed and resuspended in PBS. Yield and purity were checked by a coomassie blue stained SDS gel.

Preparation of GST beads: The Glutathione Sepharose® 4B beads were prepared according to the manufacturer instructions. Briefly, the required amount of matrix pipetted out and mixed with ten volumes of 1×PBS and centrifuged for 5 min to remove preservatives. This was repeated twice and finally 50% slurry was prepared in PBS. The beads were mixed with protein lysates prepared from bacterial culture pellet and fusion protein was purified. All the centrifugation steps were carried out at 500×g and 4°C.

GST capture assay: GST alone or GST fusion protein coupled to glutathione-Sepharose beads were incubated with 200 µg of LNCaP whole cell lysate for 1 h at room temperature in 1 ml PBS on rotator shaker. The beads were washed four times with PBS and the bound proteins were separated by 2 DE using 11 cm IPG strips (pH 3-10NL) and 12% SDS-PAGE. Proteins were visualized by colloidal coomassie blue stain. Proteins specifically bound to GST-TPD52 were identified by mass spectrometry as described previously. Further interaction of Prx1 with fusion proteins was confirmed by repeating the same experiment and followed by detection with western blotting using anti Prx1 antibody.

2.3.33 Co-Immunoprecipitation of Prx1

Immunoprecipitation was carried out by incubating 1 mg of cell lysate prepared in RIPA buffer after 24 h of transfection with Flag-TPD52 construct and 1 µg of mouse anti-Flag antibody for 2 h at 4°C. After the addition of 20 µl of Protein G-agarose, lysates were incubated for an additional 1 h at 4°C. Rabbit IgG was used as a negative control. The beads

were washed three times with the RIPA buffer, separated by SDS-PAGE, and immunoblotted with rabbit Prx 1 antibody. The protein bands were detected using HRP labelled anti-rabbit secondary antibody as described above.

2.3.34 Immunofluoroscence

IF method was used to study subcellular localization of TPD52 by direct staining cells of with specific antibodies. LNCaP cells were seeded into 3.5 cm diameter plates or 24 well formats containing a cover slip and cultured for at least 18 h. Cells were then transfected with recombinant pFLAG-CMV-1-TPD52 or empty vector using liopfectamine™ 2000 and incubated for 24 h at 37°C in CO_2 incubator. The cells attached to cover slips were washed twice with PBS. After removing PBS by gentle aspiration, the cells were fixed in 2% (v/v) formaldehyde for 10 min. For permeabilization of antibody, the cells were washed briefly with PBS, and then incubated with 0.3% Triton-X100 in PBS for 3-5 min. Then the cells were washed in PBS (2×1 min) and incubated for 1 h in blocking buffer. The primary antibody was diluted to 1000 fold in blocking buffer, and gently pipetted onto the coverslip. After 1 h, the cells were washed with PBS (3×3 min) and incubated again in blocking buffer for 15 min. The fluorescence-coupled secondary antibody diluted 1000 fold in blocking buffer was applied to the cells and incubated in dark for 30-45 min. Following by incubation, the cells were washed with PBS (3×3 min) and the cover slips were mounted on slides using the Mowiol or DAKO® Fluorescent Mounting medium and allowed to dry. The cells were observed using an inverse fluorescence microscope.

2.3.35 $(His)_6$-TPD52 expression and purification

The $(His)_6$ tag fusion protein was expressed in *E. coli* BL21 codon plus strain and purified using metal chelate affinity chromatography using Ni^{2+}-NTA column. To achieve higher purity, the protein was further purified by anion-exchange followed by gel filtration chromatography.

2.3.35.1 Preparation of His_6-TPD52 fusion proteins

$(His)_6$-TPD52 fusion protein expressing recombinant vector was generated by cloning the coding region of the human TPD52 (variant 3) cDNA from LNCaP cells into the vector pETM-11. Insertion of the *NcoI/NotI* digested PCR product into the *NcoI/NotI*

restriction sites of the vector resulted in the N-terminal His tagged TPD52. The sequence of the cloned PCR fragment was confirmed by DNA sequencing (Seqlab, Gottingen, Germany). To express the protein, vector was transformed into *E. coli* strain BL21 CodonPlus™. An overnight culture of BL21 transformed with the recombinant construct or empty vector was diluted in larger volume of LB medium with appropriate antibiotics and allowed to grow at 37°C with constant shaking to reach log phase (OD_{600} = 0.6 to 1.0). To induce protein expression 100 mM IPTG was added to final concentration of 0.2 mM and the culture was allowed to grow for additional 4 h under same conditions. Cells were harvested by centrifugation at 4500×g and 4°C for 15 min.

2.3.35.2 Purification of $(His)_6$-TPD52

To purify protein, cell pellets were resuspended in buffer (20 mM Tris-HCl, pH8.0, containing 10 mM imidazole and lysed by using French press. The cell debris was removed by centrifugation at 20000×g and 4°C for 20 min. The crude lysate was filtered through a 0.2 μm membrane and was loaded onto a MC small Hi-Trap Chelating HP column. The column was washed with 10 bed volumes of washing buffer containing 10 mM Imidazole buffer. The protein was eluted with elution buffer containing 500mM imidazole in 2ml fractions. The peak fractions were pooled and dialyzed to remove imidazole. The dialyzed sample was further subjected to anion exchanger HQ big Hi-Trap column and eluted with 20 mM Tris-HCl, pH8.0 containing 1 M NaCl. The peack fractions were further purified by size exclusion chromatography (Superdex 200, 16/60) at 4°C using 20 mM Tris-HCl, pH8.0 for equilibriation and elution. The purified protein was analysed by SDS-PAGE for purity and was concentrated appropriately for further experiments.

3 Results

3.1 Proteomic analysis of prostate needle biopsies

In the present study we analyzed prostate needle biopsies from 23 patients diagnosed with either PCa or BPH. It is known that methods used in biopsy sample collection with small needle core will give false positive or negative diagnosis for these two disease states. To overcome this problem biopsy samples were selected from patients with high probability for cancer based on diagnosis on remaining biopsies and subjected to 2-DE. We analyzed the proteome of biopsies from 11 BPH patients and 12 PCa (Table 01) by 2D-SDS-PAGE in the pH range of 4-7 and molecular weight range between 10 kDa and 120 kDa.

Table 01: List of patients included in the proteomic study together with their PSA levels and histology grading

S.No.	Diagnosis at Age	PSA-Value	DRE Palpation	Histology Diagnosis	Gleason-Score
1	56	7	inconspicuous	BPH	
2	57	10	suspect	BPH	
3	63	10	inconspicuous	BPH	
4	77	7.7	inconspicuous	BPH	
5	79	8	inconspicuous	BPH	
6	66	5.8	suspect	BPH	
7	65	6.37	inconspicuous	BPH	
8	74	7.16	inconspicuous	BPH	
9	58	10.2	inconspicuous	BPH	
10	69	14.7	inconspicuous	BPH	
11	50	5.3	inconspicuous	BPH	
12	62	11.1	suspect	PCa	3 + 3 = 6
13	68	11.3	suspect	PCa	1 + 2 = 3
14	69	11	inconspicuous	PCa	1 + 1 = 2
15	61	10.9	inconspicuous	PCa	3 + 4 = 7
16	64	7.8	suspect	PCa	2 + 3 = 5
17	59	5.95	inconspicuous	PCa	1 + 1 = 2
18	68	7.55	inconspicuous	PCa	1 + 2 = 3
19	69	6.6	suspect	PCa	2 + 3 = 5
20	71	4.7	inconspicuous	PCa	2 + 4 = 6
21	63	9	inconspicuous	PCa	2 + 3 = 5
22	62	5.1	inconspicuous	PCa	1 + 2 = 3
23	60	5.7	inconspicuous	PCa	1 + 2 = 3

On average, about 900 protein spots per gel were detected with SYPRO® ruby staining. The protein expression patterns were analysed for quantitative and qualitative differences using the PDQUEST software by comparing protein profiles of tumor tissues. Only those proteins whose expression was significantly altered (>1.5fold) in all prostate tumors examined were considered for further studies. The 2-DE image analysis and statistical analysis of protein spots showing altered expression revealed differential expression of 88 spots (Fig. 12) which corresponds to 79 different proteins (Table 02). Identification of spots by mass spectrometry showed that many of the proteins have been previously reported as differentially expressed protein in various tumors including prostate cancer [154-156]. Among the identified proteins we could find more than one spot containing the same protein with different pI, which may be due to post-translational modifications. A selection of differentially expressed proteins has been depicted on enlarged gel images in Fig. 13.

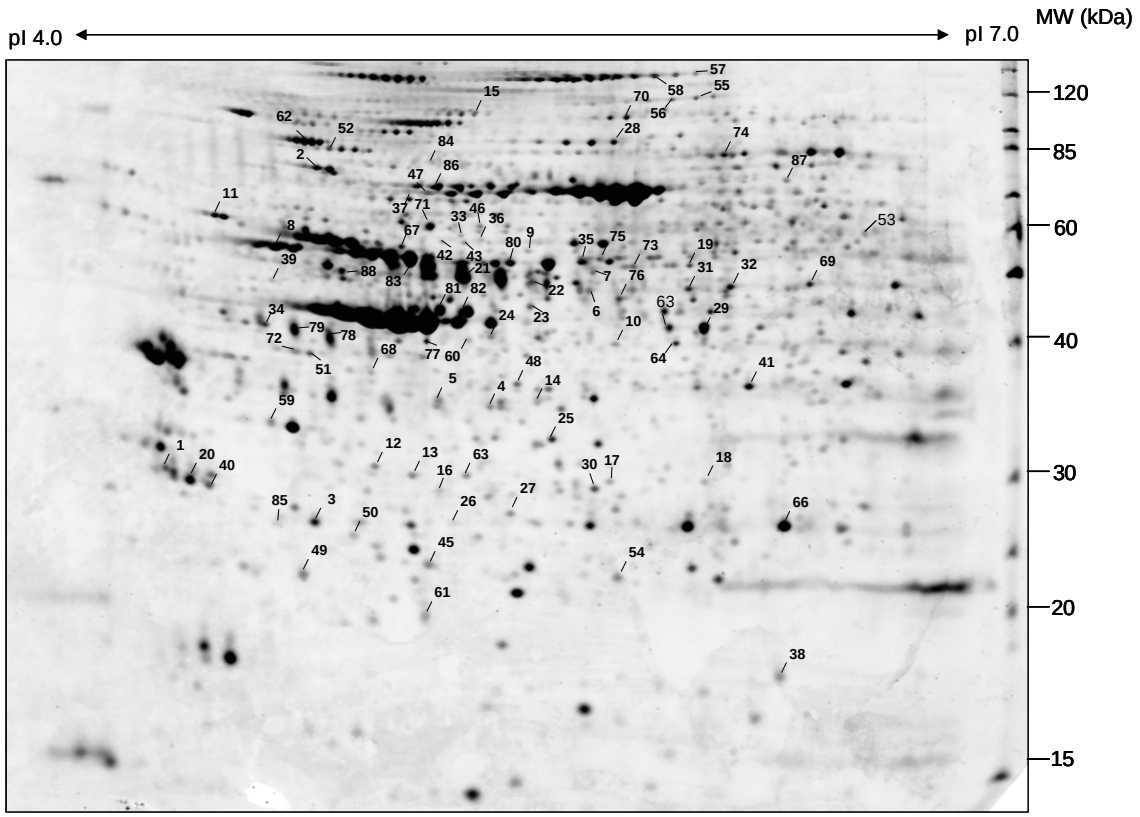

Figure 12: 2D proteome map of prostate biopsy (PCa). Proteins were resolved by IEF over the pI range 4-7, followed by 12.5% SDS-PAGE and visualized by SYPRO® Ruby staining. Significant differentially expressed proteins are labelled with numbers.

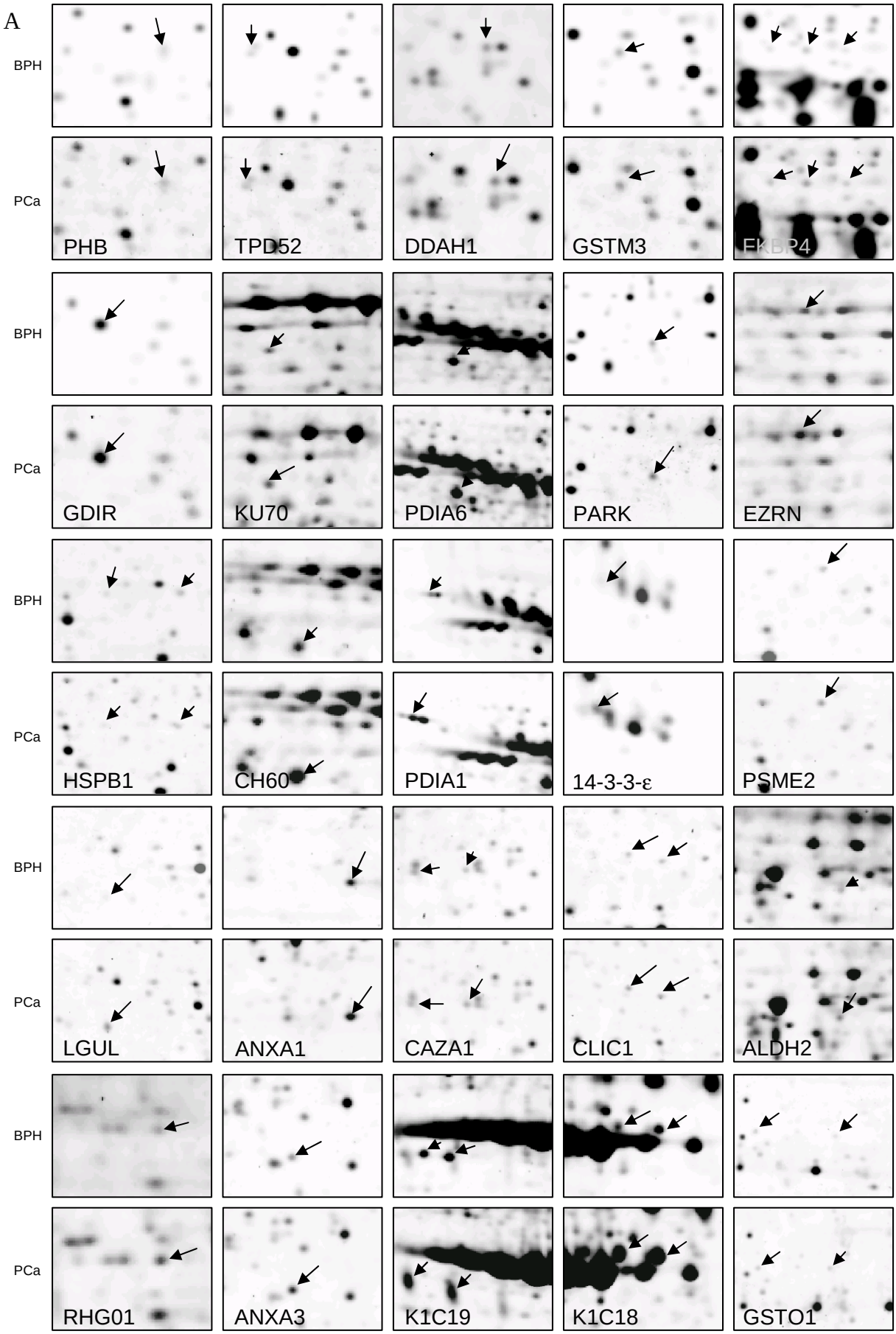
A
BPH
PCa
PHB
TPD52
DDAH1
GSTM3
FKBP4
BPH
PCa
GDIR
KU70
PDIA6
PARK
EZRN
BPH
PCa
HSPB1
CH60
PDIA1
14-3-3-ε
PSME2
BPH
PCa
LGUL
ANXA1
CAZA1
CLIC1
ALDH2
BPH
PCa
RHG01
ANXA3
K1C19
K1C18
GSTO1

B

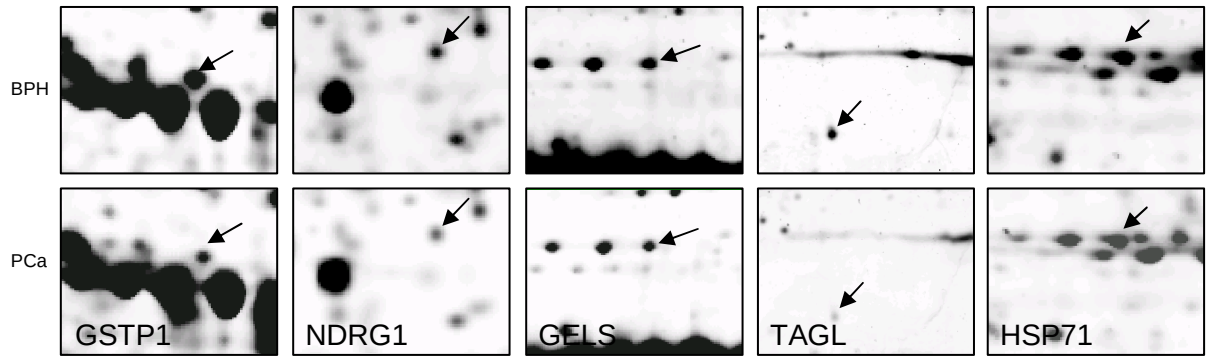

Figure 13: Enlarged images of corresponding regions of both BPH (upper panel) and PCa (lower panel). Protein spots showing upregulation (A) or downregulation (B) are indicated with arrows in both gel pictures.

Among the altered protein spots we found overexpression of prostatic acid phosphatase precursor (PPAP) (Fig. 14) consistently in all PCa samples in comparison to BPH. The results obtained for this 40-kDa protein, which is known to be up-regulated in prostate tumors, confirmed the classification of needle biopsies in PCa and BPH groups and demonstrated the reliability of our approach for proteomic analysis of prostate biopsies.

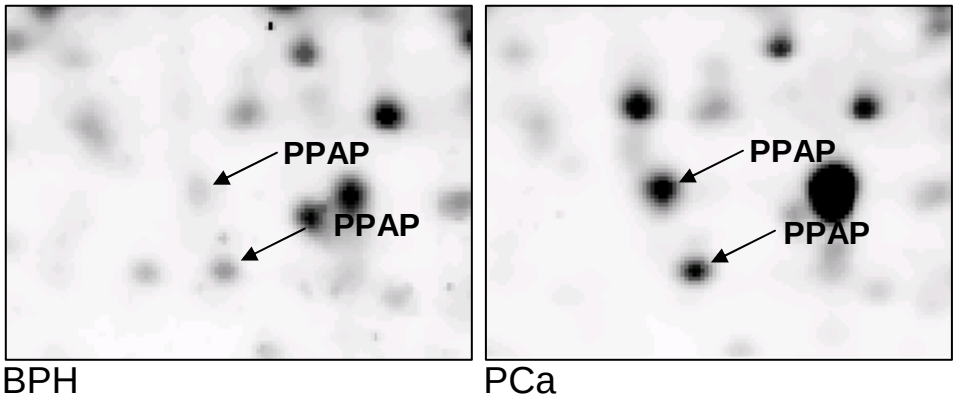

Figure 14: Enlarged region of SYPRO® Ruby stained gel images indicating prostatic acid phosphatase precursor (PPAP) up-regulation in prostate carcinoma (right panel) and benign prostatic hyperplasia (BPH) (left panel).

Table 02: Identification of 88 protein spots of 79 different proteins from tumor samples by mass spectrometry using MALDI-TOF TOF

Spot No.	Accession No.	Title_text	Swiss-Prot Entry name	Fold difference	Hit mass	Hit score	peptide matches	Sequence coverage
1	IPI00000816	14-3-3 protein epsilon	1433E	1.8	29155	323	21	69
2	IPI00003362	78 kDa glucose-regulated protein precursor	GRP78	1.53	72288	910	39	63
3	IPI00003815	Rho GDP-dissociation inhibitor 1	GDIR	1.54	23193	423	10	45
4	IPI00005969	F-actin capping protein alpha-1 subunit	CAZA1	1.70	32902	200	13	59
5	IPI00005969	F-actin capping protein alpha-1 subunit	CAZA1	1.88	32902	450	14	59
6	IPI00006114	Pigment epithelium-derived factor precursor	PEDF	1.71	46313	258	13	44
7	IPI00006663	Aldehyde dehydrogenase, mitochondrial precursor	ALDH2	4.02	56346	244	17	38
8	IPI00007752	Tubulin beta-2 chain	TBB2C	1.99	49799	567	40	71
9	IPI00007812	Vacuolar ATP synthase subunit B, brain isoform	VATB2	1.87	56465	295	24	51
10	IPI00009865	Keratin, type I cytoskeletal 10	K1C10	4.01	59483	145	18	29
11	IPI00010796	Protein disulfide-isomerase precursor	PDIA1	1.55	57081	361	20	42
12	IPI00010896	Chloride intracellular channel protein 1	CLIC1	1.72	26775	555	18	71
13	IPI00010896	Chloride intracellular channel protein 1	CLIC1	2.06	26775	279	16	67
14	IPI00013004	Splice Isoform 1 of Pyridoxal kinase	PDXK	1.57	35080	81	11	36
15	IPI00013508	Alpha-actinin 1	ACTN1	2.43	107566	468	46	56
16	IPI00017334	Prohibitin	PHB	1.83	29786	530	12	58
17	IPI00019755	Glutathione transferase omega 1	GSTO1	1.66	27548	265	14	48
18	IPI00019755	Glutathione transferase omega 1	GSTO1	2.43	27548	292	16	54
19	IPI00020567	Rho-GTPase-activating protein 1	RHG01	1.56	50404	704	26	75
20	IPI00021263	14-3-3 protein zeta/delta	1433Z	1.52	27728	495	23	73
21	IPI00021891	Splice Isoform Gamma-B of Fibrinogen gamma chain precursor	FIBG	1.50	51479	496	13	42
22	IPI00021891	Splice Isoform Gamma-B of Fibrinogen gamma chain precursor	FIBG	1.58	51479	446	14	42
23	IPI00022078	NDRG1 protein	NDRG1	2.45	42808	198	10	39
24	IPI00023006	Actin, alpha cardiac	ACTC	1.63	41992	308	13	37
25	IPI00024095	Annexin A3	ANXA3	2.26	36222	531	21	68
26	IPI00025512	Heat-shock protein beta-1	HSPB1	2.06	22768	451	14	67
27	IPI00025512	Heat-shock protein beta-1	HSPB1	2.7	22768	504	14	68
28	IPI00026314	Gelsolin precursor	GELS	1.62	85644	475	24	44
29	IPI00027341	Macrophage capping protein	CAPG	1.67	38494	221	12	45

30	IPI00030154	Proteasome activator complex subunit 1	PSME1	1.66	28705	347	16	53
31	IPI00031461	Rab GDP dissociation inhibitor beta	GDIB	1.51	50631	655	32	70
32	IPI00031461	Rab GDP dissociation inhibitor beta	GDIB	1.5	50631	515	30	70
33	IPI00032179	Antithrombin III variant	ANT3	1.7	52658	112	14	29
34	IPI00166729	Zinc-alpha-2-glycoprotein precursor	ZA2G	1.64	33851	415	22	60
35	IPI00177728	Cytosolic nonspecific dipeptidase	CNDP2	1.66	52845	322	18	45
36	IPI00216049	Splice Isoform 1 of Heterogeneous nuclear ribonucleoprotein K	HNRPK	1.78	50944	242	17	44
37	IPI00216049	Splice Isoform 1 of Heterogeneous nuclear ribonucleoprotein K	HNRPK	1.53	50944	491	24	50
38	IPI00216138	Transgelin	TAGL	2.98	22465	336	15	67
39	IPI00216171	Gamma-enolase	ENOG	2.08	47108	478	23	60
40	IPI00216318	14-3-3 protein beta/alpha	1433B	1.63	27934	390	17	71
41	IPI00218918	Annexin A1	ANXA1	1.87	38559	719	26	64
42	IPI00219005	FK506-binding protein 4	FKBP4	2.45	51641	209	22	48
43	IPI00219005	FK506-binding protein 4	FKBP4	2.78	51641	215	20	47
44	IPI00219005	FK506-binding protein 4	FKBP4	1.95	51641	147	21	47
45	IPI00219757	Glutathione S-transferase P	GSTP1	1.81	23210	383	11	59
46	IPI00220327	Keratin, type II cytoskeletal 1	K2C1	1.79	65847	175	16	27
47	IPI00220327	Keratin, type II cytoskeletal 1	K2C1	1.61	65847	132	15	30
48	IPI00220342	NG,NG-dimethylarginine dimethylaminohydrolase 1	DDAH1	1.70	30971	396	17	63
49	IPI00220766	Lactoylglutathione lyase	LGUL	2.38	20575	410	12	64
50	IPI00246975	Glutathione S-transferase Mu 3	GSTM3	1.70	26411	137	14	55
51	IPI00294536	Serine-threonine kinase receptor-associated protein	STRAP	1.85	38414	162	10	32
52	IPI00294578	Splice Isoform 1 of Protein-glutamine gamma-glutamyltransferase 2	TGM2	1.79	77280	600	35	58
53	IPI00298497	Fibrinogen beta chain precursor	FIBB	4.32	55892	294	22	50
54	IPI00298547	DJ-1 protein	PARK7	1.86	19878	353	16	84
55	IPI00304840	Splice Isoform 2C2 of Collagen alpha 2(VI) chain precursor	CO6A2	1.52	108506	246	19	23
56	IPI00304840	Splice Isoform 2C2 of Collagen alpha 2(VI) chain precursor	CO6A2	1.72	108506	343	21	25
57	IPI00307162	Vinculin isoform meta-VCL	VINC	2.17	123722	292	39	37
58	IPI00307162	Vinculin isoform meta-VCL	VINC	2.04	123722	443	41	39
59	IPI00329801	Annexin A5	ANXA5	1.62	35783	716	23	76
60	IPI00334190	Stomatin-like protein 2	STML2	1.84	38510	203	10	37
61	IPI00375676	Ferritin light chain	Q6S4P3	4.41	28399	439	7	21
62	IPI00382470	Heat shock protein HSP 90-alpha 2	HS90A	1.61	98052	588	37	37

63	IPI00384051	Proteasome activator complex subunit 2	PSME2	1.78	27213	664	15	65
64	IPI00396434	Prostatic acid phosphatase precursor	PPAP	2.64	44537	273	16	29
65	IPI00396434	Prostatic acid phosphatase precursor	PPAP	1.84	44537	348	20	33
66	IPI00465028	Triosephosphate isomerase 1 variant	TPIS	1.73	26696	345	15	73
67	IPI00465084	Desmin	DESM	1.74	53372	383	29	61
68	IPI00465121	Galphai2 protein	Q6B6N3	3.14	41522	223	18	52
69	IPI00465248	Alpha-enolase	ENOA	1.96	47008	457	23	60
70	IPI00472068	107 kDa protein	GANAB	2.11	106780	319	31	38
71	IPI00472102	60 kDa heat shock protein, mitochondrial precursor	CH60	2.6	61016	638	26	55
72	IPI00477353	Farnesyl pyrophosphate synthetase	FPPS	1.81	40507	98	7	20
73	IPI00479191	HNRPH1 protein	Q6IBM4	1.83	51197	297	17	43
74	IPI00479359	Ezrin	EZRN	2.15	69225	220	26	40
75	IPI00479877	4-trimethylaminobutyraldehyde dehydrogenase	AL9A1	1.98	56255	202	13	32
76	IPI00514510	Annexin A7	Q53HM8	3.89	52706	236	33	37
77	IPI00514598	Placental thrombin inhibitor	SPB6	1.59	42562	456	21	72
78	IPI00550818	Keratin, type I cytoskeletal 19	K1C19	2.48	44079	808	42	83
79	IPI00550818	Keratin, type I cytoskeletal 19	K1C19	1.92	44079	751	37	81
80	IPI00554648	Keratin, type II cytoskeletal 8	K2C8	2.20	53510	754	39	63
81	IPI00554788	Keratin, type I cytoskeletal 18	K1C18	2.14	47897	507	29	62
82	IPI00554788	Keratin, type I cytoskeletal 18	K1C18	2.13	47897	595	34	73
83	IPI00555812	Vitamin D-binding protein precursor	VTDB	1.512	52929	586	22	52
84	IPI00604664	NADH-ubiquinone oxidoreductase 75 kDa subunit	NDUS1	1.62	79465	304	26	46
85	IPI00619951	Tumor proTein D52 isoform 2	TPD52	2.17	22464	70	4	47
86	IPI00643932	Heat sHock 70kDa protein 1B	HSP71	1.73	69982	344	14	34
87	IPI00644712	ATP-dependent DNA helicase II, 70 kDa subunit	KU70	2.87	69799	198	11	38
88	IPI00644989	Protein disulfide-isomerase A6 precursor	PDIA6	1.59	48091	454	18	45

Database: IPI human v3.12; cut off score > 59 with p-value < 0.05, search parameters: MS/MS Ion Search, Enzyme : Trypsin, Variable modifications: Carbamidomethyl (C), Oxidation (M), Peptide Mass Tolerance: ± 50 ppm, Fragment Mass Tolerance: ± 0.45 Da, Max Missed Cleavages: 1

3.2 Prohibitin is overexpressed in prostate cancer

Among the differentially expressed proteins, a further interesting protein showing increased expression in Pca compared to BPH was identified as prohibitin (PHB) (Fig. 15 and Table 03).

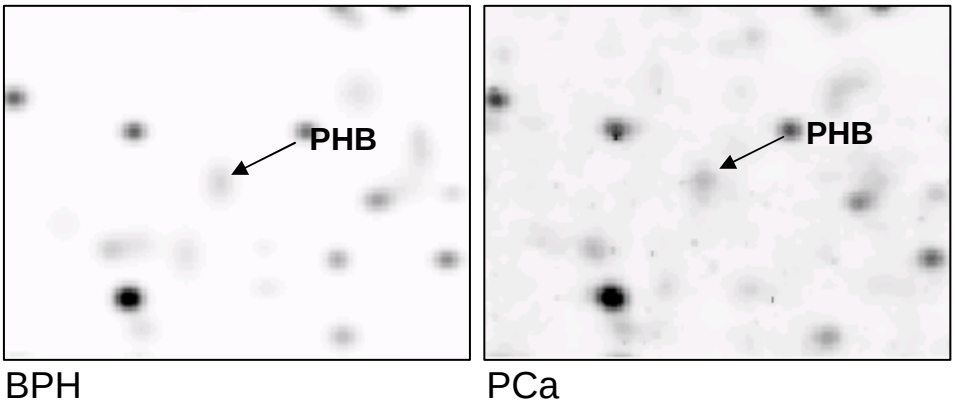

Figure 15: Enlarged region of SYPRO® Ruby stained gel images indicating prohibitin (PHB) up-regulation in prostate carcinoma (right panel) and benign prostatic hyperplasia (BPH) (left panel).

To determine whether the degree of up-regulation of this protein correlated with an increased amount of mRNA we analysed the prohibitin mRNA content in PCa and BPH biopsy specimens by quantitative real time PCR (protein and RNA had been isolated from the same biopsy, because of poor RNA quality three sample had to be discarded). RPLP0, the ribosomal protein large P0, was used as a house keeping gene to normalize expression levels. A Mann Whitney test performed at the 95% confidence interval showed significance as $p<0.001$. Real time PCR revealed a significant increase of prohibitin mRNA amount in PCa compared to BPH (Fig. 16A and B), suggesting that the increased protein expression in PCa is caused by an increased rate of transcription. The specificity of the primers for real-time PCR reaction was confirmed by melting curve analysis at the end of the PCR (Fig. 16C).

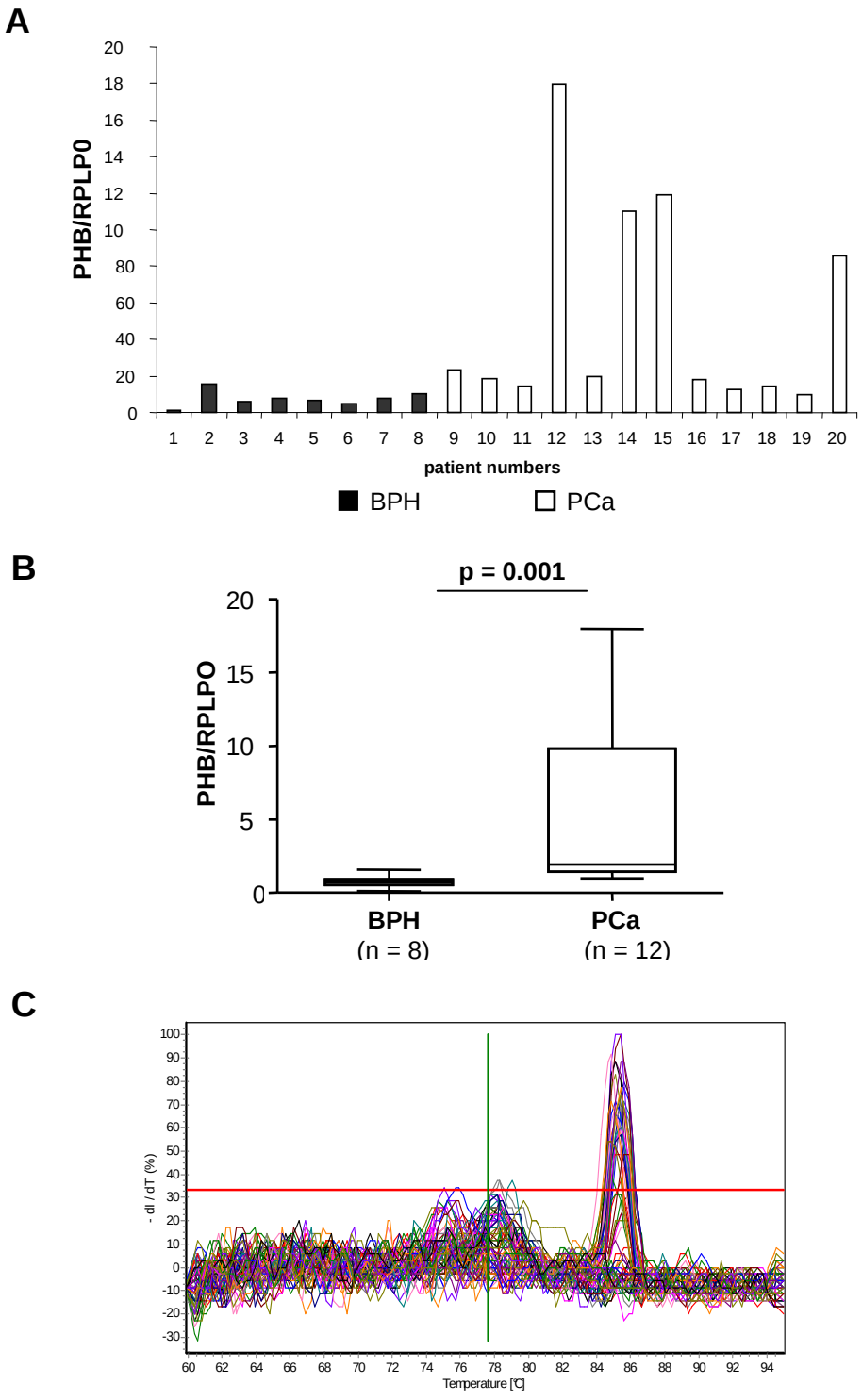

Figure 16: Quantitative reverse transcription-PCR of prohibitin (PHB) transcripts shown from benign prostate tissue (n=8) (black bars) and localized prostate cancer (n=12) (open bars); A and B: the ratio of PHB expression was normalized against RPLP0 expression (A), and this is graphically presented as *box plots* with 95% confidence intervals (B) (non-parametric two-tailed Mann Whitney test performed at 95% confidence interval). (C) Melting curve analysis indicating specificity of the primers in PCR reaction.

Table 03: Identification of 2D spot; mass spectrometry data of prohibitin using Maldi-TOF-TOF:
A protein data; B peptide data; C sequence coverage
IPI human database v3.12; cut off score > 60 with p-value < 0, 05, search parameters: MS/MS Ion Search, Enzyme: Trypsin, Variable modifications: Oxidation (M), Carbamidomethylation (C), Peptide Mass Tolerance: ± 50 ppm, Fragment Mass Tolerance: ± 0.45 Da, Max Missed Cleavages: 1; Number of queries: 105

A. protein data

Accession no.	MW (Da)	score	Title_text	pI	Sequence coverage (%)	Different peptides count	Sequenced peptides
IPI00017334	29786	530	Prohibitin	5,57	58	11	5

B. peptide data

Start-End	Observed mass	M_r (expt)	M_r (calc)	□	Missed cleavage sites	Ions Score	Peptide sequence
178-186	1023.50	1022.49	1022.49	-0.00	0	---	EFTEAVEAK
187-195	1058.52	1057.51	1057.52	-0.01	0	---	QVAQQEAER
149-157	1062.51	1061.51	1061.50	0.01	0	---	QVSDDLTER
134-143	1149.58	1148.57	1148.58	-0.01	0	65	FDAGELITQR
134-143	1149.58	1148.57	1148.58	-0.01	0	---	FDAGELITQR
84-93	1185.65	1184.64	1184.65	-0.01	0	---	DLQNVNITLR
118-128	1213.73	1212.72	1212.73	-0.01	0	---	VLPSITTEILK
94-105	1396.84	1395.83	1395.83	-0.00	0	41	ILFRPVASQLPR
94-105	1396.84	1395.83	1395.83	-0.00	0	---	ILFRPVASQLPR
106-117	1444.66	1443.65	1443.65	-0.00	0	---	IFTSIGEDYDER
106-117	1444.66	1443.65	1443.65	-0.00	0	65	IFTSIGEDYDER
240-253	1606.84	1605.83	1605.84	-0.00	1	111	KLEAAEDIAYQLSR
240-253	1606.84	1605.83	1605.84	-0.00	1	---	KLEAAEDIAYQLSR
220-239	1998.08	1997.08	1997.08	-0.00	0	---	AAELIANSLATAGDGLIELR
220-239	1998.08	1997.08	1997.08	-0.00	0	171	AAELIANSLATAGDGLIELR
158-177	2119.14	2118.13	2118.14	-0.00	0	---	AATFGLILDDVSLTHLTFGK
12-35	2371.24	2370.24	2370.24	-0.01	0	---	FGLALAVAGGVVNSALYNVDAGHR

C. Sequence coverage

58 % Matched peptides shown in **Bold Red**

```
  1 MAAKVFESIG KFGLALAVAG GVVNSALYNV DAGHRAVIFD RFRGVQDIVV
 51 GEGTHFLIPW VQKPIIFDCR SRPRNVPVIT GSKDLQNVNI TLRILFRPVA
101 SQLPRIFTSI GEDYDERVLP SITTEILKSV VARFDAGELI TQRELVSRQV
151 SDDLTERAAT FGLILDDVSL THLTFGKEFT EAVEAKQVAQ QEAERARFVV
201 EKAEQQKKAA IISAEGDSKA AELIANSLAT AGDGLIELRK LEAAEDIAYQ
251 LSRSRNITYL PAGQSVLLQL PQ
```

Using immunohistochemistry on 21 radical prostatectomized samples we determined the tissue-specific expression of prohibitin. H&E stained paraffin fixed prostate sections were examined by pathologists to confirm diagnosis of cancer (Fig. 17). Since prostate tumors are multifocal and exhibit peculiar morphological features making it difficult to confirm the diagnosis of cancer, immunostaining of parallel sections with anti Ki-67 was performed that confirmed the diagnosis of prostate cancer on sections. Further sections were used for immunodetection of prohibitin. The results indicated that there was weak staining for prohibitin (if any) in unaffected secretory epithelia (BPE), BPH and prostatitis (Fig. 18A&B). However, prohibitin was highly expressed in high-grade prostatic intra epithelial neoplasia (PIN) (Fig. 18C) and PCa (Fig. 18D). We also observed prohibitin staining in tumor cells infiltrating benign glands (Fig. 18F). Immunostaining for prohibitin revealed that this protein is located predominantly in the cytoplasm (Fig. 18D&E). Remarkably, intensive prohibitin staining was always limited to malignant cells. Therefore enhanced expression of prohibitin appears to be tumor specific.

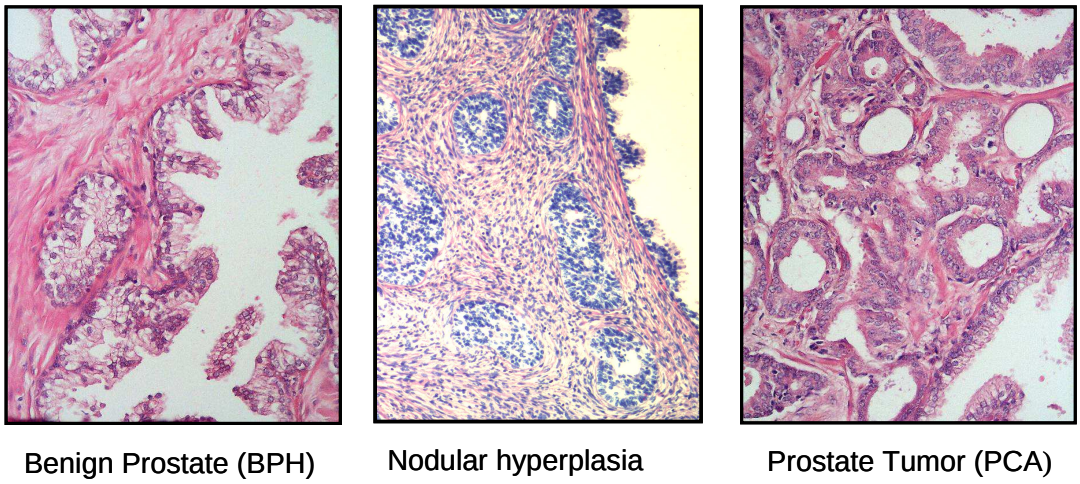

Figure 17: Haematoxylin and eosin staining for histological diagnosis of prostate carcinoma, description under the each picture indicates the confirmed diagnosis of the respective sample.

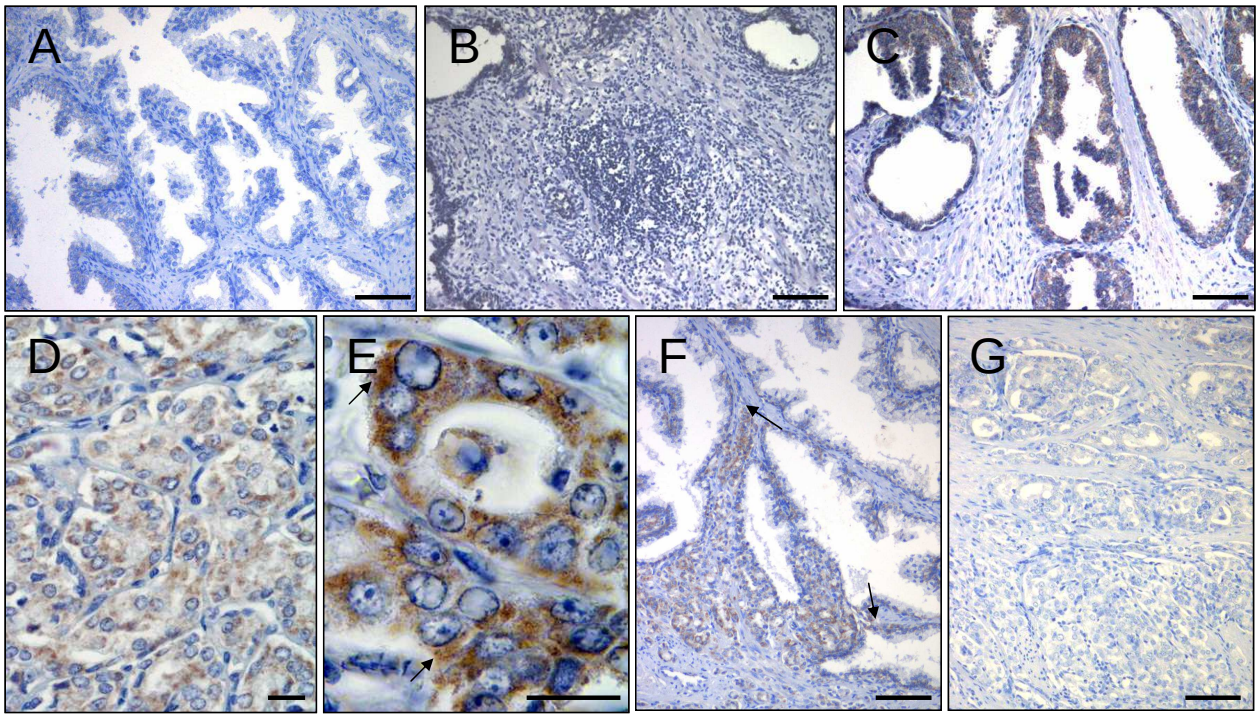

Figure 18: Immunostaining with mouse polyclonal anti-prohibitin [1:2000] and 4plus Universal Immunoperoxidase detection system for prohibitin (brown colour) on paraffin sections from radical prostatectomy: A. Benign prostate hyperplasia (BPH); B. Prostatitis; C. Prostatic intraepithelial neoplasia; D. Prostate carcinoma (PCa, Gleason score 2+3); E. PCa with 100,000 × magnification and arrows indicates immunostaining in the cytoplasm of tumor cells; F. Prostate carcinoma infiltrating into benign glands (Gleason score 4+3, arrows indicate infiltration of tumor into benign glands); G. Prostate carcinoma control for endogenous peroxidase; The bar represents 100 µm except in figures 5 D&E where it represents 20 µm.

3.3 TPD52 is overexpressed in prostate cancer

In the present protein profiling study on prostate biopsies, we identified TPD52 as overexpressed in PCa when compared with benign prostate hyperplasia (Fig 19A and Table 04). To determine whether TPD52 is overexpressed at transcriptional level too, TPD52 mRNA was estimated by quantitative real time PCR from RNA isolated from the same biopsies used for proteomic analysis. RPLP0 was used as a house keeping gene to normalize the expression levels (Fig 19B). Real time PCR data have shown a significant increase (Fig 19C) of TPD52 mRNA amount in PCa compared to BPH suggesting that upregulated protein expression in PCa is caused by an enhanced transcription rate. The melting curve analysis at the end of the PCR confirmed specificity of the primers for real-time PCR.

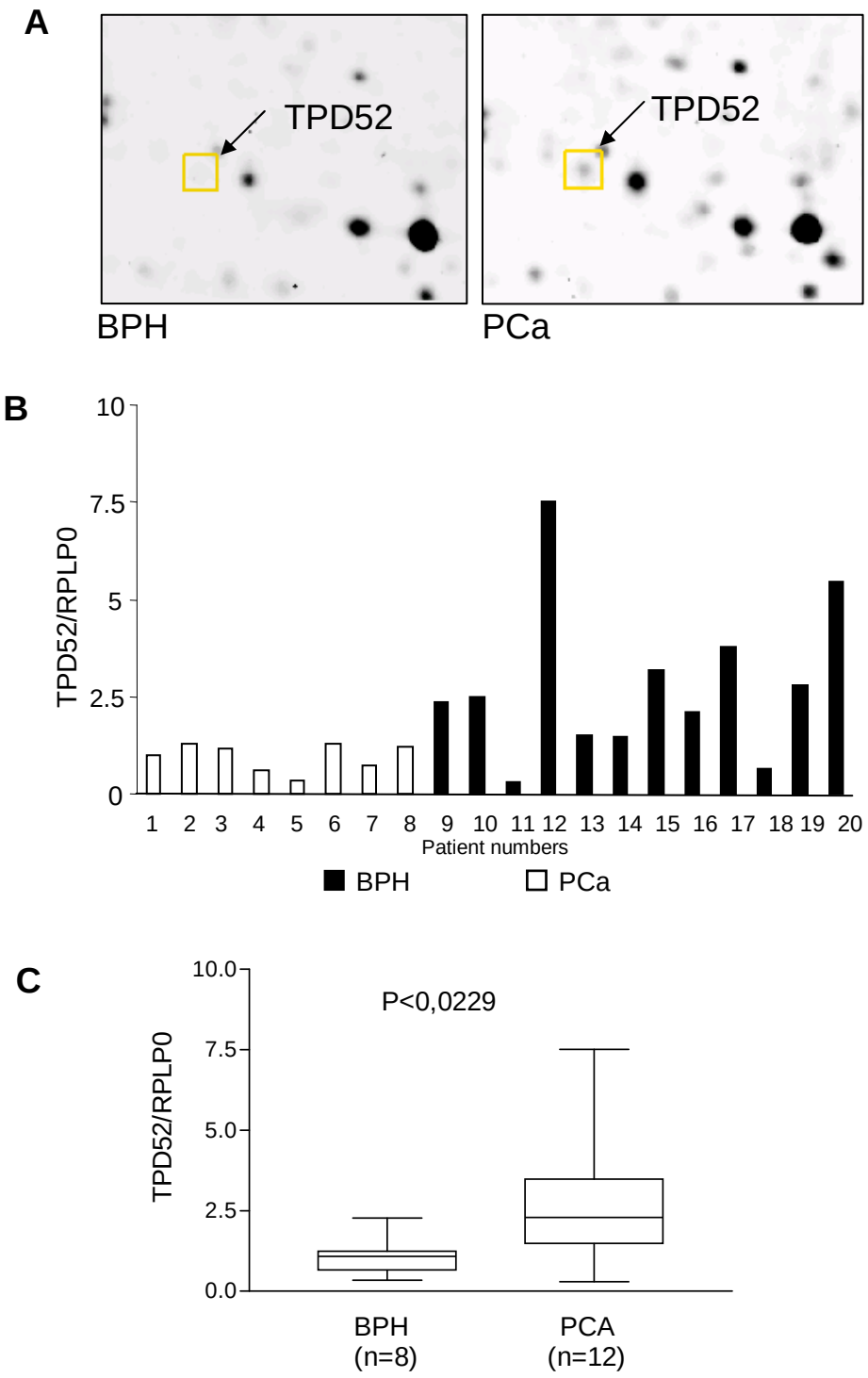

Figure 19: (A) Enlarged region of SYPRO® Ruby stained 2DE gel images indicating tumor protein D52 (TPD52) up-regulation in prostate carcinoma (right panel) and benign prostatic hyperplasia (BPH) (left panel) (B) Quantitative reverse transcription-PCR of TPD52 transcripts shown from benign prostate tissue (n=8) and localized prostate cancer (n=12) (C) the ratio of PHB expression was normalized against RPLP0 expression and this is graphically presented as *box plots* with 95% confidence intervals (non-parametric two-tailed Mann Whitney test performed at 95% confidence interval, p<0.0229).

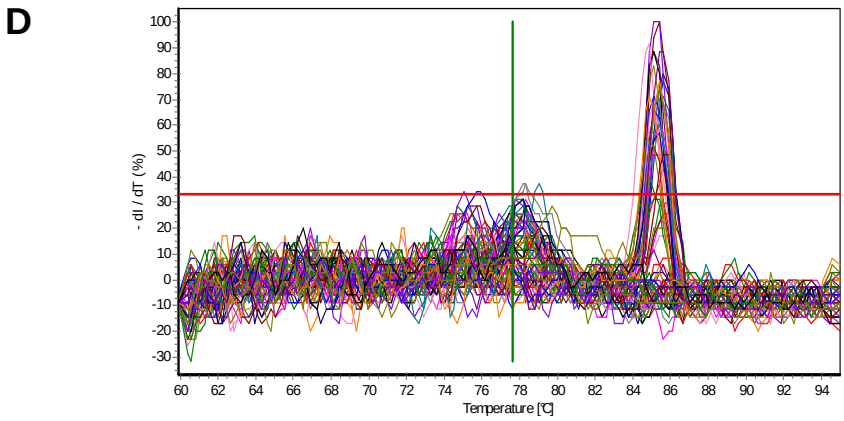

Figure 19: (D) Melting curve analysis indicating specificity of the PCR reaction.

Table 04: Identification of 2D spot; mass spectrometry data of TPD52 using Maldi-TOF-TOF:
A protein data; B peptide data; C sequence coverage. IPI human database v3.12; cut off score > 60 with p-value < 0.05, search parameters: MS/MS Ion Search, Enzyme: Trypsin, Variable modifications: Oxidation (M), Carbamidomethylation (C), Peptide Mass Tolerance: ± 50 ppm, Fragment Mass Tolerance: ± 0.45 Da, Max Missed Cleavages: 1; Number of queries: 105

A. Protein data

Accession No.	MW(Da)	Score	Title_text	pI	Sequence coverage (%)	Different peptides count	Sequenced peptides
IPI00619951	22463,5	70	Tumor proTein D52	5,3	65	8	1

B. Peptide data

Start-End	Calculated Mass	Observed Mass	Match Error PPM	Ion Score	Sequence
42-60	2099,16	2099,16	-1	-	ELAKVEEEIQTLSQVLAAK
46-60	1657,90	1657,92	13	-	VEEEIQTLSQVLAAK
70-80	1242,74	1242,75	9	-	KLGINSLQELK
98-109	1277,67	1277,71	28	-	KTSETLSQAGQK
99-109	1149,57	1149,57	-2	-	TSETLSQAGQK
110-123	1324,71	1324,72	4	-	ASAAFSSVGSVITK
159-168	1222,63	1222,63	1	20,11	SFEEKVENLK
171-202	3086,53	3086,58	17	-	VGGTKPAGGDFGEVLNSAANASATTTEPLPEK

C. Sequence Coverage 65 % Matched peptides shown in Bold Red

MDRGEQGLLR TDPVPEEGED VAATISATET LSEEEQEELR R**ELAKVEEEI QTLSQVLAAK**
EKHLAEIKR**K LGINSLQELK** QNIAKGWQDV TATSAYK**KTS ETLSQAGQKA SAAFSSVGSV**
ITKKLEDVKL QAFSHSFSIR SIQHSISMPA MRNSPTFK**SF EEKVENLK**SK **VGGTKPAGGD**
FGEVLNSAAN ASATTTEPLP
EKTQESL

3.4 Functional characterization of TPD52 in LNCaP cells

3.4.1 Cloning and expression of EGFP-TPD52

To assess the physiological effects of TPD52 expression on prostate cancer progression, EGFP-TPD52 fusion protein producing constructs were generated and expression of the fusion protein in LNCaP cells was estimated by Western blotting (Fig 20A&B) using anti EGFP antibody (Roche, Germany).

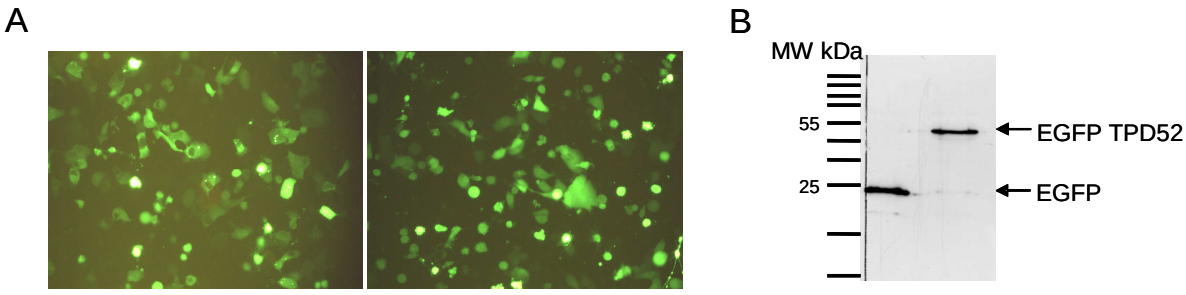

Figure 20: (A) LNCaP cells transfected with either EGFP (left panel) or EGFP-TPD52 (right panel) fusion protein producing recombinant vector. After 24 h cells were observed under microscope for expression of fusion protein. (B) Confirmation of expression of EGFP-TPD52 by Western blotting with anti-EGFP antibody.

3.4.2 Downregulation of TPD52

To study the effect of TPD52 down regulation on LNCaP cells, TPD52 was down regulated by using RNAi technology. Three different shRNA oligos were designed with the conserved sequence of all isoforms of TPD52 and cloned into pSuper-neo-gfp vector. The sequencing of recombinant vector revealed two pairs (shRNA204 and shRNA350) were successfully cloned with out any mutations. Human TPD52 (isoform 3) cDNAwas subcloned into the psiCHECK.-2 vector using the *XhoI* and *NotI* restriction sites at 3' region of *Renilla* luciferase gene. To validate the efficiency of the shRNA, siCHECK™-2-TPD52 and pSuper-shRNA204 or shRNA350 were co-transfected (1:10 ratio) into LNCaP cells. After 24 h of post-transfection, *Renilla* and firefly luciferase activities were measured using the Dual-Luciferase® Reporter assay system. The *Renilla* luciferase data has been normalized to firefly luciferase data. The data represented here is from three independent experiments in triplicates. The result indicates that the shRNA204 is the best and TPD52 is down regulated upto less than 10% (Fig 21).

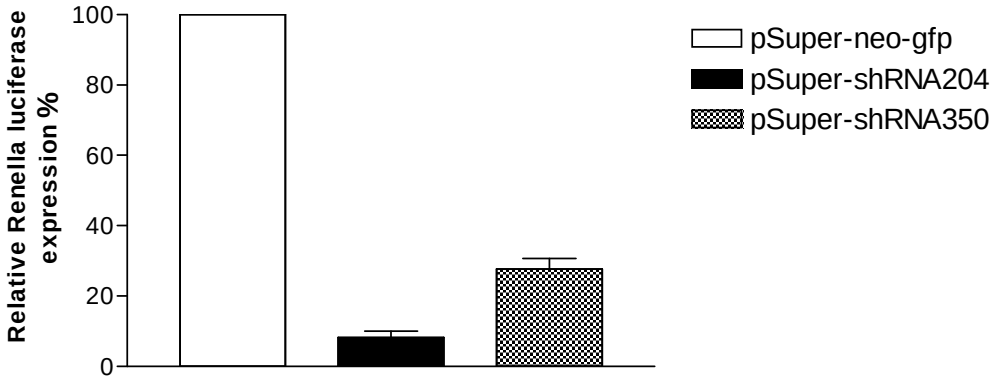

Figure 21: Luciferase assay to determine the efficiency of shRNA oligo pairs on 24 h post transient transfection of siCHECKTM-2-TPD52 and shRNA expressing or control pSuper-no-gfp vector.

To evaluate down regulation of endogenously expressed TPD52 in LNCaP cells, transfection of pSUPER.neo-gfp vector expressing shRNA into EGFP-TPD52 positive cells confirmed the downregulation of TPD52 upto 40% at transcriptional level after 24 h (Fig 22A&B). A significant downregulation was observed on protein level, as confirmed by Western blotting (Fig 23A) with anti-EGFP antibody and densitometric quantification. Corresponding bands have shown a reduced expression of EGFP-TPD52 down to 40% of control level (Fig 23B). No significant difference was observed between non-transfected and mock transfected cells.

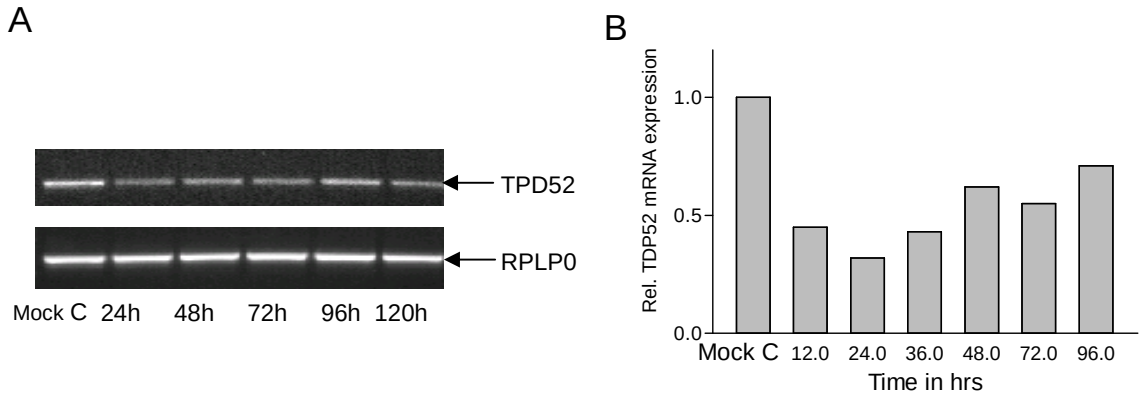

Figure 22: Down regulation of TPD52 mRNA (A) Downregulation of TPD52 by shRNA. Kinetics of TPD52 knockdown, mRNA expression was assessed by semiquantitative RT-PCR. (B) quantitative real-time PCR after LNCaP cells were transfected with vector producing specific shRNA or mock vector and incubated for the indicated times, columns, mean values of two experiments in triplicates.

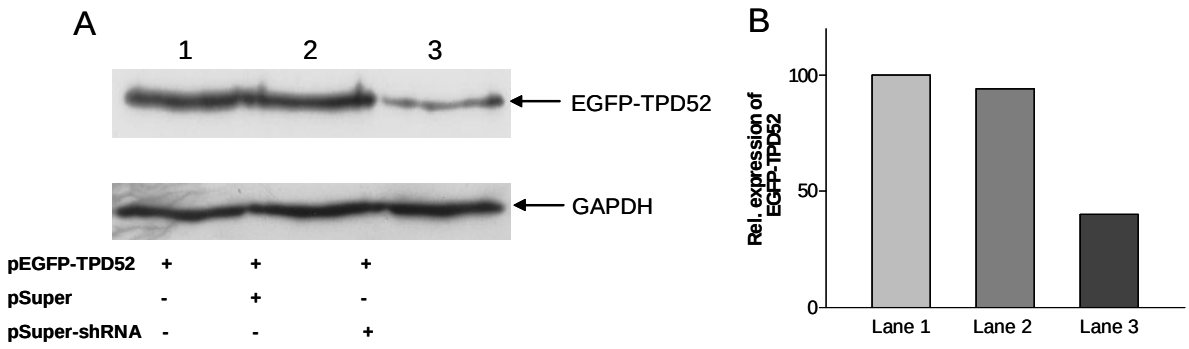

Figure 23: (A) Western blotting for EGFP-TPD52 knockdown. EGFP-TPD52 positive LNCaP cells were transfected with shRNA or control vector and incubated for 24 h. Total protein (30 µg) was separated by a 12% SDS-PAGE and detected with anti-EGFP antibody. Lane 1: EGFP-TPD52 positive cells; Lane 2: EGFP-TPD52 positive cells transfected with control; Lane 3: EGFP-TPD52 positive cells tranfected with specific shRNA. (B) Quantitation of Western blot signals showing 40% of downregulation.

3.4.3 Dysregulation of TPD52 causes changes in the proliferation rate of LNCaP cells

To determine the effect of TPD52 expression on cell proliferation, MTT assays were performed after overexpression or downregulation of TPD52 in LNCaP cells. MTT assays showed a significantly increased proliferation of the prostate carcinoma cell line LNCaP after transient overexpression of EGFP-TPD52 (Fig 24A). The proliferation of these cells was 20% higher than the proliferation of EGFP-transfected control cells 48h after transfection. Dihydroxy testosterone (DHT) was used as a control in MTT assays. On the other hand downregulation of TPD52 leads to decreased cell proliferation, an effect that could be suppressed to a certain extent when growth medium was supplemented with 1mM DHT (Fig 24B). Proliferation data has shown increased proliferation in the presence of DHT.

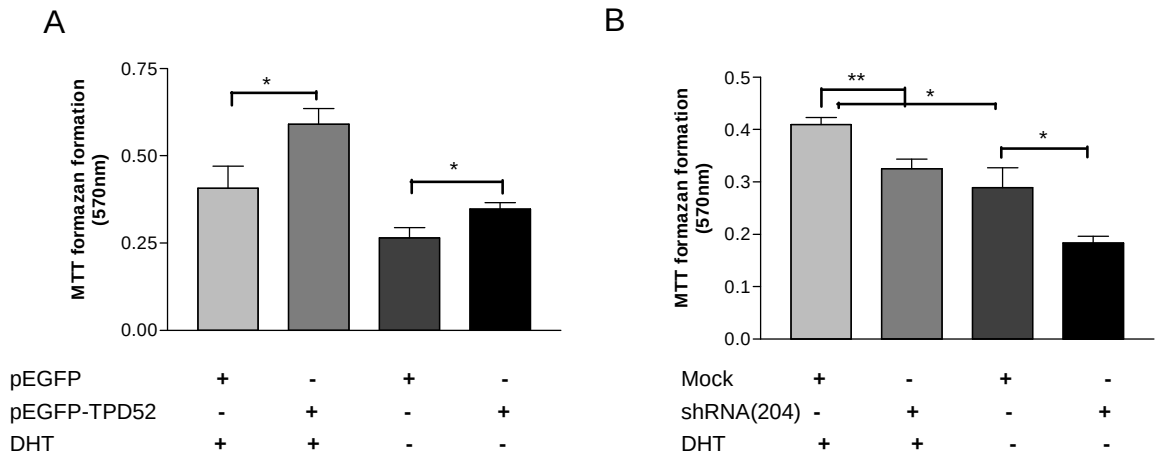

Figure 24: Influence of TPD52 overexpression on the proliferation of the prostate carcinoma cell line LNCaP. (A) Cell proliferation after over expression of TPD52 and (B) cell proliferation after down regulation of TPD52. Viability of cells was measured in a colorimetric MTT assay by the detection of formazan formation. Proliferation of control cells transfected with EGFP was set to 100%. Results are mean of four independent experiments +/- SEM and dihydroxytestosterone (DHT) was used as a control for proliferation of LNCaP cells.

3.4.5 Silencing of TPD52 by shRNA leads to apoptosis in LNCaP cells

Cell death was analysed by flow cytometry. PI was applied to LNCaP cells depleted for TPD52 expression to measure cell death. Based on flow cytometry results we observed approximately 36% cell death in TPD52 depleted LNCaP cells in comparison to mock transfected cells (Fig 25A to D). To get further insight into the mechanisms by which TPD52 downregulation induces cell death we determined the involvement of caspase activation and mitochondria membrane depolarization.

In many cell types, activation of procaspase-3 is a distinguishing feature of apoptotic cell death. Thus, we first examined whether caspase-3 is activated after downregulation of TPD52 (Fig 26A). We observed a 3.5 fold activation of caspase-3 in TPD52 knockdown LNCaP cells compared to mock transfected cells ($p \leq 0.0008$). To get further information on the apoptosis signalling triggered by TPD52 downregulation, we next examined caspase-9 activation in TPD52 depleted LNCaP cells (Fig 26B). After shRNA mediated knock down of TPD52 in LNCaP cells, caspase-9 is activated by 1.6 fold compared to control cells ($p \leq 0.0213$). Additionally, we examined the effect of TPD52 depletion on the mitochondrial membrane depolarization by determining $\Delta\psi_m$ potential after 48 h of TPD52 downregulation

in LNCaP cells (Fig 26C). In 30% of the TPD52 knockdown cells we could observe a significant decrease of $\Delta\psi_m$ ($p \leq 0.0013$), whereas less than 5% of the non-transfected or mock transfected cells suggesting that the depolarization of the mitochondrial membrane leads to cytochrome *c* release which in turn activates caspase-9 to initiate apoptosis. Taken together, activation of caspases-3, caspase-9 and the loss of mitochondrial membrane potential suggests that the downregulation of TPD52 leads to the activation of the intrinsic pathway to initiate apoptosis in LNCaP cells.

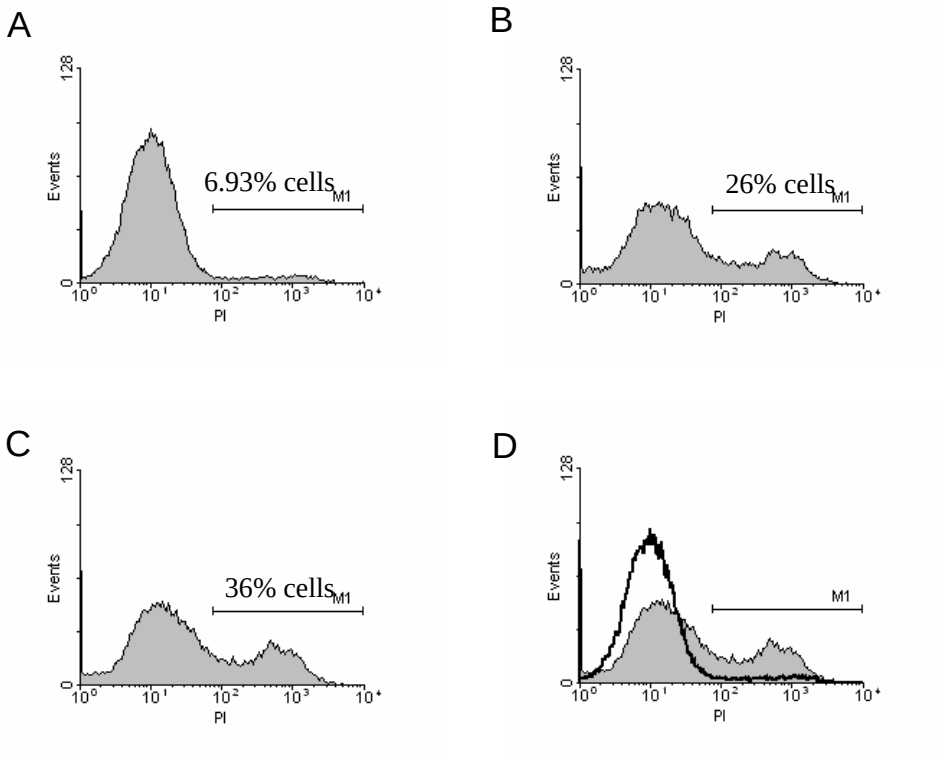

Figure 25: Downregulation of TPD52 induces cell death in LNCaP cells. Cells were transfected with specific shRNA or mock control using Lipofectamine™ 2000 and cell death measured by PI staining using FACS analysis at indicated time points. (A) Mock transfected cells (B) cells transfected with specific shRNA after 24hrs (C) after 48hrs and (D) Overlay of A and C.

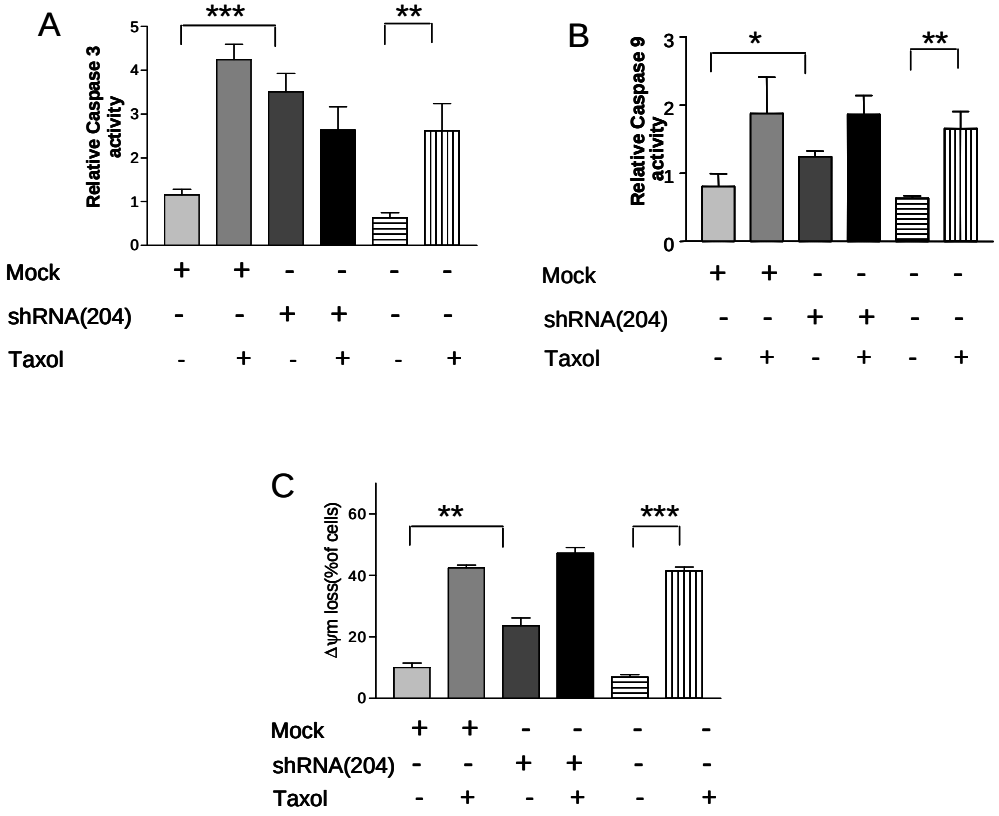

Figure 26: TPD52 down regulation activates caspase-3 (A) and caspase-9 (B) and influences mitochondrial membrane potential dissipation (C) assessed by cytofluorimetric analysis of $DIOC_6$. Columns indicate mean values of 3 independent experiments in triplicates; bars with SD.

3.4.6 Influence of TPD52 overexpression on LNCaP cell migration

Haptotactic cell migration assays with vitronectin and collagen type I demonstrated that the overexpression of EGFP-TPD52 stimulates specifically αvβ3-mediated LNCaP cell migration on vitronectin (Fig 26A, $p \leq 0.0029$), but not integrin β1-mediated cell migration on collagen type I (Fig 27B). The observed effects could not be confirmed in EGFP-TPD52 expressing MCF-7 cells (Fig 27C).

To investigate the activation of PKB/Akt pathway, EGFP-TPD52 or EGFP expressing LNCaP cells were allowed to attach to vitronectin coated plates. After intervals of 2 and 4 h, the amount of phosphorylated PKB/Akt (Ser 473) was analyzed. We observed a significantly increased phosphorylation of PKB/Akt in EGFP-TPD52 expressing cells compared to EGFP expressing cells after 4 h of incubation on vitronectin (Fig 28).

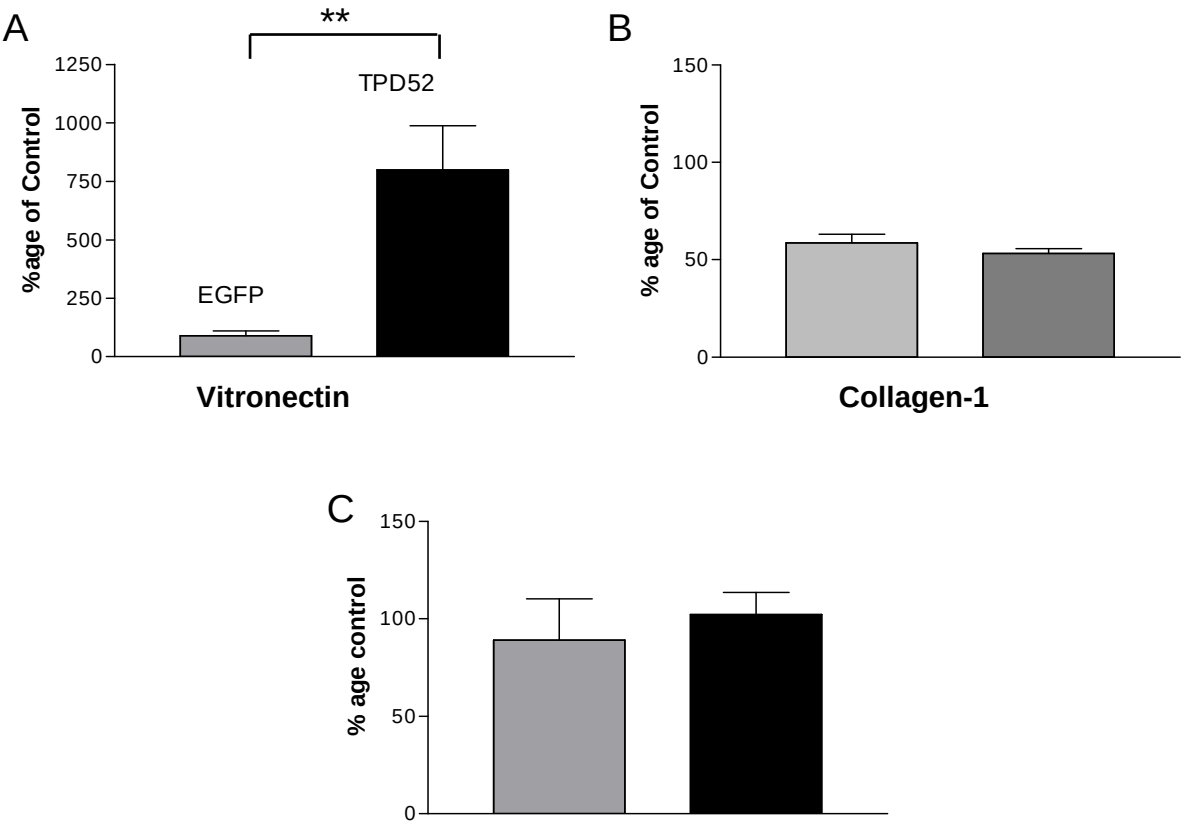

Figure 27: Overexpression of TPD52 stimulates cell migration. LNCaP cells transiently transfected with EGFP-TPD52 or EGFP as a control were analysed by haptotactic cell migration toward vitronectin $p \leq 0.0029$ (A) and collagen type I (B). (C) MCF-7 cells did not show any change cell migration with over expression of TPD52. Data represent the results from three independent experiments in triplicates and are given as mean values ± SEM.

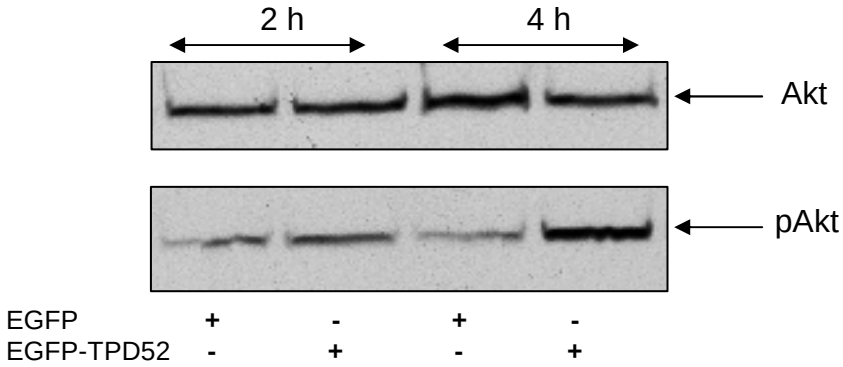

Figure 28: Adhesion of EGFP-TPD52-LNCaP cells to vitronectin increases PKB/Akt (ser 473) phosphorylation. EGFP or EGFP-TPD52 positive LNCaP cells starved in serum free medium for 24 h were harvested and seeded on vitronectin coated dishes at 37°C for indicated time intervals. Total protein of harvested cells (20 µg per lane) separated on 12% SDS-PAGE. Phosphorylation of PKB/Akt was detected by polyclonal phospho-Akt (ser 473) antibodies and loading control PKB/Akt was detected by polyclonal Akt antibodies.

3.4.7 TPD52 interacts with the peroxiredoxin1 (Prx1)

To perform GST pull down assays, optimization of protein induction with IPTG and purification with Glutathione Sepahrose® 4B has given reasonably pure protein as shown in the following figure to perform GST pulldown assays. The bound proteins on the column were eluted with 50 mM reduced glutathione in the binding buffer. The eluted protein fractions were analysed using 12% SDS-PAGE (Fig 29) confirmed the purity of the fusion protein sufficient to perform pull-down assays.

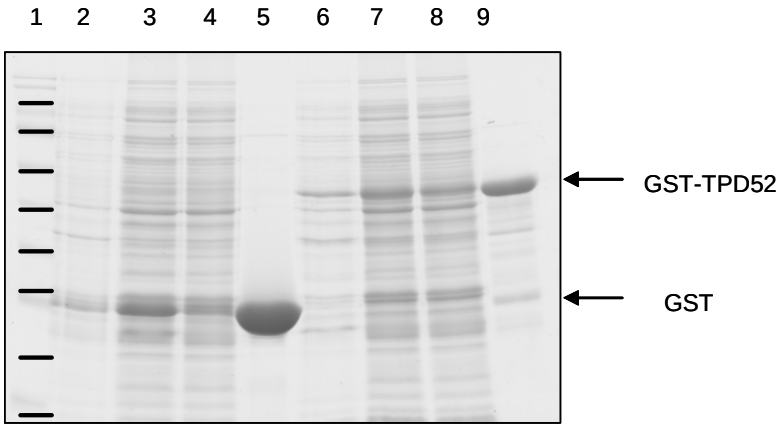

Figure 29: Expression of GST or GST-TPD52 was induced by IPTG and purified by using Glutathione Sepahrose® 4B followed by elution with reduced glutathione. Lanes 2; GST Lysate, 3; un bound, 4; wash, 5; Eluate of GST, 6; GST-TPD52 lysate, 7; unbound, 8; wash, 9; Eluate GST-TPD52.

GST pull-down assays followed by 2-DE coupled mass spectrometry indicated an interaction between TPD52 and Prx1 in LNCaP cell extracts (Fig 30). Subsequent Western blotting analysis using anti-Prx1 antibody after GST capture assay (Fig 31A) confirmed the interaction of GST-TPD52 with Prx1 but not with GST alone. To evaluate this interaction, co-immunoprecipitation was carried out from FLAG-TPD52 expressing LNCaP cell extracts with anti-FLAG antibody followed by detection with anti-Prx1 antibody (Fig 31B). These experiments confirmed the specific interaction between TPD52 and Prx1 *in vitro.*

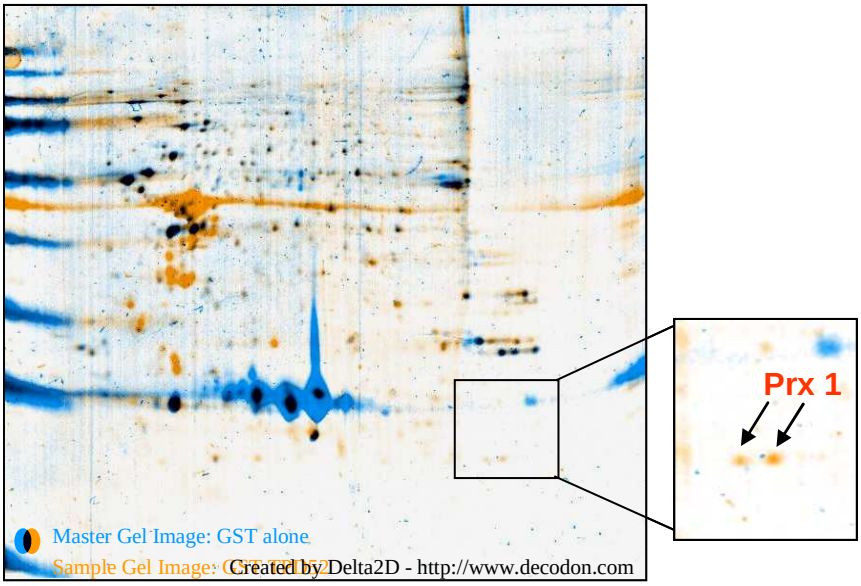

Figure 30: (A) GST pull down assay, LNCaP cell lysate incubated with purified GST, or GST TPD52 fusion proteins bound to glutathione-Sepharose beads. After washing bound proteins were prepared in rehydration buffer and subjected to 2DE. Coomassie stained gel images were overlaid by Delta 2D (Blue, proteins bound to GST and Orange proteins bound to GST-TPD52). Protein spots bound to fusion protein were identified by mass spectrometry. Enlarged region indicates Prx1 bound to GST-TPD52.

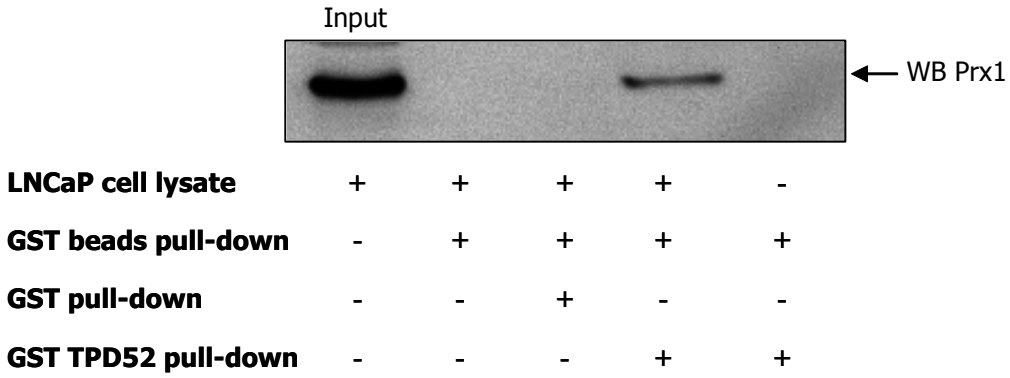

Figure 31(A)**:** GST or GST-TPD52 fusion protein bound to glutathione-Sepharose beads were incubated with LNCaP cell lysate. Bound protein was separated by SDS-PAGE and Prx1 detected by Western blotting.

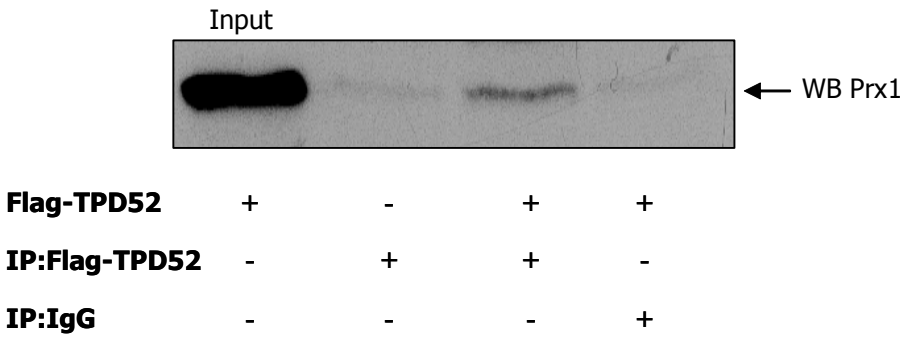

Figure 31(B)**:** Immunoprecipitation with anti-FLAG antibody. FLAG-TPD52 positive or negative cells were lysed in RIPA buffer. Immunoprecipitation was performed with anti–FLAG antibody and precipates were separated by 12% SDS-PAGE and Prx1 was detected with anti-Prx1 antibody. IgG was used as isotype control.

3.4.8 Localization of TPD52

Localization of TPD52 was investigated by indirect double immunofluorescence. To investigate localization of TPD52, Flag-TPD52 producing vector transfected into LNCaP cells were seeded on coverslips. After 24 h, cyt *c* a mitochondrial marker and Flag TPD52 were detected by rabbit anti cyt *c* and mouse anti Flag antibodies respectively. For secondary antibodies, Cy2 (green) and Cy3 (red) labels were used for cyt *c* and Flag respectively. The red fluorescence for Flag-TPD52 was observed as particulate structures (Fig 32B). The staining for TPD52 is perinuclear and particulated staining may be due to the distribution of exogenously expressed TPD52 between soluble and insoluble fractions. Immunostaining for cyt *c* in green (Fig 32A) and overlay of two images show partial co-localization of both proteins demonstrating mitochondrial distribution of Flag-TPD52 (Fig 32C). A small C-termainl flag cannot alter the localization of the fusion protein indicating mitochondrial localization of TPD52.

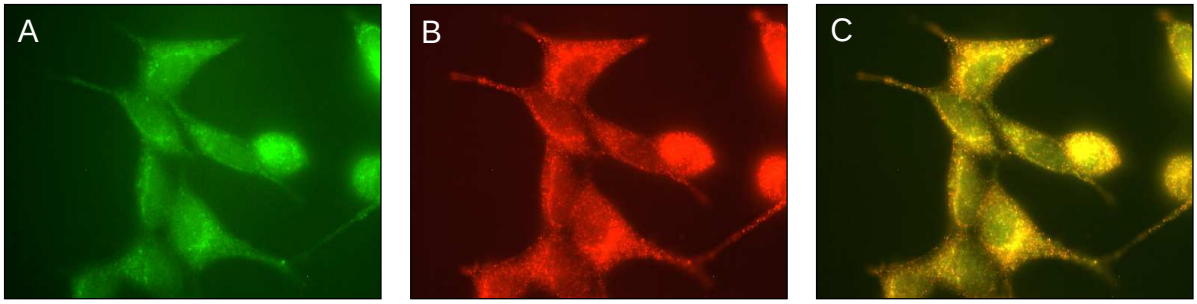

Figure 32: Mitochondrial distribution of exogenously expressed TPD52. (A) Immunofluorescence for cyt *c* in green (B) Flag-TPD52 in red and (C) Overlay of A&B indicating intracellular distribution of TPD52 in mitochondria.

3.4.9 Overexpression and purification of (His_6)-TPD52

Overexpression of the TPD52 from pETM-11 clones was performed in E. coli expression host BL21 Codon Plus. The His_6-TPD52 was successfully expressed as soluble protein. Expression was tested at different time points varying IPTG concentration at 37^0C. The level of expression with IPTG at 37^0C for 4 h was much higher as compared to other conditions. Further large volume cultures were induced for protein expression under the same conditions. Protein expression was tested by subjecting a small fraction of cell lysate to SDS-PAGE followed by coomasie staining (Figure 33). The molecular weight of the protein expressed after induction with IPTG is matching with the theoretical molecular weight of the His6TPD52.

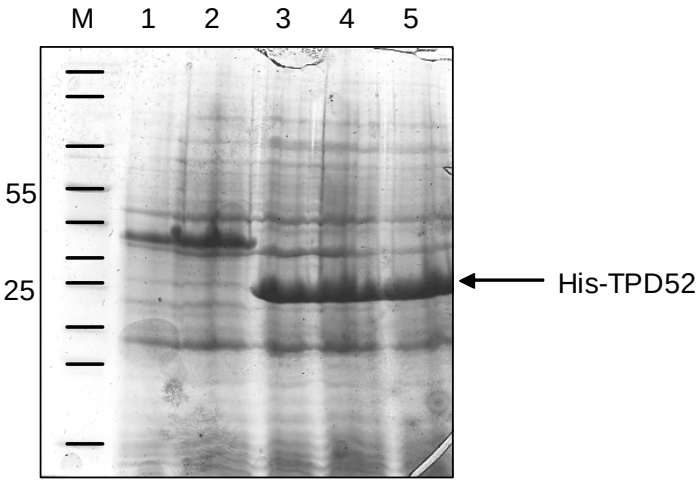

Figure 33: Induction of clones with IPTG for His6-TPD52 expression analyzed with SDS-PAGE. Lanes 1 and 2 clones with empty vector, lanes 3 to 5 are clones expressing recombinant protein after induction with IPTG.

Recombinant protein TPD52 was purified in three steps: affinity chromatography (using Ni-NTA), anion exchange chromatography (using anion exchange column HQ) followed by size exclusion chromatography (using Sephadex 16/60). The protein was eluted as a monomer by size exclusion chromatography (Figure 34). The SDS-PAGE profile shows a single band at 20 kDa and the purity of the proein was highly satisfactory to perform further experiments. The protein was stored at 4^0C and was stable for weeks without degradation. The purified protein was concentrated and used for biophysical characterization and crystallization trials.

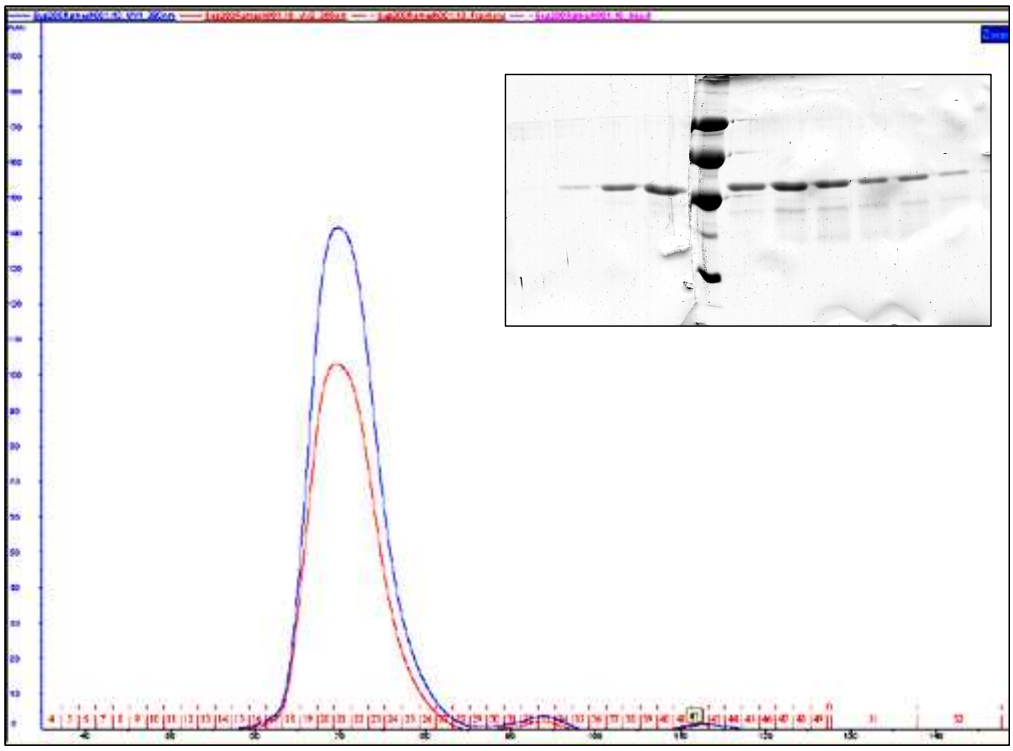

Figure 34: Gel filtration chromatography for purification of (His_6)-TPD52 after metal chelate and anion exchange chromatography. The peak fractions from 18 to 26 indicated in chromatogram checked for purity in SDS-PAGE shown in inset of the figure.

3.5 Expression of active and inactive caspases in prostate cancer

3.5.1 Histology and Grading of tumors

All prostates were evaluated by H&E staining and revealed Gleason scores between 3-8 and pT stage from 2a-3c (Table 05). During the clinical follow up after surgery (24 months) metastases were diagnosed in one patient.

Table 05 Gleason score and tumor stage of PCa samples

	Gleason score			pT		Total
	3-4	5-6	7-8	2a-2c	3a-3c	
Number of specimens	4	9	7	17	3	20

pT tumor stage.

3.5.2 Imunohistochemistry for expression of caspases and statistical analysis

Immunohistochemistry for caspase-1 showed a weak (+) cytoplasmic staining in non neoplastic tissue and in tumor tissue of all samples investigated. For caspase-9 immunostaining was observed in the cytoplasm of some prostate basal cells as well as in some tumor cells (+). The changes in expression level for caspase-1 and -9 are not significant (Table 06). Caspase-3 immunoreactivity was predominantly seen in the cytoplasm of basal cells of normal prostate tubuli (++). In most of the apical cells no immunostaining was evident (Fig. 35A). In prostate tumor tissue of all patients more than 50% of tumor cells were caspase-3 positive (++) (Fig 35B&38A,). Otherwise c-caspase-3 was strongly expressed in apical cells of non neoplastic tissue (+++, mean ± SEM 2.833 ± 0.09) whereas only few tumor cells were immunopositive for the active caspase (+, mean ± SEM 1.444 ± 0.166) ($p< 0.0001$, Fig. 35C, D & 38B). Immunostaining for caspase-6 was found in all basal and apical cells of normal prostate glands and in all tumor cells (+++) (Fig. 36A-B&38C). C-caspase-6 was strongly expressed (+++, mean ± SEM 2.00 ± 0.1617) in apical cells of normal prostate glands whereas tumor cells showed a moderate immunostaining (++, mean ± SEM 1.167 ± 0.0903) ($p< 0.0001$, Fig. 36C, D &38D). Immunohistochemical expression of Bcl-2 was seen in nearly all basal cells of non neoplastic prostate glands (+++, mean ± SEM 2.75 ± 0.099). However, tumor tissue showed a weak immune response for Bcl-2 (+, mean ± SEM 1.3 ± 0.105) ($p< 0.0001$, Fig. 37A, B&38E). In the control sections no staining was evident. The semi quantitation data for expression of all caspases and Bcl-2 was included in the Table 06.

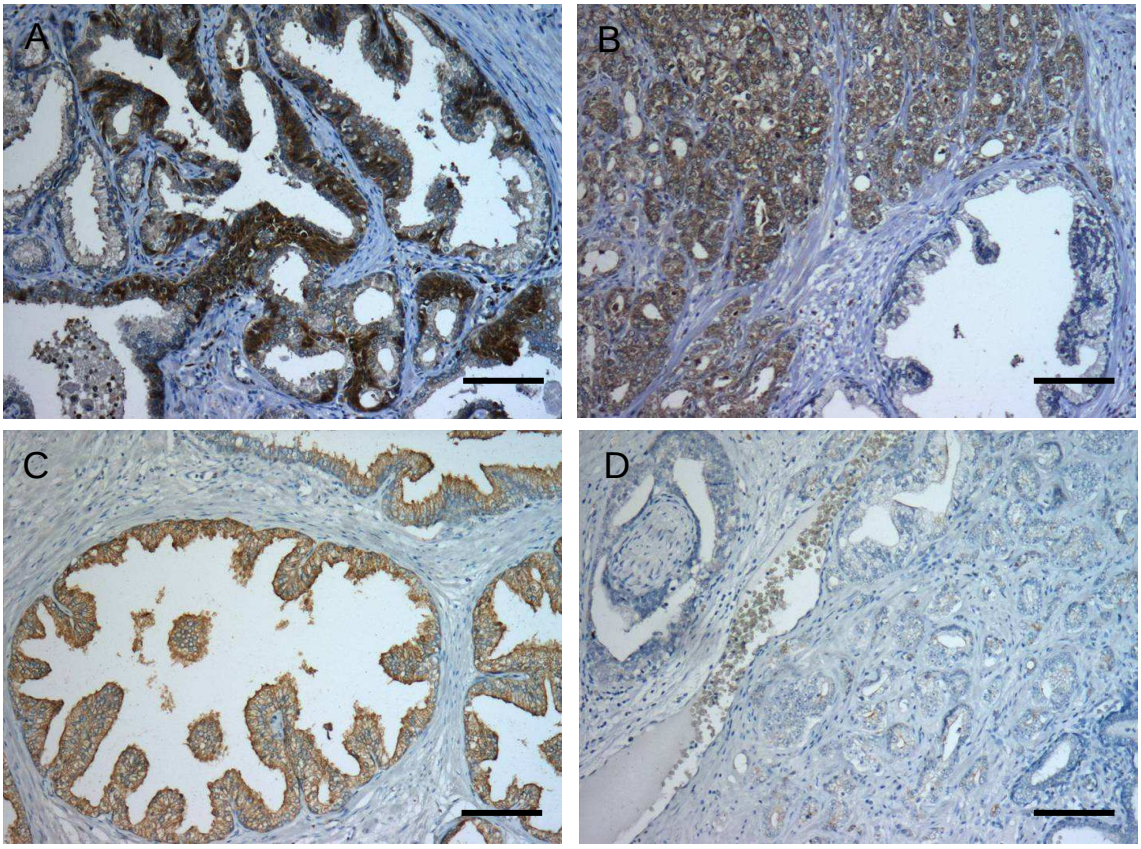

Figure 35: Immunostaining of uncleaved and cleaved caspase-3 in BPE and PCa. Uncleaved caspase-3 in BPE (A) and in PCa (B) Cleaved caspase-3 in BPE (C) and in PCa (D). Bar represents 100 µm.

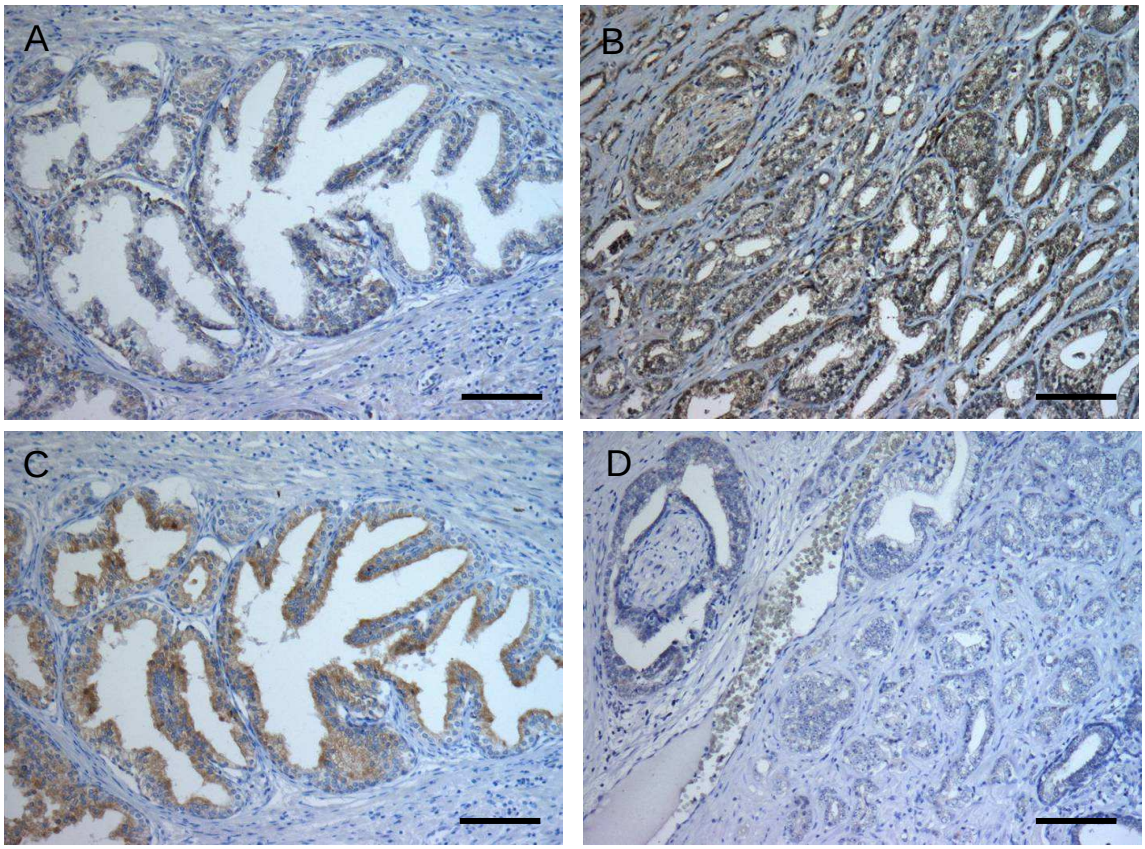

Figure 36: Immunostaining of uncleaved and cleaved caspase-6. Uncleaved caspase-6 in BPE (A) and PCa (B), cleaved caspase-6 in BPE (C) and in PCa (D) Bar represents 100 µm.

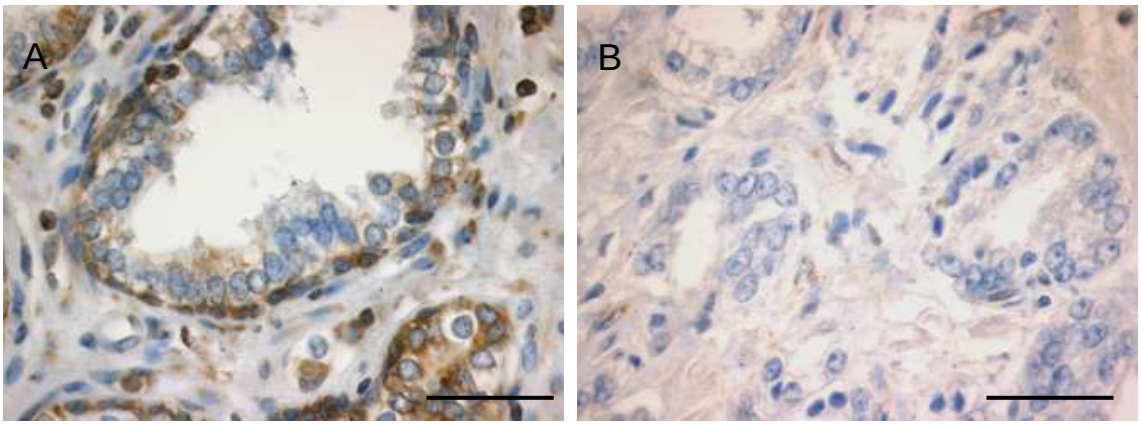

Figure 37: Immunostaining of bcl-2 in BPE (A) and PCa (B). Bar represents 20 µm.

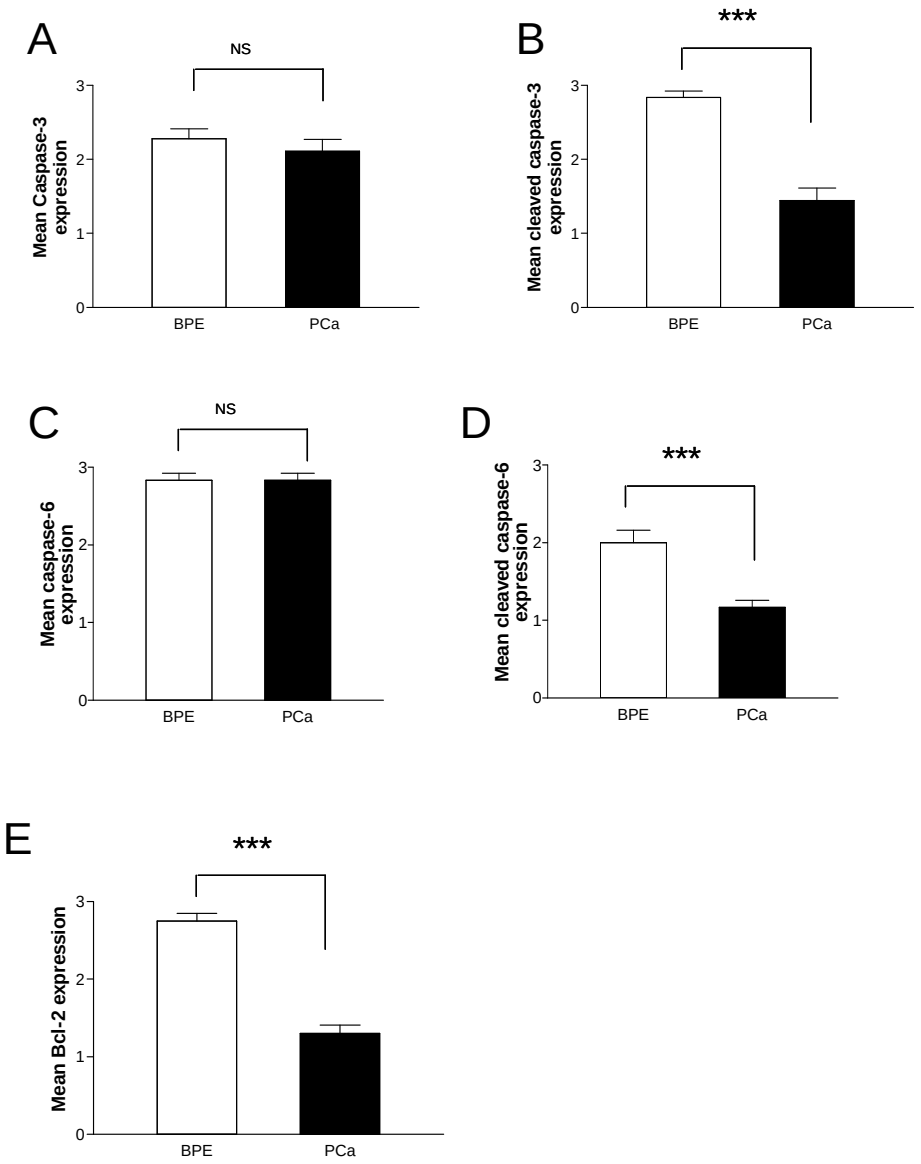

Figure 38: Mean caspase-3 (A) and cleaved caspase-3 (B) immunohistochemistry scores in normal/tumor samples. Mean caspase-6 (C) and cleaved caspase-6 (D) immunohistochemistry scores in normal/tumor samples. Mean Bcl-2 (E) expression was observed in PCa in comparison with the BPE.

Table 06: Summary of patient data and expression of caspases in normal and tumor tissue

specimen	age	Gl	pT	M	Caspase 3				Caspase 6				Caspase 1		Caspase 9		Bcl-2	
					uncleaved		Cleaved		uncleaved		cleaved							
					BPE	PCa	BPE	PCa	BPE	PCa	BPE	PCa	BPE	PCa	BPE	PCa	BPE	PCa
1	62	3+4=7	2b	0	3	3	3	1	3	3	2	1	1	1	1	1	2	1
2	52	3+3=6	2b	0	2	2	3	1	3	3	2	1	1	1	1	1	3	1
3	63	2+3=5	2b	0	2	2	3	2	3	3	2	1	1	1	1	1	3	1
4	62	2+3=5	3a	0	2	1	3	3	2	2	2	1	1	1	1	1	2	1
5	70	3+4=7	2c	1	3	1	3	1	3	3	3	1	1	1	2	1	3	1
6	62	3+4=7	2c	0	1	2	3	1	3	3	2	2	1	1	1	1	3	1
7	71	3+4=7	3c	0	2	3	3	2	3	3	1	1	1	1	1	2	3	2
8	68	2+2=4	2c	0	2	1	3	1	3	3	1	1	1	1	1	1	3	1
9	67	2+2=4	2a	0	2	2	3	1	3	3	3	1	1	1	1	1	2	1
10	68	2+3=5	2c	0	2	2	2	2	3	3	2	1	1	1	1	1	3	2
11	59	1+2=3	2b	0	2	2	3	1	3	2	3	2	1	1	1	1	3	2
12	60	2+3=5	2b	0	3	2	3	2	3	3	2	1	1	1	1	1	3	1
13	68	3+4=7	2c	0	2	3	2	1	3	3	2	1	1	1	1	1	3	1
14	66	2+3=5	2a	0	2	3	2	1	3	2	3	1	1	2	1	1	3	1
15	70	2+3=5	2b	0	3	2	3	1	2	3	1	1	2	2	1	1	3	1
16	65	2+3=5	2a	0	2	2	3	3	3	3	2	1	2	2	1	1	3	2
17	66	3+4=7	3a	0	3	2	3	1	3	3	2	1	1	1	1	2	2	2
18	65	3+5=8	2b	0	3	3	3	1	2	3	1	2	1	1	1	1	3	2
19	64	1+2=3	2a	0	*	*	*	*	*	*	*	*	1	1	2	1	2	1
20	65	2+3=5	2b	0	*	*	*	*	*	*	*	*	1	1	1	1	3	1

age at diagnosis; [Gl]: Gleason score; [pT]: tumor stage; [M]: metastasis; [BPE]: benign prostate epithelium, [PCa]: prostate cancer. *: not investigated due to limited material.

4 Discussion

4.1 Proteomic analysis of Prostate biopsies

With the latest advances for early diagnosis and the development of new therapeutics for efficient treatment, mortality rate of prostate cancer has been decreased significantly. In spite of all new treatment strategies to increase survival, PCa is the most common type of cancer found in men of western countries and is the leading cancer death next to lung and colorectal cancer. The low sensitivity and specificity of current diagnostic methods for prostate diseases underscores the need for improvement in this area. Histological investigation is usually performed on biopsies to distinguish between benign prostate hyperplasia and prostate cancer. Proteomic technologies are promising approaches to obtain further information, but so far this molecular characterization is restricted to the large amount of material available in surgical samples. In this study, we focused our proteomic analysis on biopsies to identify new biomarkers which distinguish PCa and BPH. Previously, proteomic studies on PCa identified a large number of differentially expressed proteins and some were reported as potential markers for diagnosis of localized prostate cancer [60,123-125,157]. However, these expression profiling studies have been carried out on radical prostatectomy specimens or on formalin-fixed paraffin-embedded (FFPE) tissue sections [120]. Proteomic analysis of prostate biopsies would enable biomarker investigations of pathologically characterized clinical samples. Recent advances in proteomics technology provides an excellent opportunity to characterize the proteins, modified or unmodified, involved in tumorigenesis and cancer progression. Even if in most cases only 3 of 12 pathological evaluated biopsies indicated cancer, we asked whether existing tumor microenvironment might reflect the typical cancer protein signature which we would assign both to PCa and BPH.

In the current study we performed IEF over the pI range 4-7 and SDS-PAGE gels were stained with SYPRO® ruby to achieve high sensitivity in spot detection and to ensure better quantitation of protein spots. Our data on prostate biopsy material showed differential expression of 88 spots representing 79 different proteins in PCa patients (Table 02). We included only such protein spots showing differential expression of more than 1.5 fold in all samples from PCa patients. We strongly suggests that 50% change in expression of particular protein is enough to show significant effects on physiology and pathology of the biological system. With this choice we tried to include the marker proteins with very low

expression levels because analysis criteria with higher fold change may exclude them. Recently Lin *et al.* (2007) reported proteomic data of prostate biopsies using the pI-range 3 - 10 NL in IEF and silver staining for visualization of protein spots [132]. Comparing the list of differentially expressed proteins many can be found in both records, though, Lin *et al.* did not find significant changes of proteins such as peroxiredoxin 1 and 2, HSPB1 or PPAP, a marker protein known to be upregulated in prostate cancer [158]. In our study we found upregulation of PPAP and HSPB1 in cancer patients which confirmed the presence of tumor in biopsies selected for proteomic analysis and the data published during this year (Ummanni et al. 2008). The difference may in part be due to the different methods used. By using SYPRO® ruby we applied a very sensitive stain which allows a reliable quantitation. Among the differentially expressed proteins found in both records are FKBP4 and HSPs including CH60, HSP71, HSPB1, DDAH1, PSME2, GELS, TAGL etc. [132]. This strongly supports the reliability of proteomic approaches for proteomic analysis of prostate biopsy material and demonstrates its value as a diagnostic tool which does not require radical prostatectomy.

4.2 Prohibitin can distinguish hyperplasia and cancer

Among the identified proteins one showing notably altered expression was prohibitin which was upregulated in cancer. Data from our expression analysis strongly confirmed that prohibitin is highly elevated in PCa but not in BPH. Prohibitin is an important regulator of the cell cycle involved in inhibiting DNA biosynthesis [159] and has been shown to be upregulated in gastric cancers [160,161]. Previous reports indicated that prohibitin mRNA and/or protein are highly expressed in transformed cells and tumors, rather than decreased expression in tumors as expected for a tumor suppressor protein [162-167]. As yet it is unclear whether the protein or the mRNA exhibits its tumor suppressor function. In order to investigate mRNA expression level, we analyzed the PHB expression of 20 RNA samples (8 × BPH, 12 × PCA) obtained from same biopsies used for proteome analysis by real-time SYBR Green PCR. The result suggests clear overexpression of PHB at the transcriptional level in PCa samples. We would like to point out that tumorigenesis affects the expression of almost all classical “housekeeping” genes, which may lead to unreliable results. Therefore for relative quantification of PHB expression we used the ribosomal protein large P0 (RPLP0) as a well suited normalizing gene [168].

Prohibitin has been shown to localize to the mitochondria [169,170], but nuclear localization has also-though controversially been reported for different cell types [171,172]. A recent study demonstrated translocation of prohibitin to the cytosol and showed that silencing of prohibitin expression decreases the apoptotic response to TGF-beta and TGF-beta induced cell migration in androgen responsive cells [173]. Mitochondrial prohibitin may function as a chaperone like HSP60 and mortalin. These mitochondrial chaperones play important roles in tumorigenesis and cancer development, whereas nuclear prohibitin in hormone responsive cells may provide an additional - nuclear - cell cycle regulation [174,175]. In *in vivo* studies with breast cancer cell types it has been documented that prohibitin is able to inhibit transcriptional activation by E2F [172,176]. It has also been shown that prohibitin inhibits androgen dependent growth in LNCaP cells via negative effects on the transcriptional activity of the androgen receptor (AR) and other closely associated receptors [177,178]. Moreover, the PHB family proteins are overexpressed in a large variety of human neoplasms as has been shown immunohistochemically [170]. Our study also found that prohibitin was as highly expressed in prostatic intra epithelial neoplasia as in prostatic carcinoma, but not in benign prostate epithelium or proliferative inflammatory atrophy. This suggests that prohibitin expression may occur early in the development of cancer. Immunostaining for prohibitin is cytoplasmic and it may be restricted to mitochondria. In conclusion the results from our study demonstrate the reliability of proteomic analysis of prostate biopsies to analyze global protein expression pattern of prostate biopsy specimens and to find molecular biomarkers for early diagnosis or drug targets for therapy. From the proteins identified prohibitin may be useful to distinguish PCa and BPH, however to verify this protein as a marker its role in prostate cancer needs to be elucidated.

4.3 TPD52 is overexpressed in prostate cancer

Among the identified proteins, TPD52 is overexpressed in PCa compared to BPH. In the present study, we demonstrate the physiological consequences of TPD52 expression in the androgen responsive prostate cancer cell line LNCaP. TPD52 is a member of the TPD52 gene/protein family located on 8q21 chromosome. Its encoding gene is also referred as PrLZ and is a proto-oncogene [179]. TPD52 is overexpressed in breast [180,181] prostate [182,183] as well as in ovarian cancers [184] due to gene amplification. Its overexpression

in various tumors was shown by DNA micro array analysis and high density tissue micro arrays (TMA). Its over expression due to gene amplification was confirmed by aCGH, SNP arrays and FISH analysis to measure gene copy number on clinically localized prostate cancer specimens [185-188]. The identification of TPD52 as a tumor associated antigen in breast cancer patients highlights it as a gene amplification target [189]. Expression of recombinant TPD52 in acini of rat pancreas stimulates amylase secretion [190]. In either human or mouse fibroblasts was also reported to correlate with the acquisition of epithelial characteristics of these cells [191]. As reported previously, results from our proteomic analysis to define protein signature of prostate cancer biopsies revealed overexpression of TPD52 in cancer patient material [192]. Real time PCR confirmed overexpression at mRNA level.

4.4 Functional Characterization of TPD52 in LNCaP cells

Until now there is only limited information available about the main physiological role of TPD52 in prostate cancer progression. Wang et al. examined TPD52 expression during early embryonic and adult tissues found that TPD52 expression increases with age and undergo translocation during development from early to adult tissues [193]. In the present study, we investigated the responsiveness of the LNCaP human prostate carcinoma cell line after deregulation of TPD52 expression. LNCaP is an androgen responsive cell line and the expression of TPD52 is controlled by androgens mainly testosterone which is the major circulating antigen. Therefore, we have chosen this cell line to investigate function of TPD52 in PCa progression.

4.4.1 Downregulation of TPD52 induces apoptosis

A common molecular strategy used by tumor cells to evade apoptosis, is the up-regulation of anti-apoptotic proteins or the downregulation of pro-apoptotic proteins. Gene silencing by antisense oligonucleotides or RNAi technology are useful tools to validate candidate proteins [194,195]. In the present study we used shRNA directed against all isoforms of TPD52 cloned into pSUPER.neo-GFP vector, allowing efficient knockdown of TPD52 as revealed by real-time PCR analysis and Western blotting. We found that TPD52 knockdown in LNCaP cells is accompanied by enhanced cell death. This was further confirmed as apoptosis by different methods. Caspase-3 and -9 activities in TPD52 depleted

LNCaP cells were measured and results have shown activation of caspase-3 by 3.5 and caspase-9 by 1.6 fold indicating activation of the caspase cascade on downregulation of TPD52. Furthermore TPD52 depletion affects mitochondrial membrane potential which leads to cytochrome *c* release into the cytosol. This release is responsible for the observed increase of caspase-9 activity which inturn activates caspase-3. Summing up, it is suggested that TPD52 acts upstream of the mitochondria related apoptosis. However, the exact mechanism by which TPD52 influences apoptosis needs to be investigated in detail.

4.4.2 Dysregulation TPD52 alters LNCaP cell proliferation

The expression of TPD52 proteins is linked with cell proliferation in different cancer cell types. This is underlined by reports that the expression of TPD52 in neuroepithelial cells by retroviral transduction indicated its role in cell proliferation [196,197]. The presence of androgen response elements (AREs) in the promoter region of TPD52 gene indicates that the expression of TPD52 is controlled by androgens [198]. Testosterone as the major circulating androgen can trigger AR response which in turn activates various genes for transcription in the nucleus [199]. TPD52 expression at both transcription and translational levels are positively regulated by estradiol in breast cancer cells [200] and androgens in prostate cancer cells. [201-204]. From our study, we noticed that deregulation of TPD52 expression slightly altered proliferation of LNCaP cells. Overexpression of TPD52 increases cell proliferation whereas downregulation decreases the rate of proliferation of cancer cells. DHT can induce the expression of TPD52 in LNCaP cells; proliferation assays in presence of DHT mimic this effect.

4.4.3 Cell migration and activation of Akt/PKB pathway

It has been proposed that cancer arises due to several molecular events leading to transformation of normal to tumor cells and further progression to metastasis including cell migration into the neighbouring tissue, survival and proliferation in the host tissue [205]. Understanding cell migration is also an important part of cancer research. The cells that would not migrate in normal state will start to move in cancer and this is known as metastasis. Investigation of molecular mechanisms involved in cell migration can help us to find new cures for cancer. The expression of several genes such as CARD10 [206], Vav3 [207] and integrins are important to determine the formation of metastatic cells [208,209].

Expression of mD52 (murine TPD52) in NIH3T3 cells induce the expression of several genes involved in promotion of metastasis and the genes responsible for prevention of metastasis were downregulated [210]. A very recent study reported that PrLZ gene is reactivated and its expression increases with cancer progression from primary to tumor metastasis. From our cell migration assays we found that overexpression of TPD52 in LNCaP cells promote cell migration towards vitronectin significantly whereas no change in migration towards collagen type 1 was detected. Integrins are transmembrane receptors composed of α and β subunits (Figure 39). To date, 24 different integrins with different combinations of 8 α and 18 β subunits are known [211].

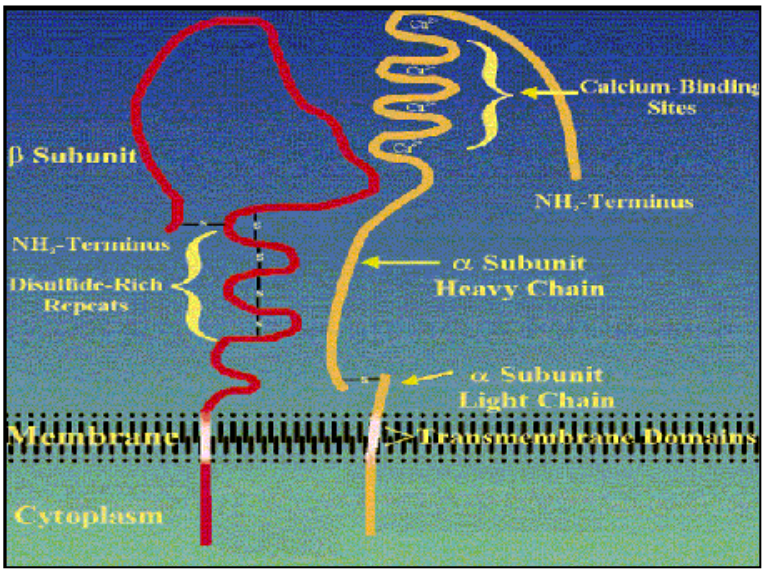

Figure 39: Integrins are transmembrane proteins which bind ligands found in the extracellular matrix. They exist in cells as "heterodimers" composed of α and β subunits. Picture courtesy Dr. Anne Cress, Arizona Cancer Center.

Integrins bind to different extracellular matrix proteins and control functions such as adhesion, migration, differentiation, proliferation, survival and motility [212]. Usually, integrins αvβ3 and αvβ5 are involved in cell migration and attachment to the extra-cellular matrix (ECM) proteins vitronectin, fibronectin, fibrinogen, laminin, osteopontin and others [213]. The integrin αvβ5 was the first identified receptor that can bind to vitronectin [214]. Vitronectin can bind to αvβ5 and αvβ3 integrin receptors. The expression of αvβ3 in LNCaP is controversial. Zheng et al. mentioned that LNCaP cells did not express αvβ3 [215].

Witkowski et al. and Chatterjee et al. reported expression of both αvβ3 integrins in LNCaP cells [216,217]. In addition to these reports, Putz et al. reported that four prostate cancer cell lines that were derived from bone marrow expressing αv and β3 integrin subunits [218]. Cell migration assays after overexpression of TPD52 in MCF-7 cells indicated no change in cell migration towards vitronectin. The MCF-7 cells chosen lack αvβ3-integrin expression, making it possible to demonstrate that overexpression of TPD52 is involved in αvβ3-mediated cell attachment to vitronectin [219,220]. Previously it has been shown that αvβ3 mediated cell migration and adhesion of LNCaP cells to vitronectin activates Akt/PI 3 kinase pathway via phosphorylation of Akt at Ser473 [221]. To investigate αvβ3 integrin mediated activation of Akt pathway on TPD52 expression, our results have shown increased Akt phosphorylation in TPD52 overexpressing cells compared to cells expressing EGFP alone. This confirmed activation of αvβ3 signalinig pathway. In αvβ3 signalinig pathway, ligation of αvβ3 with multiple ligands activates FAK, which interacts and activates PI-3 kinase. The PI-3 kinase activates PKB/Akt by phosphorylation on cell membrane and it phosphorylates several substrates to control various biological processes such as cell migration, adhesion and survival (Fig 37) [222]. A very recent study, reported that expression of PrLZ activates Akt/PKB signalling pathway in prostate cancer cells [223]. The C-terminal domain of PrLZ gene product is homologous with TPD52. Therefore we speculate, integrin mediated activation could be a possible mechanism for Akt activation by TPD family proteins. Taken together, migration studies confirm the involvement of αvβ3 integrin in TPD52 mediated migration of LNCaP cells towards vitronectin. Like breast cancer cells prostate cancer cells metastasize to the bone [222,224]. TPD52 involvement in αvβ3 mediated cell migration may play a role in bone metastasis of prostate cancer patients.

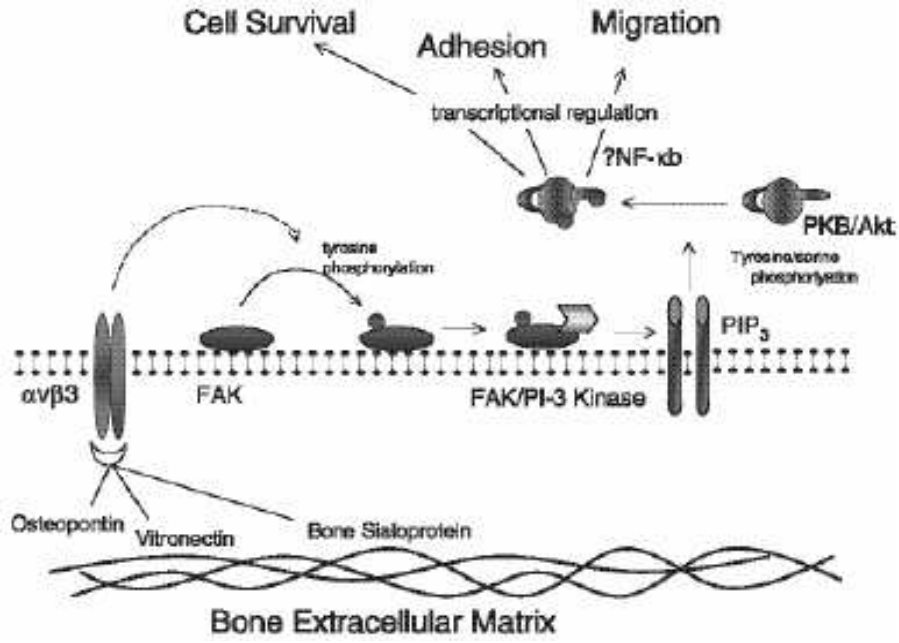

Figure 40: αvβ3 siganiling pathway in prostate cancer cells.

4.4.4 TPD52 interacts with Prx 1 in LNCaP cells

It has been reported that TPD52 interacts with MAL2 [225], a transmembrane proteolipid and annexinVI, a phospholipid binding protein in a calcium dependent manner [226]. Based on a GST pull-down approach, we identified new interacting proteins for TPD52. We found an interaction between TPD52 and Prx1 in LNCaP cells. This interaction was confirmed by co-immunoprecipitation of Prx1 with TPD52. Prx1 is elevated in most tumors such as lung cancer [227,228], breast cancer [229], bladder cancer [230], thyroid cancer [231], oral cancer [232], as well as esophageal squamous cell carcinoma [233], pancreatic adenocarcinoma [234], tongue squamous cell carcinoma [235], prostate carcinoma [236] and ras oncogene-transformed primary mammary epithelial cells [237]. The major functions of peroxiredoxins include cellular protection against oxidative stress and cell proliferation. Prx1 is not only upregulated by oxidative stress but also closely related to cell proliferation and is therefore referred as proliferation associated gene (PAG) [238]. Oxidative stress plays an important role in cancer progression [239,240]. The elevation of Prx1 expression in cancer has been hypothesized to be a consequence of self defense against tumorigenesis. Recent studies confirmed the interaction of Prx1 with AR and furthermore showed a trans-activation of its expression in LNCaP cells [241]. The data from several studies report Prx1 as tumor suppressor. However, TPD52 and Prx1 having

independent functions in neoplastic processes their physical interaction may play a vital role in prostate cancer development and need to be investigated in detail.

4.4.5 Localization TPD52

TPD52 is a cytoplasmic protein that typically displays perinuclear localization [180,242]. In pancreatic acini, TPD52 is co-localized with the endosomal marker early endosomal antigen-1 (EEA-1) and transferrin receptor in acinar cells [243]. It is also reported that TPD52 is associated with exocrine granules in rat pancreatic acinar cells [244]. Carbachol stimulation of T84 cells results in TPD52 translocation from perinuclear region to apical membrane [242]. Immunostaining for TPD52 on ovarian cancer tissue slices indicates TPD52 subcellular localization was predominantly cytoplasmic, although nuclear localization was also frequently observed in mucinous and clear cell carcinomas [184]. TPD52 is distributed between soluble and insoluble cellular fractions which are soluble with mild detergent treatment [245]. The indirect immunofluorescence for localization of exogenoulsly expressed Flag-TPD52 has shown granule like particles which may represent insoluble fraction. Double immunofluorescence detecting cyt *c*, a mitochondrial marker and Flag-TPD52 showed a partial co-localization with cyt *c*. We strongly believe that a C-terminal flag tag did not alter the subcellular distribution of TPD52 in LNCaP cells. This result indicates that the subcellular distribution of exogenouly expressed TPD52 into mitochondria in LNCaP prostate carcinoma cell line.

In conclusion, it appears that TPD52 is involved in different molecular processes, such as the regulation of apoptosis and proliferation. Its influence on cell migration suggests a role in tumor dissemination. Taken together, TPD52 may be a potential valid target to improve therapeutic strategies for better treatment of prostate cancer.

To obtain more insights about the structural features of TPD52 we want to determine its high resolution structre using protein X- ray crystallogaphy. To start with, TPD52 was successfully cloned and purified with 90% purity. The purified protein was further used for crystallization. The optimization of protein crystallization and biophysical characterization of TPD52 is in progress.

4.5 Caspases in prostate cancer

In the present study, we evaluated the immunohistochemical expression of caspases and Bcl-2 in the peripheral zone of whole mount prostate sections (the zonal anatomy and incidence of cancer explained in the introduction). We demonstrate a decreased immunostaining for active caspases-3 and -6 while expression of uncleaved caspase-3 and –6 seems not to be altered in PCa compared to BPE. Previous immunohistochemical studies revealed somehow contradictory results.

4.5.1 Active and inactive caspase-3 expression in PCa and BPE

Immunostaining for active and inactive caspases was scored in peripheral zone of the prostate sections for evaluation of their expression. Previous immunohistochemical studies revealed somehow contradictory results. For instance, immunohistochemistry studies showed the presence of caspase-3 (inactivated form) in basal as well as secretory cells of BPH. Moreover, increasing grades of PCa showed a significant loss of caspase-3 expression and it was concluded that altered caspase-3 expression may represent an additional mechanism of apoptotic resistance to androgen ablation [246]. One study showed no correlation of caspase-3 to the number of apoptotic bodies and Gleason score [247] while another study suggested that expression of caspase-3 is reduced in poorly differentiated prostate tumors than well differentiated PCa and BPE. Therefore, a prognostic significance has been suggested in disease progression [248]. Ananthanarayanan et al. found the decreased expression of active caspase-3 in high grade PIN (prostate intraepithelial neoplasia) and PCa [249] which is inline with our findings. In our results staining intensity for uncleaved caspase-3 was not altered but cleaved caspase-3 staining significantly decreased in PCa suggests an alteration of posttranslational cleavage of caspase-3 into active caspase-3. Therefore, modifications of proteolytic cleavage of its precursor form could lead to lower levels of active caspase-3. Consistently, this could represent a mechanism of apoptosis suppression and thus support the cancer development. Expression of activated caspase-3 in luminal epithelial cells suggests that these cells appear to be apoptotic. Some investigations observed that increased apoptosis is linked with increased cell proliferation [250]. This may be due to the rapid turnover of apoptotic bodies and abnormal cell proliferation followed by apoptosis. Otherwise, as increased caspase-3 expression was

correlated with increased apoptosis and high histology grade in breast carcinomas [251], cancer progression seems not be necessarily associated to the downregulation of caspase-3.

4.5.2 Active and inactive caspase-6 expression in PCa and BPE

According to current understanding, caspase-6 is an effector caspase that is activated downstream of caspase-3 during apoptosis. Activation of pro-caspase-6 by caspase-3 results in an active enzyme that is capable of cleaving an artificially introduced lamin cleavage site. This suggests that caspase-3 is activated prior to caspase-6, and may be responsible for the activation of caspase-6 [252]. However, these results are in conflict with a previous study showing that caspase-6 is capable of activating caspase-3 and, active caspase-6 initiates activation of caspase-3 as shown in rodent cerebellar granule cells [253]. Therefore these facts have drawn our attention towards the investigation of caspase-6 expression in PCa. Interestingly, immunohistochemistry studies revealed no alteration in the expression of caspase-6 but as seen for cleaved caspase-3, a significant reduction of immunoreactivity was observed for the cleaved caspase-6 in PCa compared to BPE. In recent studies, the camptothesin resistant prostate cancer cell line DU145 showed decreased expression of procaspase-6 indicating an important role of caspase-6 in drug induced apoptosis [254]. Moreover, resveratrol-induced apoptotic signalling led to caspase-6 mediated cleavage of lamin A in colon carcinoma cells [255].

4.5.3 Immunostaining for caspase-1, -9 and Bcl-2

Immunohistochemical investigations for the upstream caspases-1 and -9 revealed a weak immunostaining in tumor cells as well in benign epithelial cells. In this context it is to mention that previously the proenzyme form of caspase-1 but not its active form was detected in prostate cancer cells by western blot analysis [256].

Previous reports suggest an overexpression of Bcl-2 in PCa [257,258] and high grade PIN [259]. This is in contrast to our study, since we detected a faint staining (compared to non-neoplastic tissue) for Bcl-2 protein in PCa of all sections investigated. Recent study indicates Bcl-2 expression is not significantly altered in pre-malignant tumors [249]. Over expression of Bcl-2 is linked to restriction of cytochrome *c* release from mitochondria which in turn activates caspase-9 to induce apoptosis in PCa.

In conclusion, to the best of our knowledge this is the first study to report expression of active and inactive caspases showing that caspases are expressed constitutively in neoplastic and non-neoplastic prostate cells, whereas activation of procaspases in to active caspases seems to be dysregulated in cancer tissue which in turn alters self renewal of tissue homeostasis. Further investigations on elucidation of altered pathways for caspase activation might be worth pursuing to find novel strategies in cancer treatment.

Summary

Prostate cancer (PCa) is the most common type of cancer found in men from western countries and is the leading cancer death next to lung cancer and colorectal cancer. Proteomic studies on PCa identified a number of differentially expressed proteins and some of them were reported as potential markers, but clinical application of these markers is mostly missing. Most of the expression profiling studies have been carried out on radical prostatectomy specimens, formalin-fixed paraffin-embedded (FFPE) tissue sections, serum, urine and prostate fluids. To define the protein expression pattern of prostate biopsies, in the present study we investigated biopsy samples from benign prostate hyperplasia (BPH) and PCa patients by two-dimensional gel electrophoresis (BPH n=11 and PCa n=12) and mass spectrometry to identify potential biomarkers which might distinguish the two clinical situations. 2-DE results revealed 88 protein spots expressed differentially among hyperplasia and cancer groups with statistical significance. Interesting spots were analyzed by MALDI-TOF-MS-MS and 79 different proteins identified. The important proteins identified included, Prohibitin and NDRG1 tumor suppressor proteins, HSPs, cytoskeletal proteins, enzymes like DDAH1 and ALDH2. Prohibitin expression was investigated in detail at mRNA level and protein level using immunohistochemistry on prostatectomized specimens. We found that the level of mRNA for prohibitin correlates with the increased amount of protein indicating the involvement of changes at transcriptional level. Furthermore, immunohistochemistry revealed no staining in BPH, moderate staining in prostate intraepithelial neoplasia (PIN) and strong staining in PCa.

From the list of differentially proteins compared to PCa, TPD52 is over expressed in prostate cancer and also mRNA estimation by real-time PCR confirmed over expression of TPD52 at transcriptional level in cancer. TPD52 is a protein over expressed in prostate and breast cancer due to gene amplification but its exact physiological function is not investigated in detail. In the present study, we explored the responsiveness of LNCaP cells after dysregulation of TPD52 expression. Transfection of LNCaP cells with specific shRNA giving efficient knockdown of TPD52 resulted in a significant cell death of the carcinoma LNCaP cells. As evidenced by the activation of caspases (caspase-3 and -9) and by the loss of mitochondrial membrane potential, cell death occurs due to apoptosis. The disruption of the mitochondrial membrane potential indicates that TPD52 acts upstream of the mitochondrial apoptotic reaction. To study the effect of TPD52 expression on cell

proliferation, LNCaP cells were either transfected with EGFP-TPD52 or a specific shRNA. EGFP-TPD52 overexpressing cells showed an increased proliferation rate whereas TPD52-depleted cells showed a reverse effect. Additionally, we demonstrated that the exogenous expression of TPD52 promotes cell migration via αvβ3 integrin in prostate cancer cells through the activation of protein kinase B (PKB/Akt) pathway. In an attempt to identify new interacting proteins for TPD52, GST pulldown assays provided evidence for the physical interaction between TPD52 and Prx1 in LNCaP cells. Further, immunoprecipitation results confirmed this interaction.

Our results demonstrates that protein profiling and mRNA studies can be performed on prostate biopsies. Moreover, our study revealed a significant up-regulation of prohibitin in prostate cancer compared to BPH which may be a potential marker to distinguish PCa and BPH. From the results for functional characterization of TPD52, we conclude that TPD52 plays an important role in various molecular events particularly in morphological diversification and dissemination of PCa. It may be a promising target to investigate further in detail to develop new therapeutic strategies to treat PCa patients.

Caspases represent a family of cysteine proteases that are regarded as central executioners of apoptotic cell death. Activation of caspase cascade is an essential prerequisite in the induction of apoptosis in cellular systems. So far, in many tumors caspases were shown to be downregulated while anti-apoptotic Bcl-2 is up-regulated. To get insight in their putative role in PCa progression we determined the expression of caspase-1, uncleaved caspases 3 and 6, cleaved (activated) caspases 3 and 6, caspase-9 and antiapoptotic protein Bcl-2 in benign prostate epithelium (BPE) and prostate carcinoma.

In the current study 20 prostates were obtained from patients undergoing radical prostatectomy due to PCa. Paraffin embedded prostate whole mounts were cut at (4 µm) and investigated immunohistochemically using anti-mouse monoclonal antibodies directed against caspases 1 and 9, uncleaved caspases 3 and 6, cleaved caspases 3 and 6, and Bcl-2.
In BPE all caspases were localized in the cytoplasm of glandular cells. Comparing BPE to PCa, no differences were found for caspase-1, uncleaved caspases 3 and 6 as well as caspase-9. Immunostaining for cleaved caspases 3 and 6, however, revealed a statistically significant reduction in PCa compared to non-neoplastic tissue. Whereas in BPE Bcl-2 protein was detected in the basal compartment of epithelial gland cells no immunostaining was seen in PCa.

As our results show a decreased amount of activated caspases may be due to the alterations of posttranslational cleavage rather than expression of caspases 3 and 6. This suggests that the modification in their activation pathway could play an important role during PCa progression.

5 References

[1] **K.Moore and A.Dalley, (1999) *Clinically Oriented Anatomy*., Lippincott Williams & Wilkins, Baltimore, Maryland.**

[2] **McNeal JE (1988) Normal histology of the prostate. Am J Surg Pathol 12:619-633**

[3] **McNeal JE (1981) The zonal anatomy of the prostate. Prostate 2:35-49**

[4] **H.Steive, (1930) Männliche Genitalorgane, in: *Handbuch der mikroskopischen Anatomie des Menschen*, Springer, Berlin, 1930 pp. 1-399**

[5] **Langstaff G (1817) Cases of fungus haematodes, with observations. Medico-Chirugical Transactions 8:272-305**

[6] **Jemal A, Murray T, Ward E et al (2005) Cancer statistics, 2005. CA Cancer J Clin 55:10-30**

[7] **Hsing AW and Chokkalingam AP (2006) Prostate cancer epidemiology. Front Biosci 11:1388-1413**

[8] **Gronberg H (2003) Prostate cancer epidemiology. Lancet 361:859-864**

[9] ***Cancer society facts & figures 2005*. 2005. American cancer society, Inc. Ref Type: Report**

[10] **Hankey BF, Ries LAEdwards BK (1999) The surveillance, epidemiology, and end results program: a national resource. Cancer Epidemiol Biomarkers Prev 8:1117-1121**

[11] **Breslow N, Chan CW, Dhom G et al (1977) Latent carcinoma of prostate at autopsy in seven areas. The International Agency for Research on Cancer, Lyons, France. Int J Cancer 20:680-688**

[12] **Scardino PT (1989) Early detection of prostate cancer. Urol Clin North Am 16:635-655**

[13] **Stanford JL and Ostrander EA (2001) Familial prostate cancer. Epidemiol Rev 23:19-23**

[14] **Steinberg GD, Carter BS, Beaty TH et al (1990) Family history and the risk of prostate cancer. Prostate 17:337-347**

[15] **Lichtenstein P and Annas P (2000) Heritability and prevalence of specific fears and phobias in childhood. J Child Psychol Psychiatry 41:927-937**

[16] **Mazoyer S (2005) Genomic rearrangements in the BRCA1 and BRCA2 genes. Hum Mutat 25:415-422**

[17] Struewing JP, Hartge P, Wacholder S et al (1997) The risk of cancer associated with specific mutations of BRCA1 and BRCA2 among Ashkenazi Jews. N Engl J Med 336:1401-1408

[18] Chokkalingam AP, Pollak M, Fillmore CM et al (2001) Insulin-like growth factors and prostate cancer: a population-based case-control study in China. Cancer Epidemiol Biomarkers Prev 10:421-427

[19] Pollak M (2001) Insulin-like growth factors and prostate cancer. Epidemiol Rev 23:59-66

[20] Chokkalingam AP, McGlynn KA, Gao YT et al (2001) Vitamin D receptor gene polymorphisms, insulin-like growth factors, and prostate cancer risk: a population-based case-control study in China. Cancer Res 61:4333-4336

[21] Nam RK, Zhang WW, Trachtenberg J et al (2003) Comprehensive assessment of candidate genes and serological markers for the detection of prostate cancer. Cancer Epidemiol Biomarkers Prev 12:1429-1437

[22] Chung W, Kwabi-Addo B, Ittmann M et al (2008) Identification of novel tumor markers in prostate, colon and breast cancer by unbiased methylation profiling. PLoS ONE 3:e2079

[23] Lee WH, Morton RA, Epstein JI et al (1994) Cytidine methylation of regulatory sequences near the pi-class glutathione S-transferase gene accompanies human prostatic carcinogenesis. Proc Natl Acad Sci U S A 91:11733-11737

[24] Millar DS, Ow KK, Paul CL et al (1999) Detailed methylation analysis of the glutathione S-transferase pi (GSTP1) gene in prostate cancer. Oncogene 18:1313-1324

[25] Giovannucci E, Rimm EB, Colditz GA et al (1993) A prospective study of dietary fat and risk of prostate cancer. J Natl Cancer Inst 85:1571-1579

[26] Gann PH, Ma J, Giovannucci E et al (1999) Lower prostate cancer risk in men with elevated plasma lycopene levels: results of a prospective analysis. Cancer Res 59:1225-1230

[27] Giovannucci E (1999) Tomatoes, tomato-based products, lycopene, and cancer: review of the epidemiologic literature. J Natl Cancer Inst 91:317-331

[28] Peters U, Leitzmann MF, Chatterjee N et al (2007) Serum lycopene, other carotenoids, and prostate cancer risk: a nested case-control study in the prostate, lung, colorectal, and ovarian cancer screening trial. Cancer Epidemiol Biomarkers Prev 16:962-968

[29] Shirai T, Asamoto M, Takahashi S et al (2002) Diet and prostate cancer. Toxicology 181-182:89-94

[30] Platz EA and Helzlsouer KJ (2001) Selenium, zinc, and prostate cancer. Epidemiol Rev 23:93-101

[31] Kolonel LN, Altshuler DHenderson BE (2004) The multiethnic cohort study: exploring genes, lifestyle and cancer risk. Nat Rev Cancer 4:519-527

[32] Kyobutungi C, Ronellenfitsch U, Razum O et al (2006) Mortality from cancer among ethnic German immigrants from the Former Soviet Union, in Germany. Eur J Cancer 42:2577-2584

[33] Quinn M and Babb P (2002) Patterns and trends in prostate cancer incidence, survival, prevalence and mortality. Part I: international comparisons. BJU Int 90:162-173

[34] Cook LS, Goldoft M, Schwartz SM et al (1999) Incidence of adenocarcinoma of the prostate in Asian immigrants to the United States and their descendants. J Urol 161:152-155

[35] Shimizu H, Ross RK, Bernstein L et al (1991) Cancers of the prostate and breast among Japanese and white immigrants in Los Angeles County. Br J Cancer 63:963-966

[36] Sahmoun AE, Case LD, Jackson SA et al (2005) Cadmium and prostate cancer: a critical epidemiologic analysis. Cancer Invest 23:256-263

[37] Telisman S, Colak B, Pizent A et al (2007) Reproductive toxicity of low-level lead exposure in men. Environ Res 105:256-266

[38] Navarro Silvera SA and Rohan TE (2007) Trace elements and cancer risk: a review of the epidemiologic evidence. Cancer Causes Control 18:7-27

[39] Fritschi L, Glass DC, Tabrizi JS et al (2007) Occupational risk factors for prostate cancer and benign prostatic hyperplasia: a case-control study in Western Australia. Occup Environ Med 64:60-65

[40] Sajid KM, Khan AA, Loother BA et al (2004) Prostate specific antigen level in a fertilizer factory workers. J Coll Physicians Surg Pak 14:290-293

[41] Rubin E., (2001) Essential pathology, Lippincott Williams and Wilkins, Philadelphia.

[42] McNeal JE (1969) Origin and development of carcinoma in the prostate. Cancer 23:24-34

[43] McNeal JE (1978) Origin and evolution of benign prostatic enlargement. Invest Urol 15:340-345

[44] Garabedian EM, Humphrey PAGordon JI (1998) A transgenic mouse model of metastatic prostate cancer originating from neuroendocrine cells. Proc Natl Acad Sci U S A 95:15382-15387

[45] Kasper S, Sheppard PC, Yan Y et al (1998) Development, progression, and androgen-dependence of prostate tumors in probasin-large T antigen transgenic mice: a model for prostate cancer. Lab Invest 78:319-333

[46] McNeal JE and Bostwick DG (1986) Intraductal dysplasia: a premalignant lesion of the prostate. Hum Pathol 17:64-71

[47] Bostwick DG (1989) Prostatic intraepithelial neoplasia (PIN). Urology 34:16-22

[48] Bostwick DG, Pacelli ALopez-Beltran A (1996) Molecular biology of prostatic intraepithelial neoplasia. Prostate 29:117-134

[49] Lipski BA, Garcia RLBrawer MK (1996) Prostatic intraepithelial neoplasia: significance and management. Semin Urol Oncol 14:149-155

[50] Gleason DF and Mellinger GT (1974) Prediction of prognosis for prostatic adenocarcinoma by combined histological grading and clinical staging. J Urol 111:58-64

[51] Mellinger GT, Gleason DBailar J, III (1967) The histology and prognosis of prostatic cancer. J Urol 97:331-337

[52] C.Wittekind and L.H.Sobin, (2002) *TNM classification of malignant tumours*, in: Wiley-Liss, New York, 2002

[53] DeMarzo AM, Nelson WG, Isaacs WB et al (2003) Pathological and molecular aspects of prostate cancer. Lancet 361:955-964

[54] Naughton CK, Miller DC, Mager DE et al (2000) A prospective randomized trial comparing 6 versus 12 prostate biopsy cores: impact on cancer detection. J Urol 164:388-392

[55] Taylor JA, III, Gancarczyk KJ, Fant GV et al (2002) Increasing the number of core samples taken at prostate needle biopsy enhances the detection of clinically significant prostate cancer. Urology 60:841-845

[56] Kramer BS, Brown ML, Prorok PC et al (1993) Prostate cancer screening: what we know and what we need to know. Ann Intern Med 119:914-923

[57] Martinez M, Espana F, Royo M et al (2000) Prostate-specific antigen complexed to alpha(1)-antichymotrypsin in the early detection of prostate cancer. Eur Urol 38:85-90

[58] Polascik TJ, Oesterling JEPartin AW (1999) Prostate specific antigen: a decade of discovery--what we have learned and where we are going. J Urol 162:293-306

[59] Woolf SH (1995) Screening for prostate cancer with prostate-specific antigen. An examination of the evidence. N Engl J Med 333:1401-1405

[60] Rubin MA, Zhou M, Dhanasekaran SM et al (2002) alpha-Methylacyl coenzyme A racemase as a tissue biomarker for prostate cancer. JAMA 287:1662-1670

[61] Jiang Z, Wu CL, Woda BA et al (2002) P504S/alpha-methylacyl-CoA racemase: a useful marker for diagnosis of small foci of prostatic carcinoma on needle biopsy. Am J Surg Pathol 26:1169-1174

[62] Stenman UH (1997) Prostate-specific antigen, clinical use and staging: an overview. Br J Urol 79 Suppl 1:53-60

[63] Catalona WJ, Smith DS, Ratliff TL et al (1993) Detection of organ-confined prostate cancer is increased through prostate-specific antigen-based screening. JAMA 270:948-954

[64] Catalona WJ, Partin AW, Slawin KM et al (1998) Use of the percentage of free prostate-specific antigen to enhance differentiation of prostate cancer from benign prostatic disease: a prospective multicenter clinical trial. JAMA 279:1542-1547

[65] Parekh DJ, Ankerst DP, Troyer D et al (2007) Biomarkers for prostate cancer detection. J Urol 178:2252-2259

[66] Stephan C, Jung K, Nakamura T et al (2006) Serum human glandular kallikrein 2 (hK2) for distinguishing stage and grade of prostate cancer. Int J Urol 13:238-243

[67] Feneley MR, Young MP, Chinyama C et al (1996) Ki-67 expression in early prostate cancer and associated pathological lesions. J Clin Pathol 49:741-748

[68] Weinstein MH (1998) Digital image analysis of proliferative index: two distinct populations of high-grade prostatic intraepithelial neoplasia in close proximity to adenocarcinoma of the prostate. Hum Pathol 29:620-626

[69] Hansel DE, DeMarzo AM, Platz EA et al (2007) Early prostate cancer antigen expression in predicting presence of prostate cancer in men with histologically negative biopsies. J Urol 177:1736-1740

[70] Paul B, Dhir R, Landsittel D et al (2005) Detection of prostate cancer with a blood-based assay for early prostate cancer antigen. Cancer Res 65:4097-4100

[71] Soete G, Verellen D, Storme G (2008) Image guided radiotherapy for prostate cancer. Bull Cancer 95:374-380

[72] Lander ES, Linton LM, Birren B et al (2001) Initial sequencing and analysis of the human genome. Nature 409:860-921

[73] Venter JC, Adams MD, Myers EW et al (2001) The sequence of the human genome. Science 291:1304-1351

[74] Anderson L and Seilhamer J (1997) A comparison of selected mRNA and protein abundances in human liver. Electrophoresis 18:533-537

[75] Gygi SP, Rochon Y, Franza BR et al (1999) Correlation between protein and mRNA abundance in yeast. Mol Cell Biol 19:1720-1730

[76] Strohman R (1994) Epigenesis: the missing beat in biotechnology? Biotechnology (N Y) 12:156-164

[77] Black DL (2003) Mechanisms of alternative pre-messenger RNA splicing. Annu Rev Biochem 72:291-336

[78] Schaub M and Keller W (2002) RNA editing by adenosine deaminases generates RNA and protein diversity. Biochimie 84:791-803

[79] Han KK and Martinage A (1992) Post-translational chemical modification(s) of proteins. Int J Biochem 24:19-28

[80] Ahram M and Emmert-Buck MR (2003) Approaches to proteomic analysis of human tumors. Methods Mol Biol 222:375-384

[81] Gavin AC, Bosche M, Krause R et al (2002) Functional organization of the yeast proteome by systematic analysis of protein complexes. Nature 415:141-147

[82] Ho Y, Gruhler A, Heilbut A et al (2002) Systematic identification of protein complexes in Saccharomyces cerevisiae by mass spectrometry. Nature 415:180-183

[83] Legrain P, Wojcik JGauthier JM (2001) Protein--protein interaction maps: a lead towards cellular functions. Trends Genet 17:346-352

[84] Adams P.D., Seeholzer S, and Ohh M., (2002) Identification of associated proteins by coimmunoprecipitation. Protein-Protein interactions, in: A Molecular cloning manual, Cold Spring Harbor Laboratory Press, Cold Spring Harbor, New York, 2002 pp. 59-74

[85] Seraphin B., Puig O., Bouveret E., Rutz B., and Caspary F., (2002) Tandem affinity purification to enhance interacting protein identification. In protein-protein interactions, in: A molecular cloning manual, Cold spring Harbor Laboratory Press, Cold Spring Harbor, New York, 2002 pp. 313-328

[86] Klose J (1975) Protein mapping by combined isoelectric focusing and electrophoresis of mouse tissues. A novel approach to testing for induced point mutations in mammals. Humangenetik 26:231-243

[87] O'Farrell PH (1975) High resolution two-dimensional electrophoresis of proteins. J Biol Chem 250:4007-4021

[88] Bjellqvist B, Ek K, Righetti PG et al (1982) Isoelectric focusing in immobilized pH gradients: principle, methodology and some applications. J Biochem Biophys Methods 6:317-339

[89] Gorg A, Postel WGunther S (1988) The current state of two-dimensional electrophoresis with immobilized pH gradients. Electrophoresis 9:531-546

[90] Gorg A, Obermaier C, Boguth G et al (2000) The current state of two-dimensional electrophoresis with immobilized pH gradients. Electrophoresis 21:1037-1053

[91] Bjellqvist B, Sanchez JC, Pasquali C et al (1993) Micropreparative two-dimensional electrophoresis allowing the separation of samples containing milligram amounts of proteins. Electrophoresis 14:1375-1378

[92] Rabilloud T, Valette CLawrence JJ (1994) Sample application by in-gel rehydration improves the resolution of two-dimensional electrophoresis with immobilized pH gradients in the first dimension. Electrophoresis 15:1552-1558

[93] Richert S, Luche S, Chevallet M et al (2004) About the mechanism of interference of silver staining with peptide mass spectrometry. Proteomics 4:909-916

[94] Switzer RC, III, Merril CRShifrin S (1979) A highly sensitive silver stain for detecting proteins and peptides in polyacrylamide gels. Anal Biochem 98:231-237

[95] Gharahdaghi F, Weinberg CR, Meagher DA et al (1999) Mass spectrometric identification of proteins from silver-stained polyacrylamide gel: a method for the removal of silver ions to enhance sensitivity. Electrophoresis 20:601-605

[96] Karas M and Hillenkamp F (1988) Laser desorption ionization of proteins with molecular masses exceeding 10,000 daltons. Anal Chem 60:2299-2301

[97] Fenn JB, Mann M, Meng CK et al (1989) Electrospray ionization for mass spectrometry of large biomolecules. Science 246:64-71

[98] Perkins DN, Pappin DJ, Creasy DM et al (1999) Probability-based protein identification by searching sequence databases using mass spectrometry data. Electrophoresis 20:3551-3567

[99] Henzel WJ, Billeci TM, Stults JT et al (1993) Identifying proteins from two-dimensional gels by molecular mass searching of peptide fragments in protein sequence databases. Proc Natl Acad Sci U S A 90:5011-5015

[100] Pappin DJ, Hojrup PBleasby AJ (1993) Rapid identification of proteins by peptide-mass fingerprinting. Curr Biol 3:327-332

[101] Washburn MP, Wolters DYates JR, III (2001) Large-scale analysis of the yeast proteome by multidimensional protein identification technology. Nat Biotechnol 19:242-247

[102] Gygi SP, Rist B, Gerber SA et al (1999) Quantitative analysis of complex protein mixtures using isotope-coded affinity tags. Nat Biotechnol 17:994-999

[103] Gevaert K, Goethals M, Martens L et al (2003) Exploring proteomes and analyzing protein processing by mass spectrometric identification of sorted N-terminal peptides. Nat Biotechnol 21:566-569

[104] Veenstra TD, Prieto DAConrads TP (2004) Proteomic patterns for early cancer detection. Drug Discov Today 9:889-897

[105] Conrads TP, Hood BL, Issaq HJ et al (2004) Proteomic patterns as a diagnostic tool for early-stage cancer: a review of its progress to a clinically relevant tool. Mol Diagn 8:77-85

[106] Guevara J, Jr., Herbert BHLee C (1985) Two-dimensional electrophoretic analysis of human prostatic fluid proteins. Cancer Res 45:1766-1771

[107] Grover PK and Resnick MI (1995) Analysis of prostatic fluid: evidence for the presence of a prospective marker for prostatic cancer. Prostate 26:12-18

[108] Grover PK and Resnick MI (1997) High resolution two-dimensional electrophoretic analysis of urinary proteins of patients with prostatic cancer. Electrophoresis 18:814-818

[109] Rehman I, Azzouzi AR, Catto JW et al (2004) Proteomic analysis of voided urine after prostatic massage from patients with prostate cancer: a pilot study. Urology 64:1238-1243

[110] Laxman B, Morris DS, Yu J et al (2008) A first-generation multiplex biomarker analysis of urine for the early detection of prostate cancer. Cancer Res 68:645-649

[111] Hoque MO, Topaloglu O, Begum S et al (2005) Quantitative methylation-specific polymerase chain reaction gene patterns in urine sediment distinguish prostate cancer patients from control subjects. J Clin Oncol 23:6569-6575

[112] de Kok JB, Verhaegh GW, Roelofs RW et al (2002) DD3(PCA3), a very sensitive and specific marker to detect prostate tumors. Cancer Res 62:2695-2698

[113] Downes MR, Byrne JC, Pennington SR et al (2007) Urinary markers for prostate cancer. BJU Int 99:263-268

[114] Lexander H, Palmberg C, Auer G et al (2005) Proteomic analysis of protein expression in prostate cancer. Anal Quant Cytol Histol 27:263-272

[115] Meehan KL, Holland JWDawkins HJ (2002) Proteomic analysis of normal and malignant prostate tissue to identify novel proteins lost in cancer. Prostate 50:54-63

[116] Diaz JI, Cazares LH, Corica A et al (2004) Selective capture of prostatic basal cells and secretory epithelial cells for proteomic and genomic analysis. Urol Oncol 22:329-336

[117] Emmert-Buck MR, Bonner RF, Smith PD et al (1996) Laser capture microdissection. Science 274:998-1001

[118] Fend F, Kremer MQuintanilla-Martinez L (2000) Laser capture microdissection: methodical aspects and applications with emphasis on immuno-laser capture microdissection. Pathobiology 68:209-214

[119] Ahram M, Flaig MJ, Gillespie JW et al (2003) Evaluation of ethanol-fixed, paraffin-embedded tissues for proteomic applications. Proteomics 3:413-421

[120] Hood BL, Darfler MM, Guiel TG et al (2005) Proteomic analysis of formalin-fixed prostate cancer tissue. Mol Cell Proteomics 4:1741-1753

[121] Alaiya A, Roblick U, Egevad L et al (2000) Polypeptide expression in prostate hyperplasia and prostate adenocarcinoma. Anal Cell Pathol 21:1-9

[122] Alaiya AA, Oppermann M, Langridge J et al (2001) Identification of proteins in human prostate tumor material by two-dimensional gel electrophoresis and mass spectrometry. Cell Mol Life Sci 58:307-311

[123] Banez LL, Prasanna P, Sun L et al (2003) Diagnostic potential of serum proteomic patterns in prostate cancer. J Urol 170:442-446

[124] Hessels D, Verhaegh GW, Schalken JA et al (2004) Applicability of biomarkers in the early diagnosis of prostate cancer. Expert Rev Mol Diagn 4:513-526

[125] Kumar-Sinha C, Rhodes DR, Yu J et al (2003) Prostate cancer biomarkers: a current perspective. Expert Rev Mol Diagn 3:459-470

[126] Rehman I, Azzouzi AR, Cross SS et al (2004) Dysregulated expression of S100A11 (calgizzarin) in prostate cancer and precursor lesions. Hum Pathol 35:1385-1391

[127] Rehman I, Cross SS, Azzouzi AR et al (2004) S100A6 (Calcyclin) is a prostate basal cell marker absent in prostate cancer and its precursors. Br J Cancer 91:739-744

[128] Adam BL, Qu Y, Davis JW et al (2002) Serum protein fingerprinting coupled with a pattern-matching algorithm distinguishes prostate cancer from benign prostate hyperplasia and healthy men. Cancer Res 62:3609-3614

[129] Acevedo B, Perera Y, Torres E et al (2006) Fast and novel purification method to obtain the prostate specific antigen (PSA) from human seminal plasma. Prostate 66:1029-1036

[130] Pilch B and Mann M (2006) Large-scale and high-confidence proteomic analysis of human seminal plasma. Genome Biol 7:R40

[131] Ummanni R, Junker H, Zimmermann U et al (2008) Prohibitin identified by proteomic analysis of prostate biopsies distinguishes hyperplasia and cancer. Cancer Lett

[132] Lin JF, Xu J, Tian HY et al (2007) Identification of candidate prostate cancer biomarkers in prostate needle biopsy specimens using proteomic analysis. Int J Cancer 121:2596-2605

[133] Mischak H, Apweiler R, Banks RE et al (2006) Clinical proteomics: A need to define the field and to begin to set adequate standards. Proteomics Clin Appl 1:148-156

[134] Slee EA, Adrain CMartin SJ (1999) Serial killers: ordering caspase activation events in apoptosis. Cell Death Differ 6:1067-1074

[135] Woo M, Hakem R, Soengas MS et al (1998) Essential contribution of caspase 3/CPP32 to apoptosis and its associated nuclear changes. Genes Dev 12:806-819

[136] Harvey NL and Kumar S (1998) The role of caspases in apoptosis. Adv Biochem Eng Biotechnol 62:107-128

[137] Stegh AH and Peter ME (2001) Apoptosis and caspases. Cardiol Clin 19:13-29

[138] Nunez G, Benedict MA, Hu Y et al (1998) Caspases: the proteases of the apoptotic pathway. Oncogene 17:3237-3245

[139] Scaffidi C, Fulda S, Srinivasan A et al (1998) Two CD95 (APO-1/Fas) signaling pathways. EMBO J 17:1675-1687

[140] Luo X, Budihardjo I, Zou H et al (1998) Bid, a Bcl2 interacting protein, mediates cytochrome c release from mitochondria in response to activation of cell surface death receptors. Cell 94:481-490

[141] Thornberry NA, Bull HG, Calaycay JR et al (1992) A novel heterodimeric cysteine protease is required for interleukin-1 beta processing in monocytes. Nature 356:768-774

[142] Stennicke HR, Deveraux QL, Humke EW et al (1999) Caspase-9 can be activated without proteolytic processing. J Biol Chem 274:8359-8362

[143] Slee EA, Harte MT, Kluck RM et al (1999) Ordering the cytochrome c-initiated caspase cascade: hierarchical activation of caspases-2, -3, -6, -7, -8, and -10 in a caspase-9-dependent manner. J Cell Biol 144:281-292

[144] Li P, Nijhawan D, Budihardjo I et al (1997) Cytochrome c and dATP-dependent formation of Apaf-1/caspase-9 complex initiates an apoptotic protease cascade. Cell 91:479-489

[145] Reed JC (1994) Bcl-2 and the regulation of programmed cell death. J Cell Biol 124:1-6

[146] Reed JC (2000) Mechanisms of apoptosis. Am J Pathol 157:1415-1430

[147] F.M.Ausubel, (1990) in: Current protocols in molecular biology, 1990

[148] Chomczynski P (1993) A reagent for the single-step simultaneous isolation of RNA, DNA and proteins from cell and tissue samples. Biotechniques 15:532-537

[149] Bradford MM (1976) A rapid and sensitive method for the quantitation of microgram quantities of protein utilizing the principle of protein-dye binding. Anal Biochem 72:248-254

[150] Eymann C, Dreisbach A, Albrecht D et al (2004) A comprehensive proteome map of growing Bacillus subtilis cells. Proteomics 4:2849-2876

[151] Gleason DF and Mellinger GT (1974) Prediction of prognosis for prostatic adenocarcinoma by combined histological grading and clinical staging. J Urol 111:58-64

[152] Mellinger GT, Gleason DBailar J, III (1967) The histology and prognosis of prostatic cancer. J Urol 97:331-337

[153] Metivier D, Dallaporta B, Zamzami N et al (1998) Cytofluorometric detection of mitochondrial alterations in early CD95/Fas/APO-1-triggered apoptosis of Jurkat T lymphoma cells. Comparison of seven mitochondrion-specific fluorochromes. Immunol Lett 61:157-163

[154] Cornford PA, Dodson AR, Parsons KF et al (2000) Heat shock protein expression independently predicts clinical outcome in prostate cancer. Cancer Res 60:7099-7105

[155] Hood BL, Darfler MM, Guiel TG et al (2005) Proteomic analysis of formalin-fixed prostate cancer tissue. Mol Cell Proteomics 4:1741-1753

[156] Ruddat VC, Whitman S, Klein RD et al (2005) Evidence for downregulation of calcium signaling proteins in advanced mouse adenocarcinoma. Prostate 64:128-138

[157] Ruddat VC, Whitman S, Klein RD et al (2005) Evidence for downregulation of calcium signaling proteins in advanced mouse adenocarcinoma. Prostate 64:128-138

[158] Killian CS, Emrich LJ, Vargas FP et al (1986) Relative reliability of five serially measured markers for prognosis of progression in prostate cancer. J Natl Cancer Inst 76:179-185

[159] Roskams AJ, Friedman V, Wood CM et al (1993) Cell cycle activity and expression of prohibitin mRNA. J Cell Physiol 157:289-295

[160] He QY, Cheung YH, Leung SY et al (2004) Diverse proteomic alterations in gastric adenocarcinoma. Proteomics 4:3276-3287

[161] Ryu JW, Kim HJ, Lee YS et al (2003) The proteomics approach to find biomarkers in gastric cancer. J Korean Med Sci 18:505-509

[162] Asamoto M and Cohen SM (1994) Prohibitin gene is overexpressed but not mutated in rat bladder carcinomas and cell lines. Cancer Lett 83:201-207

[163] Byrjalsen I, Mose LP, Fey SJ et al (1999) Two-dimensional gel analysis of human endometrial proteins: characterization of proteins with increased expression in hyperplasia and adenocarcinoma. Mol Hum Reprod 5:748-756

[164] Jupe ER, Liu XT, Kiehlbauch JL et al (1996) Prohibitin in breast cancer cell lines: loss of antiproliferative activity is linked to 3' untranslated region mutations. Cell Growth Differ 7:871-878

[165] Terashima M, Kim KM, Adachi T et al (1994) The IgM antigen receptor of B lymphocytes is associated with prohibitin and a prohibitin-related protein. EMBO J 13:3782-3792

[166] Williams K, Chubb C, Huberman E et al (1998) Analysis of differential protein expression in normal and neoplastic human breast epithelial cell lines. Electrophoresis 19:333-343

[167] Jupe ER, Liu XT, Kiehlbauch JL et al (1995) Prohibitin antiproliferative activity and lack of heterozygosity in immortalized cell lines. Exp Cell Res 218:577-580

[168] Dydensborg AB, Herring E, Auclair J et al (2006) Normalizing genes for quantitative RT-PCR in differentiating human intestinal epithelial cells and adenocarcinomas of the colon. Am J Physiol Gastrointest Liver Physiol 290:G1067-G1074

[169] Ikonen E, Fiedler K, Parton RG et al (1995) Prohibitin, an antiproliferative protein, is localized to mitochondria. FEBS Lett 358:273-277

[170] Coates PJ, Nenutil R, McGregor A et al (2001) Mammalian prohibitin proteins respond to mitochondrial stress and decrease during cellular senescence. Exp Cell Res 265:262-273

[171] Thompson WE, Branch A, Whittaker JA et al (2001) Characterization of prohibitin in a newly established rat ovarian granulosa cell line. Endocrinology 142:4076-4085

[172] Wang S, Nath N, Adlam M et al (1999) Prohibitin, a potential tumor suppressor, interacts with RB and regulates E2F function. Oncogene 18:3501-3510

[173] Zhu B, Fukada K, Zhu H et al (2006) Prohibitin and cofilin are intracellular effectors of transforming growth factor beta signaling in human prostate cancer cells. Cancer Res 66:8640-8647

[174] Thompson WE, Powell JM, Whittaker JA et al (1999) Immunolocalization and expression of prohibitin, a mitochondrial associated protein within the rat ovaries. Anat Rec 256:40-48

[175] Dixit VD, Sridaran R, Edmonsond MA et al (2003) Gonadotropin-releasing hormone attenuates pregnancy-associated thymic involution and modulates the expression of antiproliferative gene product prohibitin. Endocrinology 144:1496-1505

[176] Wang S, Fusaro G, Padmanabhan J et al (2002) Prohibitin co-localizes with Rb in the nucleus and recruits N-CoR and HDAC1 for transcriptional repression. Oncogene 21:8388-8396

[177] Gamble SC, Odontiadis M, Waxman J et al (2004) Androgens target prohibitin to regulate proliferation of prostate cancer cells. Oncogene 23:2996-3004

[178] Gamble SC, Chotai D, Odontiadis M et al (2007) Prohibitin, a protein downregulated by androgens, represses androgen receptor activity. Oncogene 26:1757-1768

[179] Rhodes DR, Barrette TR, Rubin MA et al (2002) Meta-analysis of microarrays: interstudy validation of gene expression profiles reveals pathway dysregulation in prostate cancer. Cancer Res 62:4427-4433

[180] Balleine RL, Fejzo MS, Sathasivam P et al (2000) The hD52 (TPD52) gene is a candidate target gene for events resulting in increased 8q21 copy number in human breast carcinoma. Genes Chromosomes Cancer 29:48-57

[181] Pollack JR, Sorlie T, Perou CM et al (2002) Microarray analysis reveals a major direct role of DNA copy number alteration in the transcriptional program of human breast tumors. Proc Natl Acad Sci U S A 99:12963-12968

[182] Rubin MA, Varambally S, Beroukhim R et al (2004) Overexpression, amplification, and androgen regulation of TPD52 in prostate cancer. Cancer Res 64:3814-3822

[183] Wang R, Xu J, Saramaki O et al (2004) PrLZ, a novel prostate-specific and androgen-responsive gene of the TPD52 family, amplified in chromosome 8q21.1 and overexpressed in human prostate cancer. Cancer Res 64:1589-1594

[184] Byrne JA, Balleine RL, Schoenberg FM et al (2005) Tumor protein D52 (TPD52) is overexpressed and a gene amplification target in ovarian cancer. Int J Cancer 117:1049-1054

[185] Byrne JA, Tomasetto C, Garnier JM et al (1995) A screening method to identify genes commonly overexpressed in carcinomas and the identification of a novel complementary DNA sequence. Cancer Res 55:2896-2903

[186] Rubin MA, Varambally S, Beroukhim R et al (2004) Overexpression, amplification, and androgen regulation of TPD52 in prostate cancer. Cancer Res 64:3814-3822

[187] Wang R, Xu J, Saramaki O et al (2004) PrLZ, a novel prostate-specific and androgen-responsive gene of the TPD52 family, amplified in chromosome 8q21.1 and overexpressed in human prostate cancer. Cancer Res 64:1589-1594

[188] Chen SL, Maroulakou IG, Green JE et al (1996) Isolation and characterization of a novel gene expressed in multiple cancers. Oncogene 12:741-751

[189] Scanlan MJ and Jager D (2001) Challenges to the development of antigen-specific breast cancer vaccines. Breast Cancer Res 3:95-98

[190] Thomas DD, Taft WB, Kaspar KM et al (2001) CRHSP-28 regulates Ca(2+)-stimulated secretion in permeabilized acinar cells. J Biol Chem 276:28866-28872

[191] Chen SL, Zhang XK, Halverson DO et al (1997) Characterization of human N8 protein. Oncogene 15:2577-2588

[192] Ummanni R, Junker H, Zimmermann U et al (2008) Prohibitin identified by proteomic analysis of prostate biopsies distinguishes hyperplasia and cancer. Cancer Lett

[193] Wang R, Xu J, Mabjeesh N et al (2007) PrLZ is expressed in normal prostate development and in human prostate cancer progression. Clin Cancer Res 13:6040-6048

[194] Dias N and Stein CA (2002) Antisense oligonucleotides: basic concepts and mechanisms. Mol Cancer Ther 1:347-355

[195] Brummelkamp TR, Bernards RAgami R (2002) A system for stable expression of short interfering RNAs in mammalian cells. Science 296:550-553

[196] Byrne JA, Mattei MGBasset P (1996) Definition of the tumor protein D52 (TPD52) gene family through cloning of D52 homologues in human (hD53) and mouse (mD52). Genomics 35:523-532

[197] Proux V, Provot S, Felder-Schmittbuhl MP et al (1996) Characterization of a leucine zipper-containing protein identified by retroviral insertion in avian neuroretina cells. J Biol Chem 271:30790-30797

[198] Nelson PS, Clegg N, Arnold H et al (2002) The program of androgen-responsive genes in neoplastic prostate epithelium. Proc Natl Acad Sci U S A 99:11890-11895

[199] Ellis JA, Sinclair RHarrap SB (2002) Androgenetic alopecia: pathogenesis and potential for therapy. Expert Rev Mol Med 4:1-11

[200] Byrne JA, Mattei MGBasset P (1996) Definition of the tumor protein D52 (TPD52) gene family through cloning of D52 homologues in human (hD53) and mouse (mD52). Genomics 35:523-532

[201] DePrimo SE, Diehn M, Nelson JB et al (2002) Transcriptional programs activated by exposure of human prostate cancer cells to androgen. Genome Biol 3:RESEARCH0032

[202] Nelson PS, Clegg N, Arnold H et al (2002) The program of androgen-responsive genes in neoplastic prostate epithelium. Proc Natl Acad Sci U S A 99:11890-11895

[203] Rubin MA, Varambally S, Beroukhim R et al (2004) Overexpression, amplification, and androgen regulation of TPD52 in prostate cancer. Cancer Res 64:3814-3822

[204] Wang R, Xu J, Saramaki O et al (2004) PrLZ, a novel prostate-specific and androgen-responsive gene of the TPD52 family, amplified in chromosome 8q21.1 and overexpressed in human prostate cancer. Cancer Res 64:1589-1594

[205] Hanahan D and Weinberg RA (2000) The hallmarks of cancer. Cell 100:57-70

[206] Wang L, Guo Y, Huang WJ et al (2001) Card10 is a novel caspase recruitment domain/membrane-associated guanylate kinase family member that interacts with BCL10 and activates NF-kappa B. J Biol Chem 276:21405-21409

[207] Zeng L, Sachdev P, Yan L et al (2000) Vav3 mediates receptor protein tyrosine kinase signaling, regulates GTPase activity, modulates cell morphology, and induces cell transformation. Mol Cell Biol 20:9212-9224

[208] Alghisi GC and Ruegg C (2006) Vascular integrins in tumor angiogenesis: mediators and therapeutic targets. Endothelium 13:113-135

[209] Janes SM and Watt FM (2006) New roles for integrins in squamous-cell carcinoma. Nat Rev Cancer 6:175-183

[210] Lewis JD, Payton LA, Whitford JG et al (2007) Induction of tumorigenesis and metastasis by the murine orthologue of tumor protein D52. Mol Cancer Res 5:133-144

[211] Plow EF, Haas TA, Zhang L et al (2000) Ligand binding to integrins. J Biol Chem 275:21785-21788

[212] Giancotti FG and Ruoslahti E (1999) Integrin signaling. Science 285:1028-1032

[213] Varner JA and Cheresh DA (1996) Tumor angiogenesis and the role of vascular cell integrin alphavbeta3. Important Adv Oncol69-87

[214] Pytela R, Pierschbacher MDRuoslahti E (1985) A 125/115-kDa cell surface receptor specific for vitronectin interacts with the arginine-glycine-aspartic acid adhesion sequence derived from fibronectin. Proc Natl Acad Sci U S A 82:5766-5770

[215] Zheng DQ, Woodard AS, Tallini G et al (2000) Substrate specificity of alpha(v)beta(3) integrin-mediated cell migration and phosphatidylinositol 3-kinase/AKT pathway activation. J Biol Chem 275:24565-24574

[216] Witkowski CM, Rabinovitz I, Nagle RB et al (1993) Characterization of integrin subunits, cellular adhesion and tumorgenicity of four human prostate cell lines. J Cancer Res Clin Oncol 119:637-644

[217] Chatterjee S, Brite KHMatsumura A (2001) Induction of apoptosis of integrin-expressing human prostate cancer cells by cyclic Arg-Gly-Asp peptides. Clin Cancer Res 7:3006-3011

[218] Putz E, Witter K, Offner S et al (1999) Phenotypic characteristics of cell lines derived from disseminated cancer cells in bone marrow of patients with solid epithelial tumors: establishment of working models for human micrometastases. Cancer Res 59:241-248

[219] Brooks PC, Klemke RL, Schon S et al (1997) Insulin-like growth factor receptor cooperates with integrin alpha v beta 5 to promote tumor cell dissemination in vivo. J Clin Invest 99:1390-1398

[220] Wong NC, Mueller BM, Barbas CF et al (1998) Alphav integrins mediate adhesion and migration of breast carcinoma cell lines. Clin Exp Metastasis 16:50-61

[221] Zheng DQ, Woodard AS, Tallini G et al (2000) Substrate specificity of alpha(v)beta(3) integrin-mediated cell migration and phosphatidylinositol 3-kinase/AKT pathway activation. J Biol Chem 275:24565-24574

[222] Hullinger TG, McCauley LK, DeJoode ML et al (1998) Effect of bone proteins on human prostate cancer cell lines in vitro. Prostate 36:14-22

[223] Zhang H, Wang J, Pang B et al (2007) PC-1/PrLZ contributes to malignant progression in prostate cancer. Cancer Res 67:8906-8913

[224] Cooper CR, Chay CHPienta KJ (2002) The role of alpha(v)beta(3) in prostate cancer progression. Neoplasia 4:191-194

[225] Wilson SH, Bailey AM, Nourse CR et al (2001) Identification of MAL2, a novel member of the mal proteolipid family, though interactions with TPD52-like proteins in the yeast two-hybrid system. Genomics 76:81-88

[226] Tiacci E, Orvietani PL, Bigerna B et al (2005) Tumor protein D52 (TPD52): a novel B-cell/plasma-cell molecule with unique expression pattern and Ca(2+)-dependent association with annexin VI. Blood 105:2812-2820

[227] Chang JW, Jeon HB, Lee JH et al (2001) Augmented expression of peroxiredoxin I in lung cancer. Biochem Biophys Res Commun 289:507-512

[228] Chang JW, Lee SH, Jeong JY et al (2005) Peroxiredoxin-I is an autoimmunogenic tumor antigen in non-small cell lung cancer. FEBS Lett 579:2873-2877

[229] Noh DY, Ahn SJ, Lee RA et al (2001) Overexpression of peroxiredoxin in human breast cancer. Anticancer Res 21:2085-2090

[230] Quan C, Cha EJ, Lee HL et al (2006) Enhanced expression of peroxiredoxin I and VI correlates with development, recurrence and progression of human bladder cancer. J Urol 175:1512-1516

[231] Yanagawa T, Ishikawa T, Ishii T et al (1999) Peroxiredoxin I expression in human thyroid tumors. Cancer Lett 145:127-132

[232] Yanagawa T, Iwasa S, Ishii T et al (2000) Peroxiredoxin I expression in oral cancer: a potential new tumor marker. Cancer Lett 156:27-35

[233] Qi Y, Chiu JF, Wang L et al (2005) Comparative proteomic analysis of esophageal squamous cell carcinoma. Proteomics 5:2960-2971

[234] Shen J, Person MD, Zhu J et al (2004) Protein expression profiles in pancreatic adenocarcinoma compared with normal pancreatic tissue and tissue affected by pancreatitis as detected by two-dimensional gel electrophoresis and mass spectrometry. Cancer Res 64:9018-9026

[235] Yanagawa T, Omura K, Harada H et al (2005) Peroxiredoxin I expression in tongue squamous cell carcinomas as involved in tumor recurrence. Int J Oral Maxillofac Surg 34:915-920

[236] Lin JF, Xu J, Tian HY et al (2007) Identification of candidate prostate cancer biomarkers in prostate needle biopsy specimens using proteomic analysis. Int J Cancer 121:2596-2605

[237] Prosperi MT, Ferbus D, Karczinski I et al (1993) A human cDNA corresponding to a gene overexpressed during cell proliferation encodes a product sharing homology with amoebic and bacterial proteins. J Biol Chem 268:11050-11056

[238] Prosperi MT, Apiou F, Dutrillaux B et al (1994) Organization and chromosomal assignment of two human PAG gene loci: PAGA encoding a functional gene and PAGB a processed pseudogene. Genomics 19:236-241

[239] Ames BN, Gold LSWillett WC (1995) The causes and prevention of cancer. Proc Natl Acad Sci U S A 92:5258-5265

[240] Weitzman SA and Gordon LI (1990) Inflammation and cancer: role of phagocyte-generated oxidants in carcinogenesis. Blood 76:655-663

[241] Park SY, Yu X, Ip C et al (2007) Peroxiredoxin 1 interacts with androgen receptor and enhances its transactivation. Cancer Res 67:9294-9303

[242] Kaspar KM, Thomas DD, Taft WB et al (2003) CaM kinase II regulation of CRHSP-28 phosphorylation in cultured mucosal T84 cells. Am J Physiol Gastrointest Liver Physiol 285:G1300-G1309

[243] Thomas DD, Weng NGroblewski GE (2004) Secretagogue-induced translocation of CRHSP-28 within an early apical endosomal compartment in acinar cells. Am J Physiol Gastrointest Liver Physiol 287:G253-G263

[244] Groblewski GE, Yoshida M, Yao H et al (1999) Immunolocalization of CRHSP28 in exocrine digestive glands and gastrointestinal tissues of the rat. Am J Physiol 276:G219-G226

[245] Groblewski GE, Wishart MJ, Yoshida M et al (1996) Purification and identification of a 28-kDa calcium-regulated heat-stable protein. A novel secretagogue-regulated phosphoprotein in exocrine pancreas. J Biol Chem 271:31502-31507

[246] O'Neill AJ, Boran SA, O'Keane C et al (2001) Caspase 3 expression in benign prostatic hyperplasia and prostate carcinoma. Prostate 47:183-188

[247] Sohn JH, Kim DH, Choi NG et al (2000) Caspase-3/CPP32 immunoreactivity and its correlation with frequency of apoptotic bodies in human prostatic carcinomas and benign nodular hyperplasias. Histopathology 37:555-560

[248] Winter RN, Kramer A, Borkowski A et al (2001) Loss of caspase-1 and caspase-3 protein expression in human prostate cancer. Cancer Res 61:1227-1232

[249] Ananthanarayanan V, Deaton RJ, Yang XJ et al (2006) Alteration of proliferation and apoptotic markers in normal and premalignant tissue associated with prostate cancer. BMC Cancer 6:73

[250] Leoncini L, Del Vecchio MT, Megha T et al (1993) Correlations between apoptotic and proliferative indices in malignant non-Hodgkin's lymphomas. Am J Pathol 142:755-763

[251] Vakkala M, Paakko PSoini Y (1999) Expression of caspases 3, 6 and 8 is increased in parallel with apoptosis and histological aggressiveness of the breast lesion. Br J Cancer 81:592-599

[252] Kang JJ, Schaber MD, Srinivasula SM et al (1999) Cascades of mammalian caspase activation in the yeast Saccharomyces cerevisiae. J Biol Chem 274:3189-3198

[253] Allsopp TE, McLuckie J, Kerr LE et al (2000) Caspase 6 activity initiates caspase 3 activation in cerebellar granule cell apoptosis. Cell Death Differ 7:984-993

[254] Reinhold WC, Kouros-Mehr H, Kohn KW et al (2003) Apoptotic susceptibility of cancer cells selected for camptothecin resistance: gene expression profiling, functional analysis, and molecular interaction mapping. Cancer Res 63:1000-1011

[255] Lee SC, Chan J, Clement MV et al (2006) Functional proteomics of resveratrol-induced colon cancer cell apoptosis: caspase-6-mediated cleavage of lamin A is a major signaling loop. Proteomics 6:2386-2394

[256] Winter RN, Kramer A, Borkowski A et al (2001) Loss of caspase-1 and caspase-3 protein expression in human prostate cancer. Cancer Res 61:1227-1232

[257] McDonnell TJ, Troncoso P, Brisbay SM et al (1992) Expression of the protooncogene bcl-2 in the prostate and its association with emergence of androgen-independent prostate cancer. Cancer Res 52:6940-6944

[258] Tu H, Jacobs SC, Borkowski A et al (1996) Incidence of apoptosis and cell proliferation in prostate cancer: relationship with TGF-beta1 and bcl-2 expression. Int J Cancer 69:357-363

[259] Johnson MI, Robinson MC, Marsh C et al (1998) Expression of Bcl-2, Bax, and p53 in high-grade prostatic intraepithelial neoplasia and localized prostate cancer: relationship with apoptosis and proliferation. Prostate 37:223-229

Acknowledgements

I wish to express my sincere thanks to everyone who helped, inspired and guided throughout this project.

It is very difficult to express my gratitude to my supervisor and Guru **Prof. Dr. Reinhard Walther** for introducing me to the prostate cancer research and providing an end less support during these years. Yours empathic and caring personality has given colors to my life since I met you. Thank you for providing a stimulating and nice environment in which I learned a lot and became more mature scientifically, for encouragement and allowing me to collaborate with other groups in the University of Greifswald. Thank you very much for your amazing response on my day to day scientific as well as non-scientific questions, patience and bearing me for last three years. You are the kindest hearted person I have ever met in my life. I would have been lost without you during the high time of my lab work with my problems.

I wish to thank **Dr. Heike Junker** who is my lab supervisor. I can not forget her support that was always there whenever I was in need through out my stay in Griefswald. Thanks for everything you have done for me.

I would like to thank **Dr. Steffen Teller** for your help since my first day in cell culture lab and suggestions through out my work. You are always willing to discuss about the work and results. Without you it would have not been possible for me to do good experiments in cell culture.

Prof. Dr. Jürgen Giebel, Thank you very much for your valuable time for support, endless discussions, and morphological evaluation of prostate sections for immunohistochemistry and nice criticism while writing manuscripts from my project. I cannot forget cappuccino sessions we always had together following our meetings in Griefswald.

PD Dr. med. Uwe Zimmermann, Thank you for your support as urologist, collecting the biopsies and ideas giving from clinician's point of view.

I thank mass spec collaborators **Dr. Simone Venz** and **Dr. Christian Scharf** for identification and data processing of protein spots very quickly time to time.

Thanks to **Prof. Dr. Winfried Hinrichs** for allowing me to use facilities in your laboratory and introducing me to biophysical methods.

I also express my heartfelt thanks to **Dr. Rajesh Kumar Singh** for your friendship, encouragement and motivation when I ever I felt depressed and for helping me so much whatever I need through my study time in Greifswald. Thank you for reading and suggestions while writing my dissertation.

I am indebted to my lab co-worker **Gabriele Würtz** for her help to get through the difficult times, and for all the emotional support, entertainment, and care you provided. You helped me a lot in Griefswald from day one to till date.

I also express my heartfelt thanks to **Dr. Gabriele Wolf, Dr. Antje Bast** and **Anke Karkour** for your friendship and for help whenever I was in need through out my study time in Greifswald.

I am grateful to the secretary **Christiana Grothmann** for her understanding, all day to day help at her office and to convey all my messages to Prof. Walther. I am also thankful to **Brigitte Parlow** and **Ines Schultz** for their support during my work.

I can not forget to mention my thanks to ***Alfried-Krupp von Bohlen und Halbach Stiftung, Graduiertenkolleg Tumorbiologie*** and speaker of the graduate college **Prof. Dr. Christian A. Schmidt** for the financial support of my stay as well as research in Greifswald.

I wish to thank my entire extended family for providing a loving environment.

Most importantly, I wish to thank my parents, **Shri. Gopal and Smt. Lalithamma**. They bore me, raised me, supported me, taught me, and loved me. To them I dedicate this thesis.

Last but not the least; I want to express my special thanks to my lovely wife **Kavitha** for her remarkable patience and support. She was very supportive and understanding. Often, whenever I said, “I do not have time to go out” during the high time of my PhD she never complained. While writing this dissertation she has taken care of every thing time to time at my work desk.

Thanks to all and my sincere apology if I missed anyone who deserved to be mention.

Erklärung

Hiermit erkläre ich, daß diese Arbeit bisher von mir weder an der Mathematisch-Naturwissenschaftlichen Fakultät der Ernst-Moritz-Arndt-Universität Greifswald noch einer anderen wissenschaftlichen Einrichtung zum Zwecke der Promotion eingereicht wurde.

Ferner erkläre ich, daß ich diese Arbeit selbständig verfaßt und keine anderen als die darin angegebenen Hilfsmittel benutzt habe.

Curriculum Vitae

RAMESH UMMANNI : **Hyderabad, India**

PERSONAL Information

Date of Birth	: 15-05-1978
Father's Name	: U.Gopal
Gender	: Male
Marital status	: Married
Perm. Address	: S/o U.GOPAL East Narasapuram Post Singanamala (Mandal), Anantapur Dist. Andhra Pradesh, India 515435
Nationality	: Indian
Languages	: English, Telugu

Education and work experience

1983-1993	: Primary and Secondary school, Andhrapradesh, India
1993-1995	: Board of Intermediate Education, Andhrapradesh, India
1995-1998	: Bachelor of Science (Biochemistry), Sri Krishnadevaraya University, India
1998-2000	: Masters of Science (Biochemistry), Nagrjuna University, India
2000-2003	: Lecturer in Biochemistry, GVR&S PG College for Women, Nagarjuna University, India
2003-2005	: Research fellow at Centre for Cellular and Molecular Biology (CCMB), Inida
2005-2008	: Ph.D. student of the Institute of Medical Biochemistry and Molecular Biology, Ernst-Moritz-Arndt University of Greifswald, Germany.